

**POWER LINE COMMUNICATION (PLC) CHANNEL  
MEASUREMENTS AND CHARACTERIZATION**

by

**Modisa Mosalaosi**

Dissertation Submitted in fulfilment of the requirements for the degree

Master of Science in Engineering: Electronic Engineering

in the

College of Agriculture, Engineering and Science



**UNIVERSITY OF KWAZULU-NATAL**

2014

Supervisor: **Prof. Thomas Joachim Odhiambo Afullo**

As the candidate's Supervisor I agree to the submission of this thesis.

Signed .....

Date.....

Name: Prof. Thomas J. O. Afullo

## DECLARATION - PLAGIARISM

I, **Modisa Mosalaosi**, declare that

1. The research reported in this thesis, except where otherwise indicated, is my original research.
2. This thesis has not been submitted for any degree or examination at any other university.
3. This thesis does not contain other persons' data, pictures, graphs or other information, unless specifically acknowledged as being sourced from other persons.
4. This thesis does not contain other persons' writing, unless specifically acknowledged as being sourced from other researchers. Where other written sources have been quoted, then:
  - a. Their words have been re-written but the general information attributed to them has been referenced
  - b. Where their exact words have been used, then their writing has been placed in italics and inside quotation marks, and referenced.
5. This thesis does not contain text, graphics or tables copied and pasted from the Internet, unless specifically acknowledged, and the source being detailed in the thesis and in the References sections.

Signed .....

Date.....

## PUBLICATIONS

The list of publications related to this work are given including their overlapping chapters:

[Overlapping Chapter 3]

M. Mosalaosi, Thomas J. O. Afullo, “Broadband Analysis and Characterization of Noise for In-Door Power-Line Communication Channels”, *Progress In Electromagnetics Research Symposium Proceedings (PIERS)*, Guangzhou, China, pp. 719-723, Aug. 25-28, 2014.

[Overlapping Chapter 4]

M. Mosalaosi and Thomas J. O. Afullo, “Dispersive Characteristics for Broadband Indoor Power-Line Communication Channels”, *Southern Africa Telecommunication Networks and Applications Conference (SATNAC)*, Port Elizabeth, South Africa, Aug. 30 – Sep. 03, 2014

[Overlapping Chapter 5]

M. Mosalaosi and Thomas J. O. Afullo, “Broadband Characteristics for Multi-Path Power Line Communications Channels: Indoor Environments”, (submitted to) *IEEE Transactions on Power Delivery*.

Signed.....

## **ACKNOWLEDGEMENTS**

First and foremost I have to thank my parents, Mr and Mrs Thokweng, for their love and support throughout my life. Thank you both for giving me strength to reach for the stars and chase my dreams, even when it had to be so far from you. I extend my gratitude to my siblings who supported my adventures and stood by me in many ways to mention.

I would like to sincerely express my deepest appreciation to my supervisor, Professor T. J. O. Afullo for his guidance and support throughout this study, and especially his confidence in me. With his attitude and substance of intellect, he continually and persuasively conveyed the spirit of adventure and excitement in this research. Without his contribution in stimulating suggestions and encouragement, this dissertation would not have been possible.

Furthermore, I would also like to acknowledge with much appreciation the crucial role of the technical staff for making it possible to gather all the necessary material required to build our test bed. Mr Jabulani Gumede, your tirelessness, energy and attention to detail played a key role in our data acquisition campaign so I thank you. I extend my acknowledgements to Ms F. Zwane for the discussions and knowledge sharing, thank you for making the time. Finally, all the contributions towards this work were made possible by the lord God and may all the glory be his.

## ABSTRACT

The potential of the power line to transport both power and communication signals simultaneously has been realized and practiced for over a century, dating back to the 1900's. Since the key aspect of power line communications being its expansivity, its implementations were largely as a retrofit technology. This motivation of power line communication is typical for low-, medium-, and high voltage distribution networks. Beyond the "last mile" part, there's an uprising appeal for intra-building networks currently targeted for home automation (smart homes/buildings) and in-building networking. The optimum use of the existing power line channels has been a focus area for researchers and designers, with the inherent channel hostility proving a serious drawback for high speed data communications.

The low-voltage electrical network has unpredictable noise sources, moreover it has two other main disadvantages as a communication channel. The first short coming has to do with the unknown characteristics of the power cable and topology of the network, the second arises from the time-dependent fluctuation of the impedance level of the power line as the loads are switched into and out of the power line network in an unpredictable manner. These factors determine the behaviour of the power line channel when a high frequency signal is impressed on it. This study has shown that the behaviour of indoor power line channels can be captured using a multipath based model even with limited qualitative and/or quantitative knowledge of the network topology. This model is suitable for typical indoor power line channels where knowledge of the topology is near impossible. Some of the feed parameters are obtained through measurements. With sufficient adjustment of control parameters, this model was successfully validated using sample measured channels from the numerous measurements.

Through noise measurements, this study has established that impulsive noise is the rifest in the frequency band of interest. The impulsive energy rises well above background noise, which translates to possible data "black outs". The statistics of the components of this noise are presented. A model of sufficient simplicity is used to facilitate the qualitative description of the background noise through its power spectral density. Two descriptions are provided in terms of the worst and best case scenarios of the background noise occurrences. The model has a good macroscopic capture of the noise power spectral density, with narrow-band interference visible for the worst case noise.

Due to the multipath nature of the power line channel, this study also presents the dispersive characteristics of the power line as a communication channel. The power delay profile is used to determine parameters such as first arrival delay, mean excess delay, root mean square delay spread and maximum delay spread. The statistics of these parameters are presented. Also, the coherence bandwidth of power line channels is studied and its relationship with the *rms* delay spread is developed. It is in view of this work that further research in power line communication and related topics shall be inspired.

## **TABLE OF CONTENTS**

---

<b>DECLARATION-PLAGIARISM</b>	(II)
<b>PUBLICATIONS</b>	(III)
<b>ACKNOWLEDGEMENTS</b>	(IV)
<b>ABSTRACT</b>	(VI)
<b>1. INTRODUCTION</b>	<b>- 1 -</b>
1.1 Power Line Communication	- 1 -
1.2 PLC History	- 2 -
1.3 PLC Impairments	- 4 -
1.3.1 Intrinsic Attenuation and Radiation	- 4 -
1.3.2 Power Line Communication Noise	- 7 -
1.4 PLC Regulations and Standardization	- 8 -
1.5 Research Objectives	- 9 -
1.6 Thesis Organization	- 10 -
<b>2. LITERATURE REVIEW</b>	<b>- 11 -</b>
2.1 Introduction	- 11 -
2.2 Properties of Electrical Power Networks	- 11 -
2.2.1 High Voltage Networks	- 12 -
2.2.2 Medium Voltage Networks	- 13 -
2.2.3 Low Voltage Networks	- 13 -
2.3 Characteristics of Power Lines	- 14 -
2.3.1 Capacitance and Inductance	- 14 -
2.3.2 Impedance	- 15 -
2.4 PLC Noise	- 15 -
2.5 PLC Channel Modelling	- 17 -
2.5.1 Time Domain Approach: The Multipath Model	- 18 -
2.5.2 Frequency Domain Approach: Transmission Line Theory Models	- 20 -
2.6 Impulsive Noise Modelling	- 21 -
2.6.1 Middleton Class A Noise Model	- 22 -
2.6.2 Bernoulli-Gaussian Model	- 23 -
2.6.3 Poisson-Gaussian Model	- 24 -
<b>3. BROADBAND ANALYSIS AND CHARACTERIZATION OF NOISE FOR IN-DOOR POWER-LINE COMMUNICATION CHANNELS</b>	<b>- 26 -</b>
3.1 Introduction	- 26 -
3.1.1 Background Noise	- 28 -
3.1.2 Impulsive Noise:	- 29 -

3.2	Noise Measurements	- 31 -
3.3	Impulsive Noise	- 31 -
3.4	Measurements Results	- 32 -
3.4.1	Periodic Impulsive Noise Synchronous With the Mains	- 33 -
3.4.2	Periodic Impulsive Noise Asynchronous With the Mains	- 34 -
3.5	Asynchronous Impulsive Noise	- 35 -
3.6	Background Noise	- 36 -
3.7	Chapter Summary	- 40 -
<b>4.</b>	<b>DISPERSIVE CHARACTERISTICS FOR BROADBAND INDOOR POWER-LINE COMMUNICATION CHANNELS</b>	<b>- 41 -</b>
4.1	Introduction	- 41 -
4.2	Measurement Setup & fundamentals	- 41 -
4.3	Channel Impulse Response (CIR)	- 42 -
4.4	Power Delay Profile (PDP)	- 43 -
4.5	Time-Delay Spread Parameters	- 44 -
4.5.1	First-Arrival Delay $\tau_A$	- 44 -
4.5.2	Mean Excess Delay $\tau_e$	- 44 -
4.5.3	RMS Delay Spread $\tau_{rms}$	- 44 -
4.5.4	Maximum Excess Delay $\tau_m$	- 45 -
4.6	Results Analysis	- 45 -
4.7	Coherence Bandwidth	- 46 -
4.8	Chapter Summary	- 48 -
<b>5.</b>	<b>BROADBAND CHARACTERISTICS FOR MULTI-PATH POWER LINE COMMUNICATION CHANNELS: INDOOR ENVIRONMENTS</b>	<b>- 50 -</b>
5.1	Introduction	- 50 -
5.2	Measurement Description & Instrumentation	- 51 -
5.3	Channel Frequency Response (CFR) Measurements	- 53 -
5.4	Practical PLC Channel Modelling	- 54 -
5.4.1	Channel Response Characteristics	- 54 -
5.4.2	Channel Impulse Response (CIR)	- 57 -
5.4.3	Channel Model Parameters	- 60 -
5.5	Chapter Summary	- 61 -
<b>6.</b>	<b>CONCLUSIONS AND FUTURE DIRECTIONS</b>	<b>- 62 -</b>
6.1	Summary of Results	- 62 -
6.2	Possible Future Work	- 64 -
	<b>REFERENCES</b>	<b>- 65 -</b>



## **LIST OF FIGURES**

---

### **Chapter 1**

Figure 1.1: MV to LV transmission system (<http://imgarcade.com/1/low-voltage-transmission-lines/>)

-2-

Figure 1.2: Conductor cross-sectional area at a) DC current b) Low frequency ac current and c) High frequency ac current

-5-

Figure 1.3: PLC system External fields at 100 kHz and 10 MHz [46]

-6-

Figure 1.4: Even-mode current driven power line [46]

-7-

### **Chapter 2**

Figure 2.1: typical electrical power system

[<http://venturebeat.files.wordpress.com/2010/10/grid.jpg>]

-12-

Figure 2.2: PLC communication system [69]

-16-

Figure 2.3: Single branch PLC channel

-19-

Figure 2.4: Sample Impulsive noise [82]

-22-

### **Chapter 3**

Figure 3.1: Noise in PLC systems

-28-

Figure 3.2: Coupling Circuit

-31-

Figure 3.3: Synchronous Impulsive Noise showing the dominant 100 Hz components

-32-

Figure 3.4: Asynchronous Impulsive Noise

-33-

Figure 3.5: detailed synchronous impulsive noise over two mains cycles

-33-

Figure 3.6: Impulsive noise captured in a laboratory with view of the dominant 50 Hz synchronous components

-34-

Figure 3.7: Detailed view of registered periodic impulsive noise for half mains cycle

-34-

Figure 3.8: Detailed view of registered periodic asynchronous noise

-35-

Figure 3.9: Minimum Spectral Noise

-37-

Figure 3.10: Maximum Spectral Noise

-37-

Figure 3.11: Time-of-the-day noise characteristics

-38-

Figure 3.12: Sample noise measurements and their models (a) University lab (b) measurement lab (c) post-graduate office, and (d) comparison of models with those of Esmailian *et al* [114]

-39-

### **Chapter 4**

Figure 4.1: (a) Channel determination setup In-Building and (b) Coupling Circuitry

-42-

Figure 4.2: Sample Channel IR (absolute)

-43-

Figure 4.3: A typical PDP plot

-43-

Figure 4.4: Cumulative distributions (CDFs) of the time delay parameters

-46-

Figure 4.5: FCFs of sample measured channels

-47-

Figure 4.6: Scatter plot of coherence bandwidth against RMS delay spread

-48-

## **Chapter 5**

Figure 5.1: Measurement setup	-52-
Figure 5.2: (a) Channel determination setup In-Building and (b) Coupling Circuitry	-52-
Figure 5.3: Coupler Characteristics	-53-
Figure 5.4: Channel Response of Real In-door Channels and their Average Responses (bottom right corner)-54-	-54-
Figure 5.5: Attenuation parameters estimation	-56-
Figure 5.6: Impulse Response of figure (3) Channels and their corresponding group delays	-58-
Figure 5.7: Modelled real CTFs and Their Phase Characteristics	-59-

## **LIST OF TABLES**

---

Table 3.1: Statistical Parameters of Impulsive Noise	-36-
Table 3.2: Background noise parameters	-38-
Table 4.1: Time delay parameters	-45-
Table 5.1: Impulse response summary of eight sample channels	-58-
Table 5.2: Model parameters for three simulated channels of Figure 3	-60-

## CHAPTER ONE

### INTRODUCTION

#### 1.1 Power Line Communication

The significant increase in demand for broadband multimedia services in recent years continues to grow at a rapid rate. Broadband internet connectivity, for instance, has a tremendous demand and increasingly becoming a basic fundamental for homes and businesses. Currently there is a variety of technologies employed to provide broadband connectivity to and within consumers' homes and offices. However, power line communications (PLC) presents an appealing opportunity for broadband multimedia connectivity to the last mile solution and has thus received an overwhelming amount of research interest. PLC derives benefit from already-existing electrical wiring networks to provide high speed data services. PLC exploits in-building electrical wiring to build local area networks (LANs) delivering high speed networking services such as broadband internet access, voice over IP (VoIP) and home entertainment services effectively to every plug in the residential or business premises. The driving incentive of using PLC is that it uses infrastructure that is much more ubiquitous than any other wired media (telephone loops, Ethernet, fibre optic), hence does not require new wiring installations.

In most cases, building a home network using the existing AC electrical wiring is easier than trying to run wires, more secure and more reliable than radio wireless systems like 802.11b and relatively inexpensive as well [1]. Although the practical use of PLC has been in existence since the 1900's, it's only of recent (90's) that power line communication has gained momentum. Traditionally, PLC applications were limited to narrowband services such as voice and control signals over high voltage (HV) and medium voltage (MV) networks, peak demand management (load shedding) as well as automatic meter reading (AMR) over low voltage (LV) networks. To date, the advancement in technology and production in association with consumer demand for broadband services has facilitated a rapid growth in the internet market. Consequently, this has established the need for home networks and home automation solutions of which power line communication is an ideal candidate.

Data transfer over a medium that was never designed for makes for a curious and challenging prospect. In the frequency band closest to the power frequency (50 Hz), PLC systems do not experience as much hostility as they would at frequencies much further up the spectrum. Unfortunately, at low frequencies only limited data rates can be achieved since frequency is the sole controlling element of bandwidth. The demand for broadband services dictates that higher frequency bands be used and as frequency increases so do the complications. The other major concern at high frequencies is that the copper network behave like complex antennas which not only poses an efficiency concern but also that of the environment and interference to other systems operating at or neighbouring frequencies.

## 1.2 PLC History

PLC technology has been in operation for over a century, unbeknown to the general public but the utility companies have used it to implement their own telephone systems over distribution lines since the 1920's [2], [3]. Another extensive use of this technology out of public knowledge has been load shedding, e.g. switching off hot water geysers from a central monitoring location during peak hours [4]-[6]. However, only in recent times have consumers become adept in the promises of this "free" power line network when America and European countries started to permit production and sales of power line modems for home networks and home automation [7]-[9]. Transmission over HV lines became very popular due to their early existence long before dedicated telephone loops were established and extended considerably into rural areas [2]. The utility companies themselves had a compelling need for bidirectional communication for the management of their power stations, sub-stations, distribution lines, as well as synchronization and energy distribution.

The ability of both the HV and MV power lines to carry out reliable data transmission became clearer as decades went by, simply because these lines have a simple topology with predictable transfer characteristics. Linkage between the different voltage levels of the power network typically requires bypassing of transformers at the conversion points, spoiling the simplicity of the topology [10]. Such transformers are as seen in figure 1.1 deployed to transform from MV to LV to feed residential settlements.

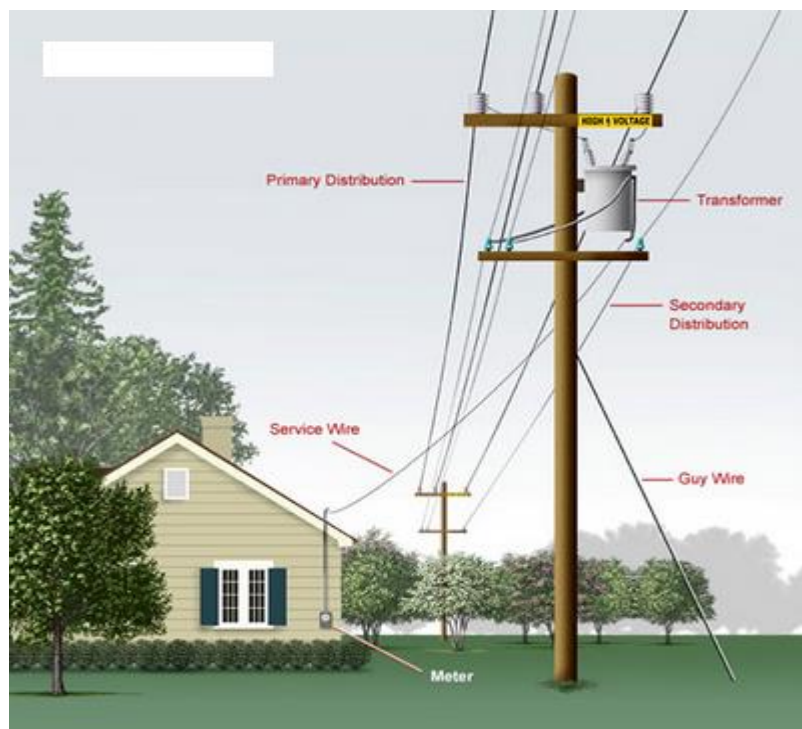


Figure 1.1: MV to LV transmission system (<http://imgarcade.com/1/low-voltage-transmission-lines/>)

In developing countries, the spread of telephone systems is currently restricted, whilst power line networks are far-reaching. Their pervasive nature presents an opportunity to facilitate the desperate need for broadband services. Internet access over power lines is viewed as a viable solution to bring about telephony, education, banking as well as remote medical consultations in third world countries. This explains the recent enthusiasm shown by some African and South American researchers in pursuit of this PLC and related topics [11]-[17].

The complex nature of the low voltage networks makes for unreliable data transmission, hence this branch of PLC has been historically ignored and consequently lagged behind. The only application perceived to have had reasonable justification, before the 90's, was load control to limit peak energy demand. Known as ripple control or ripple carrier signalling, this approach has been in use since the 1930's [2], [18]. Due to the low carrier frequency (<3 kHz) and the inherent hostility of the LV topology, transmission systems used very high power (even in the order of kilowatts) for successful communication [4]. Since the inception of PLC technology, the main attraction for utility companies has been the implementation of automatic meter reading (AMR), though it only gathered momentum in the 1970's [19]-[23]. Researchers today however envisage usage beyond data acquisition for billing of electricity, water and gas consumption; but anticipate more advanced roles that could be implemented in the near future. These would include channel state parameters such as noise data and signal level required for continuous monitoring of the signal-to-noise ratio (SNR) across all channels for channel adaptation and to help make decisions on channel status and assignments.

Research into the applicability of PLC systems for home automation began to rise during the 1980's and 1990's [24], [25]. This is owing to the exponential growth in the market for consumer electronics in parallel with the capacity for intelligent systems as well as home networking and automation. Some of the target applications are remote control of lighting, heating and air-conditioning, multimedia, and alarm systems. Buildings could be programmed to intelligently decide the number of lights required at any particular point in time based on in-house activity and/or occupancy. Energy management systems may be put in place tailored for specific household routines by calibrating heating "on" and "off" periods. Multimedia applications may include scheduled recording of radio and/or television programs with view of re-running them through the home network at one's convenience.

The establishment of local area networks (LANs) became popular in the 1990's due to personal computers (PCs) becoming inexpensive [26], [27]. The emergence of the World Wide Web or internet in the later years as well as a rapid growth in the number of PCs found in homes in developed countries gave rise to internet usage from the consumer's home comfort for instant access to information, media, shopping and banking [28]. Power line communication is an ideal candidate for this intra-building computer networks and home automation. Owing to this, some companies have flooded the market with

low speed narrow band home networking products since the 1990's [29], [30]. In the 2000's, broadband high speed technologies became operational as a result of relaxed regulations in different countries [9], [31]-[34]. A number of standards were specified by the HomePlug alliance [35] as the technology developed. First off is the HomePlug 1.0 which was released in June 2001 and supports data rates up to 14 Mbps followed by the HomePlug AV specification which was released in 2005 and increased physical layer (PHY) peak data rates from 14 to 200 Mbps. Later in June 2010 another specification was released, the HomePlug Green PHY, regarded as the "sibling" to the HomePlug AV with target applications such as smart energy with lower power consumption, lower cost and decreased throughput compared to its predecessor. On September 30, 2010 another broadband PLC standard was approved in the IEEE's 1901 standard and now the HomePlug AV is validated and ratified as an international standard.

### **1.3 PLC Impairments**

The physical characteristics as well as the topology of electrical networks was never designed with data transmission at high frequencies in mind. Power line as a communication medium presents inherent impairments that a designer has to work around or accept their impact as a base loss. Besides these inherent impairments, the very systems that the electrical utility sort to supply electricity, consume considerable amounts of the transmission signal and presents a harsh environment by feeding harmonics and noise back into the grid randomly. The challenge of designing PLC systems stems from these key issues.

#### **1.3.1 Intrinsic Attenuation and Radiation**

The intrinsic properties of the electrical wiring have a direct influence on the attenuation level at different frequencies in the 1 – 30 MHz frequency band. Transmission with low frequency modulation (~100 kHz) will result in low attenuation as compared to transmission at ~10 MHz for example. This is due to the skin effect which causes about 10 times smaller effective conductor area since the frequency is higher by a factor of 100 [36]. This effect is depicted in figure 1.2. Due to the self-inductance of the conductor, the resultant conductor impedance is proportional to the transmission frequency [37]. The higher the frequency the more difficult it becomes for the signal to traverse the wiring. Moreover, power devices and other loads have an adverse impact on the low frequency systems since these inductive loads and particularly resistive loads conduct low frequencies well, thereby draining the energy from the communication signal [38], [39]. Conversely, the R-L loads has less effect on the high frequency systems as inductive loads permit an insignificant amount of the high frequency current to pass through. Capacitive and numerous protective devices such as varactors and zener diodes are however deleterious to transmission of high frequency signals [3].

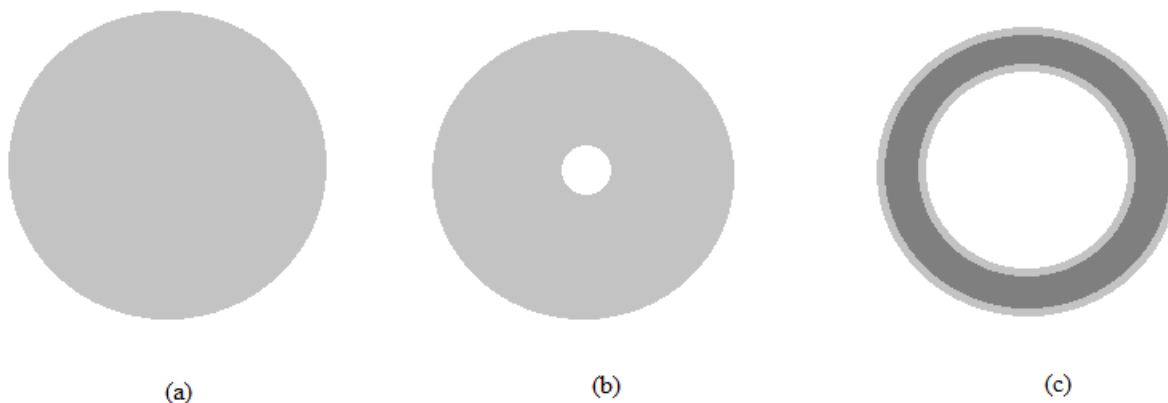


Figure 1.2: Conductor cross-sectional area at a) DC current b) Low frequency ac current and c) High frequency ac current

The prosperity of a PLC system is primarily influenced by the topology of the network it's deployed in [40]. The simplicity in terms of topology common with both medium and high voltage networks promotes point-to-point communications through a single line between two points [3]. This allows for simplicity in facilitating impedance matching using single lines or ring [41] and/or make signal attenuation more predictable. It would therefore be more rewarding to deploy high data rates systems on such topologies at low transmit power than it would be on more complex ones. Transformers interconnecting sections of the power network typically needs to be by-passed for proper transmission from one section to the other [10], thereby spoiling the simplicity.

The electrical power lines' physical layout in low voltage residential areas adopts a more complex multi-tap (branched) topology also typified as star topology [3], [4], [40]. All the branches in the LV network experience different signal attenuation levels with the mismatches at the branch nodes giving rise to multiple reflections of the propagation signal [40], [42]. It is this characteristic of the LV network that results in it been open and unpredictable. The branches in the network are terminated by random loading profiles as consumers plug appliances in and out of the network in a disorderly manner, leading to abrupt and severe impedance fluctuations. The unpredictability of the network loading conditions increases as the complexity of the network increases. These fluctuations makes it difficult for impedance matching and thus only a small portion of the transmitted signal will be available at the receiver [43]. As a result of the abovementioned shortcomings, low voltage PLC systems designers resort to low data rates communications or higher power levels for faster data rates.

The unshielded nature of the electrical wiring is a cause for concern at high frequencies in terms of its ability to radiate into free space as well as intercept other radios operating in the same band. There is a direct impact on potential radiation of a PLC network due to its topology. Common-mode currents that



often leak back to earth through parasitic capacitances form large antenna-like loops, thereby radiating much of the common-mode energy. In [44] and [45], a description of the radiating mechanisms for both differential and common-mode currents is given, while in [46] it is shown that guided-wave radiation is dominant at 100 kHz up to a distance of 170 m from the source while at 10 MHz the radiated field dominates even in the near field (< 10 m). Moreover, according to [46] (see figure 1.3), for the same transmit power at 10 MHz a PLC system will cause up to 80 dB more radiated emission compared to a 100 kHz system.

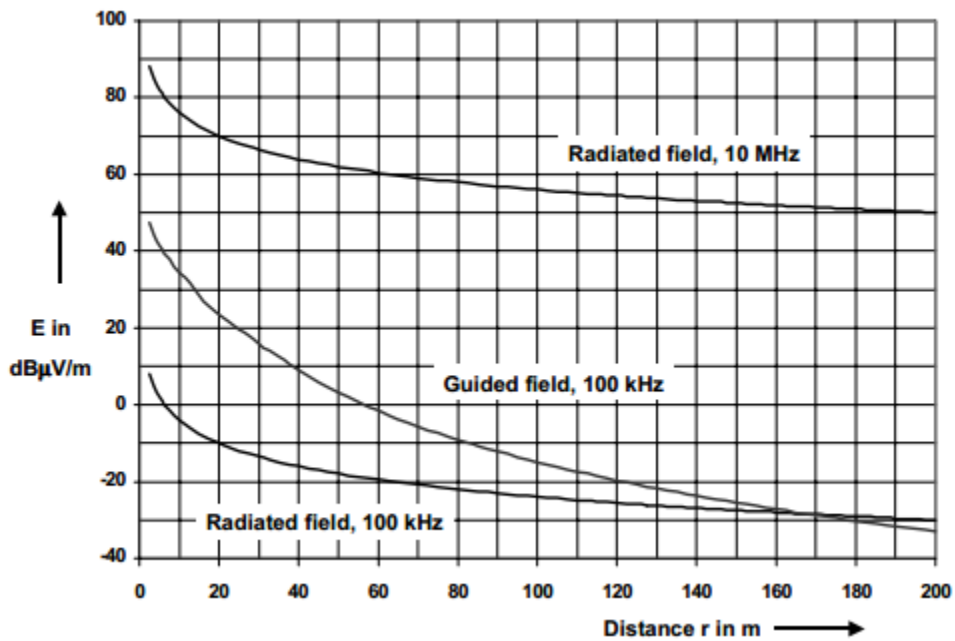


Figure 1.3: PLC system External fields at 100 kHz and 10 MHz [46]

Originally, the external electromagnetic (EM) fields of a PLC system are due to the even-mode current [44]. Figure 1.4 shows two types of external fields. The field of the guided wave and that of the radiated wave. At 100 kHz, the signal has a wavelength of 3 km which is large compared to the dimensions of the radiating structure. Therefore the radiated part of the field is very small and the guided field dominates in the immediate vicinity of the wires [46]. On the other hand, at 10 MHz, the signal has a wavelength of 3 m and the electrical wires of the indoor network become very effective radiators. Conveniently, PLC systems operating at high frequencies are more viable in terms of network conditioning since high frequencies require smaller (cheaper) reactive components [47]. One technique of network conditioning is to keep the signal “blind” off the branches whose path strays from that which is intended. Consequently, the signal preserves the energy enabling it to travel further. However, this technique when employed for low frequency signals requires expensive series inductors capable of carrying the load current [48]-[50].

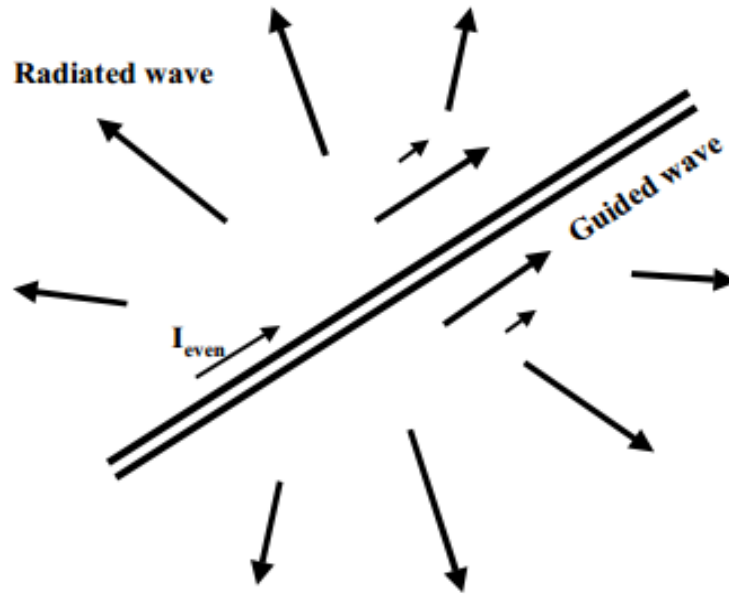


Figure 1.4: Even-mode current driven power line [46]

In high frequency PLC systems, ferrite cores clamped around the appropriate conductor could be used to improve its self-inductance thereby adequately blocking the signal in that branch. This improves the topology of the network and accordingly the undesired dissipation of the communication signal in the down-stream LV load fluctuations prevented to a certain degree [47]. Also noteworthy is the elimination of the high frequency noise signals brought about by the loads which terminates numerous branches. Thus, if there's adequate justification of cost towards performance improvement, this approach can be used to design a more conducive channel in terms of both noise and topology [47].

### 1.3.2 Power Line Communication Noise

Power line communication noise remains one of the prime impediments towards successful communication through this channel, barring the unpredictable time-variant nature of its transfer characteristics. As mentioned in section 1.3.1, numerous consumer loads connected to the electrical network not only presents fluctuating impedance to the transmitted signal, but also impairs the PLC channel through their switching behaviour. Again, the simpler topology found in the medium and high voltage electrical networks results in fewer noise sources while the low voltage network is heavily populated with noise generators. Typical noise sources in the MV and HV power line networks include lightning strikes and other atmospheric discharges, low-level corona discharges and circuit breaker transients [13]. Other noise peaks can be observed during switching of capacitor banks on MV lines employed for power factor correction.

Whilst the interconnecting transformers spoil the simplicity of the MV and HV networks, they do however help filter out some of the noise generated in these networks preventing it from reaching the LV network. Therefore, the noise observed in the LV networks is predominantly due to the switching and operation of intra-building appliances as well as that which originates external to the building from radiation interference. Disturbances that affect the mains waveform have an impact on PLC systems, though these disturbances remain the responsibility of the utility company. These disturbances are categorized as under-voltages, over-voltages, frequency fluctuations and harmonic distortions and occasionally outages [51]. Power line communication modems require power to operate, their operation will thus be terminated during an outage event unless on-board temporal power is provided. Uninterruptible power supplies (UPS) could be used to keep the local PLC systems in operation.

The noise superimposed onto the data signal, typically from the switching operation of the connected appliances, can be classified into four categories [52] namely i) noise synchronous to the mains signal, ii) periodic but asynchronous noise, iii) smooth spectrum noise and iv) single event impulsive noise. The discussion of these noise classes can be found in [3], [4] or [13]. This kind of classification is considered instrumental in developing noise mitigation strategies towards improving PLC systems. Periodic disturbances such as those classified under i) and ii) are considered predictable and hence their modelling and alleviation is less challenging than those unpredictable as classified under iv). Single-event (aperiodic) noise's stochastic study has proven to be the hindrance towards modelling noise characteristics of the PLC channel due to its time-variant nature. Nonetheless, researchers have attempted to describe and predict this randomly occurring fluctuations statistically [43], [53]-[58].

#### **1.4 PLC Regulations and Standardization**

In order to make certain that a power line communication system operates in a conducive environment and that it does not hamper the smooth operation of other communication technologies, there is need for standardization. There exists several standard bodies and groups with many established standards aimed at providing guidance and regulating the operational specifications of power line communications systems. There has been a progressive development of standards over time as discussed in section 1.2, nonetheless, it remains a work-in-progress. PLC systems exhibit both telecommunications (high frequency low power) and electrical (low frequency high power) properties, hence this has become the underlying motivation for the need for unprecedented regulatory bodies. To prevent interference to and from other communication systems, the power line channel, PLC products and services must adhere to and work under certain operational regulations such as electromagnetic compatibility (EMC), electric safety, and nets and communication services [59].

The emergence of any new technology is always accompanied by lack of standardization and absence of regulation thereof. As it was with the first telephone systems [60], early PLC systems were developed

without any particular standards in place simply because its large-scale economic implementation promise could not be foreseen. However, to this date, the economic appeal has grown a great deal and so did the need for regulation by governments for deployment and operation. The approval of the IEEE 1901 standard has facilitated the international standardization of the HomePlug AV standard as a baseline technology for the FFT-OFDM PHY within the standard.

The standardization process tends to be a lengthy prospect, usually emanating from the differences between the respective stakeholders. As with many other standards, the United States of America (USA) is content with having their own standards. They have arguably a large enough market to develop and sustain the technology within their confines. However, in Europe, multiple committees are established and together with regulatory bodies have to identify common grounds [13]. Some of the technical issues that require specifications are i) radiation emission limits and background noise (they both have an impact on the signal-to-ratio), ii) frequency bands, iii) measurement standards e.g. coupling as well as iv) maximum modem output power levels [61], [62]. For elementary and equitable regulations, frequency bands are separated to define PLC systems with those operating under 1 MHz (precisely < 525 kHz) referred to as low frequency or LF-PLC, while those operating above 1 MHz (precisely > 1.6 MHz) referred to as high frequency or HF-PLC [44]. A thorough discussion on various regulations and details of standards can be found in [62], including the allowable field strengths and corresponding distances at which they should be measured.

## **1.5 Research Objectives**

Power line communication has recently emerged as a viable technology for provision of numerous multimedia services for home and office such as internet access, local area networking, etc. utilizing the in-building electrical wiring. Power lines are the most ubiquitous wired networks with a huge potential to provide the in-demand high speed broadband communication services, eliminating the need for new infrastructure. However, their design and structure presents a hostile environment towards high speed data communications as they were only designed for low frequency signal transmission. Accordingly, they exhibit high attenuation, multipath fading as well as random time-varying impulsive noise.

In this work, the characteristics of power lines are investigated through a measurement campaign carried out within the University premises. The objectives of this study are as follows:

- Measure, study and characterize the behaviour of impulsive noise in practical power line networks.
- Measure, study and characterize the behaviour of background noise in practical power line networks.

- The statistical computations from data collected shall aid towards the development of realistic PLC noise models.
- Power line networks present a multipath propagation scenario during transmission, a result of which can be described as dispersive. This work also aspires to study the dispersive characteristics of the power line, which directly impacts on the choice of modulation techniques and coding schemes for PLC systems.
- Finally, to model the power line using a multipath based approach given the limited knowledge of the network topology, cable type and/or loading profile.

## **1.6 Thesis Organization**

This work is comprised of six chapters. The first chapter introduces the concept of power line communications, its history and evolution. The review of some of the key contributions in this field is presented in chapter two. This review entails efforts on PLC channel modelling, noise characterization and modelling. The next three chapters, chapter 3, 4, and 5, are focused on the contributions made by the author as reflected under publications. Their focus is on noise, channel dispersion, and channel modelling respectively. This dissertation is concluded by a summary of the three main chapters mentioned above.

## CHAPTER TWO

### LITERATURE REVIEW

#### 2.1 Introduction

The fundamental principle of power line communication (PLC) is utilizing the existing electrical power line networks for communications purposes. For a greater period of their existence, power line have fulfilled its duties as a medium for transmission and distribution of low frequency electrical signals. Primitive power line communication was restricted to low speed applications such as remote metering and operations management services that serve the needs of utility companies. This narrow scope of PLC functionality has improved a great deal recently, owing to the tremendous increase in demand for high speed broadband multimedia communication services.

This chapter aims to provide insight into some of the contributions in literature with regards to power line communication. The development of new PLC technology and systems requires extensive knowledge of the structure and properties of the power line network for its consideration as a viable channel. The historical development and current advances in the PLC technology are outlined. Channel and noise modelling approaches and developments are also outlined. This chapter serves as a knowledge basis that will be used in later sections of the dissertation to investigate existing techniques and develop approaches to serve the aim of enhancing the performance of PLC systems.

#### 2.2 Properties of Electrical Power Networks

Power line communication systems exploit the existing electrical grid infrastructure to transport communication signals aimed at delivering broadband data services to the consumer. The primary purpose of the electrical power network is, nonetheless, the transmission and distribution of AC power signal at 50 or 60 Hz (50 Hz in Africa and other parts of the world, 60 Hz in North America) from the power generating plants to the customers. Accordingly, electrical networks differ significantly in topology, structure and physical characteristics from conventional communication channels like twisted pair, Ethernet cables, coaxial cables, and optical fibres. The viability of the PLC channel for high speed data transfer requires a comprehensive understanding of the channel's structure and its underlying properties.

Electrical networks are classified based on their voltage levels into three classes [63]: the high-voltage (HV) level (110 – 330 kV), the medium-voltage (MV) level (10 – 30 kV) and the low-voltage (LV) level (0.4 kV). These three segments of the electrical network are interconnected by transformers. The transformer present a data transmission blockage at high frequencies as it will only allow low frequency electrical signals to pass. Figure. 2.1 shows a typical structure of an electric power system.

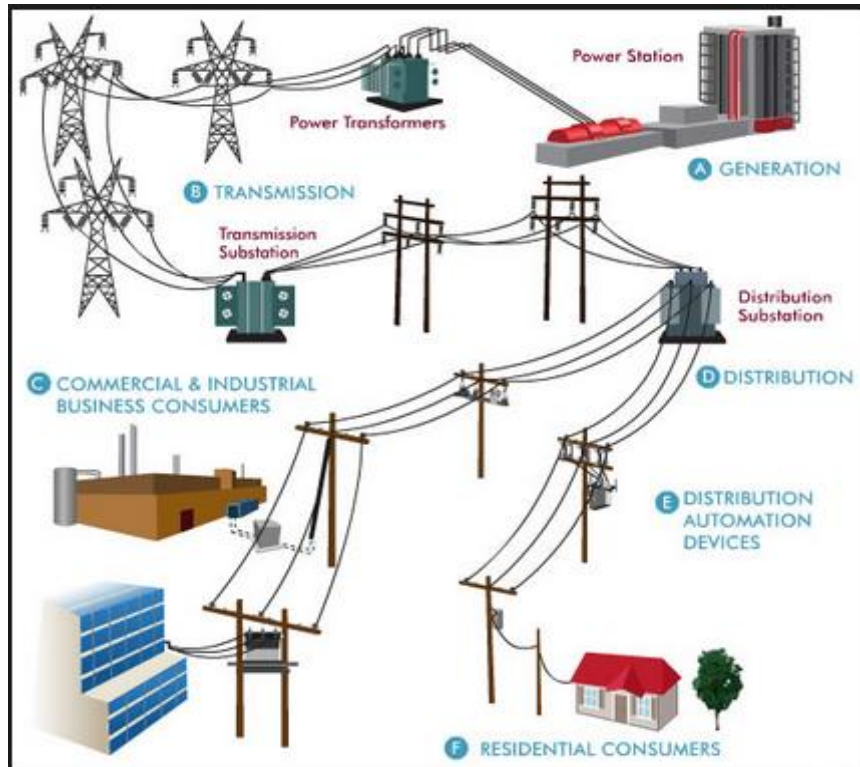


Figure 2.1: typical electrical power system  
 [http://venturebeat.files.wordpress.com/2010/10/grid.jpg]

### 2.2.1 High Voltage Networks

High voltage power lines are used for the transmission of electrical power generated at the power plant to multiple substations, traversing long geographical distances of up to several hundred kilometres. High voltage power networks form the electric power backbone for the utility company. HV power transmission is usually carried out through overhead three phase conductors. This level of voltage is preferred for transportation over long distances essentially to reduce the energy losses. The main losses present in high voltage lines are the heat loss caused by the resistance of the power line material and leakage losses [63]. A convenient selection of the wire material and appropriate dimensioning of electrical cables can restrict heat losses to acceptable levels. Corona losses are likely to occur due to the discharge activities in the vicinity of the conductors caused by high electric field strengths at high voltages. Thinner conductors are more prone to these discharge effects when employed to transport high voltage signals. Moreover, corona discharge can produce concentrated high frequency impulses which may cause interference with radio broadcasting utilizing the low and medium frequency bands.

Communication over high voltage lines at high frequencies is also subject to interference, reducing system reliability. Two dominant types of high frequency interference are specified in high-voltage overhead lines [63]: the first is the periodic short-duration impulsive interference generated by switching events and atmospheric discharges. It tends to have a broadband spectra in the frequency

domain. Since the conductors are carrying high voltages, the resulting impulses are characterized by very high magnitudes which may lead to dangerous peaks arriving at the receiver. The second type of interference prevalent in HV lines is a persistent broadband interference having a fairly high power spectral density (PSD). This interference is brought about by discharge activities and can be modelled as white Gaussian noise (WGN) with its PSD strongly dependent on weather conditions increasing drastically in the presence of rain, frost and fog. Due to severe interference and attenuation at high voltages, HV power lines are not suitable for data transmission [64]. Alternatively, fibre optic cables are generally installed along high voltage routes for control and monitoring purposes as well as for data transmission exploiting their high capacity.

### **2.2.2 Medium Voltage Networks**

Medium voltage networks are typically employed to supply electricity to rural areas, small towns and independent industrial companies. Generally, MV electrical power lines carry voltage levels ranging between 10 kV and 30 kV and have typical lengths of about 5 – 25 km [63]. Overhead lines and underground cables are both used in the medium voltage range for the transmission and distribution of electrical power. However, in densely-populated urban areas, underground cables are normally preferred. Unlike overhead high voltage lines, medium voltage overhead lines tends to require relatively smaller poles and smaller wire cross-sections because of the smaller voltage they carry. With regards to the physical structure, MV lines are mainly made of copper and aluminium with various cross-section shapes including round, sector-shaped and oval [63]. The preferred insulation for medium voltage power line networks is usually Polyvinyl chloride (PVC) or vulcanized polyethylene (VPE). Regarding data transmission, medium voltage lines form the back bone of the electric utility data communications over power lines [64].

### **2.2.3 Low Voltage Networks**

The low voltage network is the last portion of the electrical network supplying electrical power to the consumers at 100 – 400 volts. In Europe underground cables are mainly used in this voltage level [63], [65]. However, in South Africa, low voltage overhead lines are still visible in urban areas. In terms of the physical structure, low voltage lines are similar to medium voltage lines and are composed of copper or aluminium with PVC or VPE insulation. The length of LV electrical power lines normally extends up to 500 m from the MV/LV transformer station to the consumer's premises. Power line communication technologies utilize the low voltage electrical wiring to deliver communications services to the home or office. Furthermore, in-building networking solutions can be established through the power line network.



## 2.3 Characteristics of Power Lines

Power lines form the medium of transmission in PLC systems. Since the primary purpose of these lines is the transmission of electric signals at 50 or 60 Hz, their design did not take into consideration the possibility for data transport at higher frequencies. This section serves to provide an overview of the technical characteristics of electrical wiring pertaining to their usability and/or suitability for data transmission.

### 2.3.1 Capacitance and Inductance

The power line network distributes electrical power to various devices connected to the network. The devices connected to the power network are characterized by a certain inductance ( $L$ ) and capacitance ( $C$ ) each of which depends on the amount of current flowing through the device's circuit. The inductance of an electrical circuit defines the amount of magnetic flux caused by the current running through the circuit. Depending on the value of inductance (amount of flux), it can be limited within the circuit or may interfere with other circuits if it's large enough. If an electric current ( $I$ ) induces a magnetic flux ( $\emptyset$ ), the inductance ( $L$ ) can be defined [66] by:

$$L = \frac{\emptyset}{I} \quad (2.1)$$

If the circuit is driven by an alternating current (AC) with voltage ( $V$ ), at a frequency ( $f$ ), the following expression can be used:

$$L = \frac{V}{j2\pi fI} \quad (2.2)$$

The capacitance of an electric circuit represents a measure of the amount of electrical energy stored for a given potential created between two adjacent conductive surfaces with opposite charges [66]. The capacitance is defined in terms of the electric charge ( $Q$ ) and the voltage ( $V$ ) between the two surfaces according to the following:

$$C = \frac{Q}{V} \quad (2.3)$$

For the AC voltage supplied by the power line network, the capacitance ( $C$ ) can be defined by the following:

$$C = \frac{I}{j2\pi fV} \quad (2.4)$$

### 2.3.2 Impedance

The overall opposition to the flow of current in alternating current (AC) circuits is measured by impedance. The impedance ( $Z$ ) of a cable is made of resistive, capacitive and inductive components and can be expressed in a complex form by [66]:

$$Z = R + jL2\pi f + \frac{1}{jC2\pi f} \quad (2.5)$$

For circuits only operated by a direct current (DC), the impedance will be equivalent to a pure resistance. Normal operation in electrical networks entails continuous connection to or disconnection from of appliances in the power network. Accordingly, the input impedance seen by a PLC device connected to the network in the vicinity of such loads may be variable and unpredictable. This inconsistency makes it difficult to model the power line channel to determine its suitability for simultaneous transmission of communication signals. Poor or lack of matching of the loads in the electrical network to the cable's characteristic impedance leads to reflections from the loads back along the cable towards the source. The severity of the reflections depends on the output impedances of the loads, with significant reflections able to deter the communication signal from reaching the receiver with sufficient energy. This channel variation caused by plugging and/or unplugging of electrical appliances makes for a difficult prospect in modelling PLC channels. Section 2.5 presents some of the attempts in literature towards modelling of power line channels.

### 2.4 PLC Noise

One of the significant features of electrical networks, particularly in the “last mile” area and in-building wiring, is the susceptibility to a variety of signals. Understanding of the different interference sources in the electrical power network is key to establishing reliable high speed PLC data systems. Generally, the electrical devices connected to the network or its proximity are the main sources of interference. This is, however, not always a result of any kind of malfunction in the power network as some of the electrical machinery and devices can cause interference even during their normal operation. In addition, switching electrical appliances (on and off) causes impulsive current and voltage peaks propagating along the electrical wiring. Typical noise-generating electrical devices include light dimmers, fluorescent and halogen lamps, universal motors and so forth [67], [68]. Another kind of impairment affecting broadband power line communications (BPL) is with regards to electromagnetic interference (EMI) and electromagnetic compatibility (EMC) of power lines. The unshielded electrical wiring is susceptible to radiation effects from radio services operating in the same radio frequency (RF) band. Broadband power line devices typically operate in the frequency range 2 – 30 MHz. Radio services operating within this frequency range such as amateur radio have been using parts of the medium frequency (MF) and high frequency (HF) bands for decades.

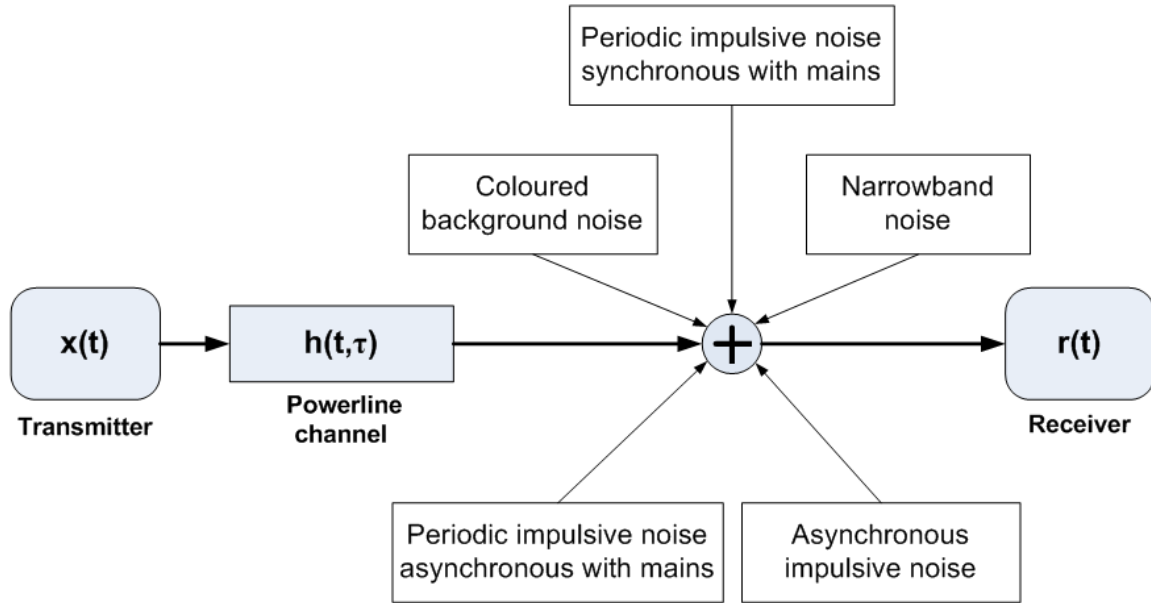


Figure 2.2: PLC communication system [69]

Accordingly, contrary to conventional communication channels, power line communication noise cannot be described by the classical approach of additive white Gaussian noise (AWGN). The noise present in power lines is often categorized into classes. As reported in [63], noise at a wall power outlet is summarized into three main categories: coloured background noise, narrowband interference and impulsive noise. According to [70], there are five types of noise: coloured background noise, narrowband noise, periodic impulsive noise synchronous to the mains frequency and asynchronous impulsive noise. Figure 2.2 depicts a PLC link under a noisy scenario encountered during data transmission. The transmitted signal  $x(t)$  passes through a PLC channel represented by its channel transfer function  $H(f)$ . Various types of noise are added to  $x(t)$  before its arrival at the receiver. The different types of noise scenarios that are depicted in Fig. 2.2 are described with more details as follows:

- *Coloured background noise*: this type of noise is usually assumed to be the aggregate result of various sources of white noise characterized by different noise amplitudes at different portions of the frequency band [71]. Coloured background noise is typically characterized by a fairly low power spectral density (PSD). This PSD tends to decrease with an increase in frequency. Its highest value is in the frequency band closest to the power signal frequency (50 Hz or 60 Hz) up to about 20 kHz [63].
- *Narrowband Noise*: this type of noise occurs at narrow portions of the frequency band with a relatively high PSD. Narrowband interference appears in the form of sharp peaks of noise amplitudes in the frequency domain. It is generally caused by the radio stations broadcasting their signals in the frequencies typically within the 1 – 22 MHz range. Nonetheless, narrowband

interference may occur at lower frequency bands. Its occurrence at such low frequencies is due to the switching of electrical appliances such as television sets, power supplies, fluorescent lamps or computer screens [63].

- *Periodic Impulsive Noise Synchronous to the Mains Frequency*: the main cause of periodic impulsive noise is the switching of rectifiers in DC power supplies [71] and phase control in electric devices such as light dimmers, which takes effect synchronously with the power signal frequency. Cyclic voltage peaks of impulsive nature are generated at every zero-crossing of the mains signal leading to repetition rates of the multiples of the mains frequency (i.e. 50 or 100 Hz for 50 Hz power grids). These type of impulses are generally characterized by short durations and a PSD that decreases with frequency.
- *Periodic Impulsive Noise Asynchronous to the Mains Frequency*: this periodic interference occurs with repetition rates in the range of 50 – 200 kHz. Impulses of this type are generated as a result of switching of power supplies.
- *Asynchronous Impulsive Noise*: the main cause of asynchronous impulsive noise is switching transients that occur in various parts of the electric network. Measurements in [70] show that typical impulses of this type have durations ranging from some microseconds to a few milliseconds. The threat posed by this random noise occurring in bursts on high speed PLC data communication is quite significant. Effectively, the need for robust modulation techniques and powerful channel coding schemes is highlighted.

The first three noise types described above generally remain stationary over long periods of time (i.e. seconds, minutes or hours) and can be summarized as background noise [63], [70], [72]. The last two types have a random time-varying nature and can be described as impulsive noise. A review of the different approaches to modelling impulsive noise will be given in section 2.6.

## **2.5 PLC Channel Modelling**

The emergence of new communication systems demands an extensive knowledge and understanding of the characteristics of the transmission medium for effective communication. The choice of the transmission technique and other design parameters is based on the channel transfer properties and the capacity offered by the channel. Therefore, suitable models that can describe the transmission behaviour over the channel with sufficient precision are required. As mentioned before, the electrical power line channel is not designed for high speed data transmission, hence modelling this channel is a very difficult task and forms one of the major technical challenges [65], [71], [73], [74]. In addition to the impulsive noise dilemma that was discussed in the previous section, electrical networks exhibit strong branching topologies due to their intricate distribution structures, which gives rise to significant degradation of transmission quality. Signal propagation along power lines does not only take a single path from the transmitter to the receiver. Multiple paths are possible due the numerous routes created by the numerous

branches. Furthermore, reflections from the loads connected at the branch end points lead to the reception of multiple delayed copies (echoes) of the transmitted signal. Several attempts to model the power line as a communication channel can be found in the literature, for example [75]-[78]. However, existing models for the transfer function of power line channels are based on two fundamental approaches: time domain and frequency domain [65]. Time domain models are typically based on averaged measurement trials of obtained results. On the other hand, frequency domain models, are based on a deterministic approach. These two approaches are briefly reviewed in the following two sub-sections.

### 2.5.1 Time Domain Approach: The Multipath Model

The topology and structure of power line networks differs from those of conventional telecommunication networks. In PLC networks, the link between a substation and the customer's premises is not presented by a point-to-point connection as in the case of communication networks such as telephone local loops. As shown previously in Figure. 2.1, the link from a transformer substation consists of a distribution link forming a bus topology and house connections with variable lengths representing branches from the distributor cable. The house connection is terminated at a house connection box, which is then succeeded by numerous branches in the in-building wiring. Due to the heavy presence of branching and impedance mismatches in the power line network, multiple reflections occur giving rise to a multipath propagation scenario with frequency selectivity. Furthermore, this frequency selectivity causes frequency-dependent attenuation and thus should be considered in the PLC modelling process. Generally, signal attenuation in power lines is the result of coupling losses which depends on the PLC transmitter design and line losses depending on the length of the cable [73]. In addition to the frequency-dependent attenuation, the channel transfer characteristic is also time-varying and depends on the location of the receiver since different appliances are constantly been plugged in and out of the network causing changes in the transfer function. Models of the power line channel transfer function that describe the multipath propagation effects have been proposed by Phillips [76] and Zimmermann and Dostert [75], [79]. According to [75], the channel transfer function  $H(f)$  that describe the signal propagation in PLC channels in the frequency range from 500 kHz to 20 MHz is given by the following:

$$H(f) = \sum_{i=1}^{N_p} c_i \cdot e^{-(a_0 + a_1 f^k) \cdot d_i} \cdot e^{-j2\pi f \tau_i} \quad (2.6)$$

where  $N_p$  is the number of meaningful propagation paths,  $c_i$  and  $d_i$  are the weighting factor and length of the  $i$ th path respectively. In this model the multipath scenario is represented by a superposition of

signals arriving from  $N_p$  different paths. Frequency-dependent attenuation is described by the parameters  $a_0, a_1$  and the exponent  $k$ . In this model, the first exponential represents the attenuation factor, whereas the second exponential describes the echo scenario where  $\tau_i$  is the path delay and is given by the following:

$$\tau_i = \frac{d_i \sqrt{\epsilon_r}}{c_0} = \frac{d_i}{v_p} \quad (2.7)$$

where  $\epsilon_r$  is the dielectric constant of the insulating material,  $c_0$  is the speed of light and  $v_p$  is the propagation velocity. To demonstrate the multipath signal propagation in power lines, a simple example extracted from [75] is illustrated in Figure. 2.3. This simple topology, commonly known as the T-network, consists of a power line with a single branch represented by the line segment from point B to point D in the figure. The three segments of the link (i.e. (1), (2) and (3)) are assumed to have different lengths and different characteristic impedances. Consider that points A and C (transmitter and receiver respectively) are matched to their line characteristic impedances, then it follows that only points B and D can cause reflections in the link. These reflections occurring at points B and D will lead to an infinite number of propagation paths from point A to point C (e.g. A-B-C or A-B-D-B-D-...C). The transmission and reflection factors in each branch determines the weighting factor each propagation path will have, which is denoted by  $g_i$  in the transfer function given in equation (2.6).

Generally, the parameters of the model in equation (2.6) can be obtained from measurements of the PLC channel complex transfer characteristics.

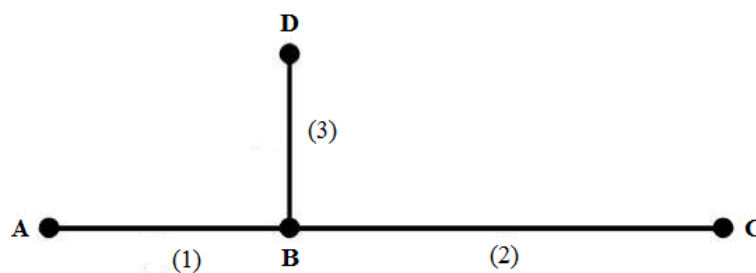


Figure 2.3: Single branch PLC channel

The magnitude of the channel frequency response can be used to determine the values of the attenuation parameters (i.e.  $a_0, a_1$  and  $k$ ). The path parameters ( $g_i, d_i$  and  $\tau_i$ ) can be obtained from the impulse response of the channel. The number of paths is typically in the range 5 – 50 paths [71].

## 2.5.2 Frequency Domain Approach: Transmission Line Theory Models

The power line channel can be modelled using deterministic approaches provided a detailed knowledge of the communication link between the transmitter and the receiver is available. Thus, knowledge of the network topology, physical properties of the cable, and load impedances should be available. Two models based on a two-conductor and a multi-conductor transmission line (MTL) theory are briefly reviewed.

### *Two-Conductor Transmission Line Models*

Various researchers have utilized the two-conductor transmission line theory to model the power line channel as can be found in [77] and [78]. Typically, these models use either scattering or transmission matrix approach [65]. A two-conductor transmission line, with ground being the second conductor supports four modes of signal propagation. The signal travels along the line in two spatial modes each having two directions of propagation [65]. The two spatial modes are the differential and common mode. The dominant mode that carries the data signal in the desired direction along the transmission line is the differential mode. Differential signalling can be used to excite the propagation in the differential mode only, and reduce the propagation in the common mode which is normally induced by external noise. To achieve good rejection of unwanted external signals, the two conductors must be well balanced as any imbalance between them promotes common mode propagation. The two-conductor model does not address the effects of wiring and grounding practices in the transmission behaviour. In addition, the model neglected the effect of electromagnetic compatibility issues in the estimation of the common mode currents. Additionally, the two-conductor model does not explain the propagation in the presence of a third conductor present in single-phase power lines leading to a MTL situation. Consequently, the attempts to model the power line channel based on a two-conductor transmission line approach did not fully explain the propagation behaviour along power lines [65].

### *Multi-Conductor Transmission Line Models*

Electrical Power cables used in single-phase connections normally consist of three or four conductors, which limits the applicability of the two-conductor transmission line model in explaining the propagation behaviour. Therefore, the modelling of the power line channel in the presence of a third or fourth conductor should rather consider multiple-conductor transmission line theory. In MTL, a transmission line consisting of  $N$  conductors and ground is partitioned into  $N$  simple TL's, each representing a single propagation mode [79]. Accordingly, the signal at the input of an MTL is broken into  $N$  modal components, each of which traverses the corresponding modal TL. Recombination of the modal components of the signal takes place at the output ports. The coupling between each port and each modal TL is obtained using the weighting factors in the voltage and current transformation matrices. If a three-conductor power cable is used, then six propagation modes exist in the line resulting from three spatial modes (i.e. differential, pair and common). Each of the three spatial modes has two

directions of propagation. The desired signal current generally travels in the differential mode. The signal in the pair-mode corresponds to the current flowing from the ground wire and the other two wires, whereas the signal in the common mode of operation corresponds to the overall imbalance between the modes and is directly related to the cable installation practices [74]. In indoor PLC systems, there is usually an imbalance between the propagation modes which results in coupling between the propagation modes [74]. Frequency-domain channel models based on TL theory offer the advantage of low computational complexity that is almost independent of the power line link topology [65]. Nevertheless, a comprehensive knowledge of the transmission link must be available *a priori*. The model requires details about the topology, properties of the cables used and impedance values at the end of every branch involved. The validity of the model can easily be nullified if an appreciable amount of knowledge of such parameters is not available. In a practical scenario, such knowledge of the power line network is nearly impossible, which makes modelling the power line using the frequency-domain models based on TL theory unrealistic. The time-domain approach described in section 2.5.1, however does not require such details about the network. For this reason, the time-domain multipath model is preferred over frequency-domain models and it is thus utilized in this dissertation to simulate typical channel scenarios in PLC networks. Its applicability is validated through measurements.

## 2.6 Impulsive Noise Modelling

High-speed communications over power lines is confronted with a significant challenge in terms of asynchronous impulsive noise. Practical measurements show that this type of noise can have large energy leading to a significant degradation in the performance of PLC systems [71], [81]. Its ability to frequently sweep complete data symbols is a cause for concern in the research community as well as designers of PLC devices and systems. In [82], it is reported through practical measurements in power lines that the typical strength of a single impulse is more than 10 dB above the background noise level and can exceed 40 dB. Measurements in [70] indicate that the PSD of impulsive noise generally exceed the PSD of background noise by a minimum of 10 – 15 dB in most parts of the 0.2 – 20 MHz band. Furthermore, this difference may even rise to more than 50 dB at certain parts of the band. Figure 2.4 shows a sample impulse having a duration of approximately 50  $\mu$ s. In the time-domain, three random variables characterize the impulsive noise that occurs in power lines and other communication mediums. These are: impulse width, amplitude and inter-arrival time (IAT). Several attempts to derive the probability distribution statistics of these three parameters based on practical measurements in power line networks can be found in [82] and [83]. The impulse width and amplitude both represents the energy carried by a single impulse. The frequency of the impulses (the reciprocal of IAT) along with the impulse energy describe the power of the impulsive noise. Numerous statistical approaches have been put forward in literature in an attempt to model impulsive noise as described in the following sub-sections. Background noise on the other hand is usually modelled as white Gaussian noise (WGN) [82].



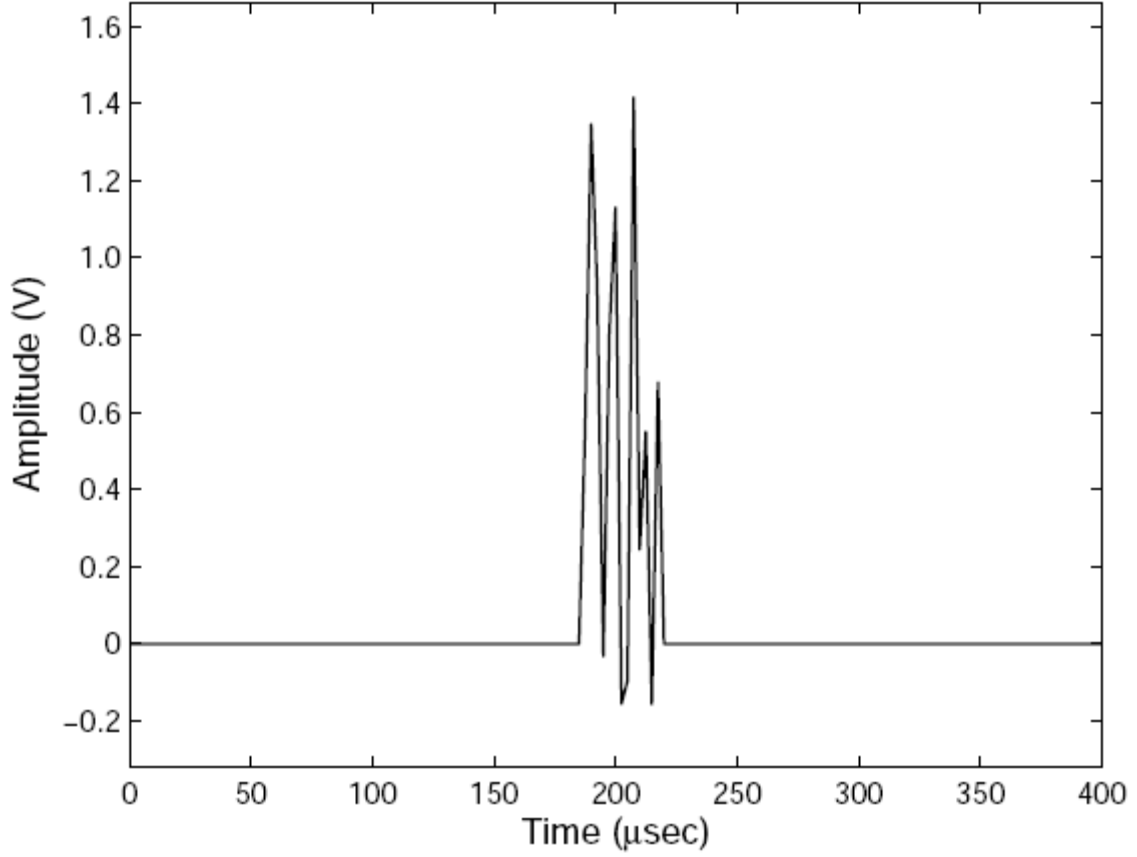


Figure 2.4: Sample Impulsive noise [82]

### 2.6.1 Middleton Class A Noise Model

Middleton in [84]-[86] classifies the electromagnetic (EM) noise or interference into three main classes: Class A, Class B and Class C (the sum of Class A and Class B). Various researchers concede that the Middleton Class A noise model satisfactorily describes the statistical characteristics of the impulsive noise in PLC environments as in [81], [87]-[89] as well as in other communication environments [90]. This model integrates both background and impulsive noises. Following the Middleton Class A model, the overall noise is a sequence of independent and identically distributed (i.i.d.) complex random variables with the probability density function (PDF):

$$p(z) = \sum_{m=0}^{\infty} e^{-A} \frac{A^m}{m!} \frac{1}{2\pi\sigma_m^2} \exp\left(-\frac{z^2}{2\sigma_m^2}\right) \quad (2.8)$$

where the variance  $\sigma_m^2$  is defined as:

$$\sigma_m^2 = (\sigma_g^2 + \sigma_i^2) \frac{\left(\frac{m}{A}\right) + \Gamma}{1 + \Gamma} \quad (2.9)$$

where the parameter  $A$  is called the impulsive index and is determined as the product of the average rate of impulses per unit time and average impulse duration. The variances  $\sigma_g^2$  and  $\sigma_i^2$  denote the power of background noise and impulsive noise respectively. The ratio between background noise and impulsive noise is given by the parameter  $\Gamma$ . Therefore:

$$\Gamma = \frac{\sigma_g^2}{\sigma_i^2} \quad (2.10)$$

It can be deduced from (2.8) that the PDF of the Middleton Class A noise is actually a weighted sum of Gaussian PDFs with mean equal to zero. Accordingly, the mean and variance of this process can be obtained by the following [81]:

$$\mu_z = E\{z\} = \int z \cdot p(z) \cdot dz = \sum_{m=0}^{\infty} e^{-A} \frac{A^m}{m!} \frac{1}{2\pi\sigma_m^2} \int z \cdot \exp\left(-\frac{z^2}{2\sigma_m^2}\right) = 0 \quad (2.11)$$

$$\sigma_m^2 = E\{z^2\} = \sum_{m=0}^{\infty} e^{-A} \frac{A^m}{m!} \frac{1}{2\pi\sigma_m^2} \int z^2 \cdot \exp\left(-\frac{z^2}{2\sigma_m^2}\right) = \frac{e^{-A}\sigma_g}{\Gamma} \sum_{m=0}^{\infty} \frac{A^m}{m!} \left(\frac{m}{A} + \Gamma\right) \quad (2.12)$$

The Middleton Class A model was originally developed to describe the man-made EM interference with impulsive behaviour. Despite the fact that this model has been considered by many researchers to describe impulsive noise, its applicability to model impulsive noise in power line networks remains inconclusive.

## 2.6.2 Bernoulli-Gaussian Model

Owing to its simplicity, the Bernoulli-Gaussian model is frequently used to model impulsive noise in power line networks and other communication channels [91]-[95]. In a Bernoulli-Gaussian model of impulsive noise, the occurrence of impulsive noise is modelled according to the Bernoulli process  $b(m)$ , whereas the amplitude of the impulses is modelled according to the Gaussian distribution  $n(m)$  [96]. A Bernoulli process is an i.i.d. sequence of ones and zeros with a probability that the process takes a value of '1' ( $p(b(m) = 1) = \alpha$ ); therefore, the process takes a value of '0' with a probability of  $1 - \alpha$ . The probability mass function (pmf) of a Bernoulli process is defined by:

$$P_b[b(m)] = \begin{cases} \alpha & \text{for } b(m) = 1 \\ 1 - \alpha & \text{for } b(m) = 0 \end{cases} \quad (2.13)$$

The mean and variance of the Bernoulli process are given by:

$$\mu_b = E[b(m)] = \alpha \quad (2.14)$$

$$\sigma_b^2 = E\{[b(m) - \mu_b]^2\} = \alpha(1 - \alpha) \quad (2.15)$$

The amplitudes of impulses are obtained from a Gaussian distribution with zero mean and variance  $\sigma_n^2$ , which has the following probability density function (pdf):

$$G[n(m)] = \frac{1}{\sigma_n \sqrt{2\pi}} \exp\left(-\frac{n^2(m)}{2\sigma_n^2}\right) \quad (2.16)$$

### 2.6.3 Poisson-Gaussian Model

A simple and efficient way that is often used to model impulse noise is the Poisson-Gaussian model [89], [91], [92]. In [92], it has been determined through measurements that in residential power line networks, the arrival of impulsive noise resembles a Poisson distribution. In the Poisson-Gaussian model, the impulse arrival time is modelled according to the Poisson process and the impulsive noise amplitudes are modelled as a Gaussian process of zero mean and variance  $\sigma_n^2$ . Thus, the impulsive noise will occur according to a Poisson distribution with a rate  $\lambda$  units per second, so that the probability of an event of  $m$  arrivals in unit time is:

$$P_p(m) = P_p(M = m) = e^{-\lambda} \frac{\lambda^m}{m!}, \quad m = 0, 1, 2, \dots \quad (2.17)$$

However, the amplitude of impulsive noise is modelled as a Gaussian process with a mean of zero and variance  $\sigma_n^2$  as described in the previous section. To model the total noise that occurs in PLC transmission in the discrete time domain, the background noise  $w_k$  is usually assumed to be an AWGN [77], [91]. The impulsive noise  $i_k$  can be defined using the Poisson-Gaussian model as:

$$i_k = b_k g_k \quad (2.18)$$

where  $b_k$  denotes the arrival of impulses according to the Poisson process and  $g_k$  is a white Gaussian process characterizing the impulse amplitudes. This model can be physically thought of as each transmitted symbol being independently struck by an impulse with a probability of  $b_k$  having a random Gaussian amplitude of  $g_k$  [90]. If the signal  $a_k$  is transmitted over power lines impaired by impulsive noise, the received signal can be represented by:

$$r_k = a_k + w_k + i_k \quad (2.19)$$

The probability density function of the total noise  $n_k$  is given by [90]:

$$p(n_{kR}, n_{kI}) = (1 - \alpha)G(n_{kR}, 0, \sigma_w^2) + \alpha G(n_{kR}, 0, \sigma_w^2 + \sigma_i^2)G(n_{kI}, 0, \sigma_w^2 + \sigma_i^2) \quad (2.20)$$

where  $\alpha$  is the probability of occurrence of impulsive noise and  $G(x, \mu, \sigma^2)$  is the Gaussian pdf with mean  $\mu$  and variance  $\sigma^2$  and as defined in equation (2.16).

Based on the measurements carried out in actual indoor power line channels, the noise characteristics were investigated. The summary of our findings with regards to the parameters of the impulsive noise statistics shows consistency with findings elsewhere in terms of its amplitude, duration and interval time in time domain. The parametric model used to capture background noise of PLC channels in the frequency domain in terms of its spectral density shows a good improvement on the results. We have used the same three-parameter model popular in literature but we have modified the measurement algorithm to eliminate the influence of narrowband interference from other radio services operating within the same band.

The time-domain multipath approach discussed in section 2.5.1 is employed in chapter 5 of this dissertation and it has proved to describe the PLC channel adequately. However, to further enhance the usability of this model, we have introduced another approach which considers the time variability of the channel. Its performance is evaluated by considering the statistical variation of its parameters, which allows us to capture an ensemble of different power line topologies. The model parameters are considered to be random variables.

## CHAPTER THREE

### BROADBAND ANALYSIS AND CHARACTERIZATION OF NOISE FOR IN-DOOR POWER-LINE COMMUNICATION CHANNELS

#### 2.1 Introduction

Power line communication (PLC) has emerged as an alternative solution for connectivity at home and offices in recent times [69]. The universal existence of power-line networks in buildings and residential areas present a convenient and inexpensive communication media. However, developing PLC systems turns out to be a massive challenge for the communication engineer having to deal with such a harsh channel [97]. The difference between power line networks and other conventional media such as twisted pair and coaxial cable is significant in terms of topology, structure and physical properties. The transfer characteristics of PLC channels are time-varying and frequency dependent with deep fades as high as 60 dB [98]. Additionally, PLC noise cannot be described as additive white Gaussian noise (AWGN) as is the case for conventional communication Channels. With high data rates (~1Gbps) in demand nowadays, the PLC band is expanded [99]. These goals can be achieved by improving the resource allocation efficiency [100], with regards to the transfer function [101], [102] and the stochastic noise detail [103]. Thus, obtaining realistic power line channel noise models remain a key goal for the PLC community worldwide. Practical modems' performance fluctuates widely and these variations are a consequence of the presence of different appliances connected to the network [104], electromagnetic interference (EMI) [105], power supplies and switching loads [106]. Its development for multimedia broadband applications thus requires an extensive knowledge of the major peculiarities which influences communication over this channel. PLC channels are susceptible to noise inherent in power networks, leading to performance degradation. In this work, we have set up a measurement system designed to capture the noise both in frequency and time domain for practical power networks. The main observable components of the indoor PLC noise are: background noise, impulsive noise, and narrowband interferences. The impulsive components of PLC noise are observed to be time variant, random in nature, have high power spectral density (PSD) and lasts for very small time durations. A greater portion of the impulsive noise has cyclostationary behaviour, though with different amplitudes and widths. The repetition rates of these impulses are synchronous with the mains harmonics of 50 Hz and 100 Hz, the supply frequency in South Africa. Others have irregular occurrences and much higher repetition rates; hence they are unpredictable in nature. This noise is referred to as asynchronous impulsive noise [107].

These noise terms are key design parameters for modulation schemes in broadband PLC, popularly orthogonal frequency division multiplexing (OFDM), with its conventional receivers assuming additive white Gaussian noise (AWGN) [108]. The time variability of PLC noise is presented

alongside its statistical analysis based on a series of measurements performed on numerous power line scenarios. The relevance of this time variance is evaluated in actual channels. The significant difference in amplitudes of the impulsive noise is observed and characterized statistically. The power spectral density for both the worst case and best case background noise scenarios is presented. Finally, we present the results of the noise PSD captured with a parametric model and compare our results with findings from other parts of the world.

Noise in PLC systems remains one of the major peculiarities that influence communication performance over this channel. This is particularly the case in the “last mile” and in-building parts of the electrical network. Its contribution to the hostility of the channel alongside multipath, selective fading and attenuation justifies its consideration when designing PLC systems. To successfully employ power lines for reliable high-speed data transmission, it is necessary to study and understand the numerous noise scenarios that exist in the PLC network. Noise generated by internal and external devices connected either to or in close proximity to the power line transmission network persistently cause impairment in PLC systems. Inherently, the normal operation of electrical machinery and appliances causes interference. The noise at any power outlet is the sum of all the noises produced by different appliances connected to the line plus background noise. Typical noise-generating electrical appliances include halogen and fluorescent lamps, light dimmers, universal motors and so forth [67], [68]. PLC noise varies with time largely in response to the varying loading profile of the network as consumers plug appliances in and out of the network at random.

Broadband power line communication (BPL) is also affected by electromagnetic interference (EMI) and electromagnetic compatibility (EMC) of power networks. Electrical wiring is susceptible to irradiation from other radio services operating in the same radio frequency (RF) band. Broadband PLC networks operate in the 1-30 MHz band and portions of this band are also employed by AM, FM, as well as amateur radio. These services have been using the medium frequency (MF) and high frequency (HF) bands for decades.

It is clearly not the responsibility of the cable makers to provide shielding against possible interference as PVC provides enough insulation for the intended purpose. The challenge therefore remains for PLC engineers and researchers to find alternative ways of mitigating the effects of narrowband interference.

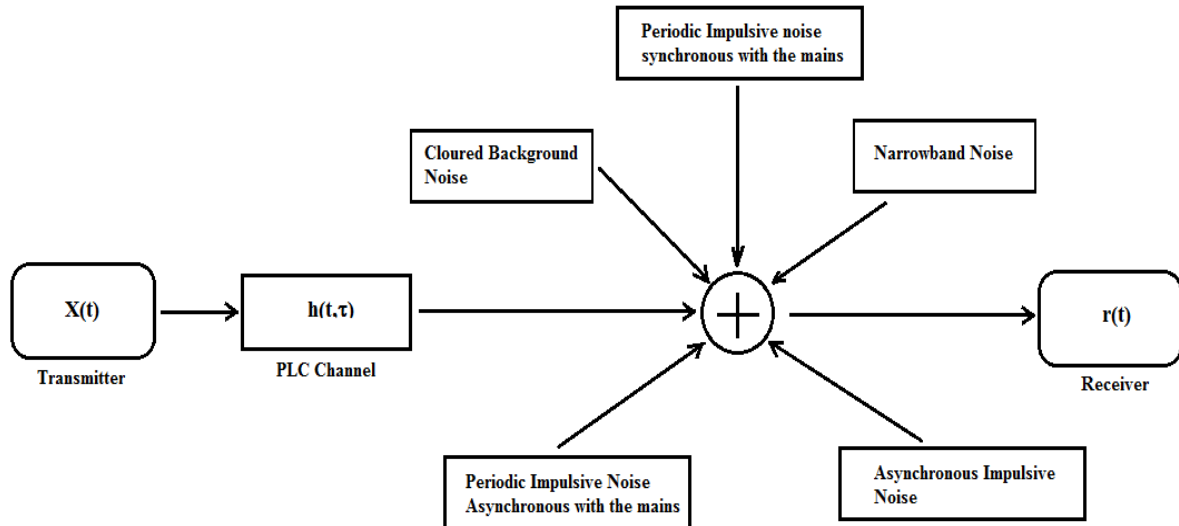


Figure 3.1: Noise in PLC systems

The noise scenario during PLC transmission as depicted in figure (3.1) is indicative that, as opposed to other traditional communication channels, PLC noise cannot be described by the additive white Gaussian noise (AWGN) model. This model assumes that the noise power spectral density (PSD) is constant and has a Gaussian distribution of amplitude across the communication band. Often times in PLC systems, noise is classed into different categories. In [63] after noise measurements at a wall outlet, three main categories were used to summarize the noise: coloured background noise, narrow-band interference, and impulsive noise. However, according to [70], five categories have been derived: coloured background noise, narrowband noise, periodic impulsive noise synchronous with the mains frequency, periodic impulsive noise asynchronous with the mains frequency, and asynchronous impulsive noise. The transmitted signal propagates through the PLC channel of a certain transfer function,  $H(f)$ . On arrival at the receiver, the transmitted signal contains all the noise components added to it as it traverses the channel. A detailed explanation of the different noise impairments under their respective classes is as follows:

### 3.1.1 Background Noise

- a) Colored Noise: This noise is the total sum of numerous sources of white noise with variable amplitudes across the frequency band [71]. Colored background noise is generally characterized by a reasonably low power spectral density (PSD). Typically caused by common building and residential electronic appliances, this PSD tends to decrease as the frequency increases. It attains high values in the frequency band near the power mains frequency (50 Hz or 60 Hz) up to about 20 kHz [63].
- b) Narrow-band Interferences: This type of noise occurs at narrow functions of the frequency band but with a rather high PSD. Narrow-band noise appears as sharp peaks

of high amplitudes in the frequency domain. The main issue with utilizing electrical wiring for communication is its lack of shielding. At high frequencies these lines behave like antennas, thus they have the ability to intercept transmissions in the same frequency bands. Interference is thus sourced from external radio stations broadcasting in the 1-30 MHz range such as AM, FM as well as amateur radio. However, narrow-band interference is also possible at much lower frequencies due to switching of electrical appliances such as power supplies, television sets, fluorescent lamps, or computer monitors [63].

### **3.1.2 Impulsive Noise:**

- a) Periodic impulsive noise synchronous with the mains frequency: This type of noise is peculiar with silicon controlled rectifiers (SCRs) commonly used in DC power supplies and phase control in devices such as light dimmers, which occurs synchronously with the mains frequency, 50/100 Hz in South Africa (60/120 Hz in the US) [71]. Periodic voltage impulsive peaks are generated at every zero-crossing of the mains signal which leads to repetition rates of multiples of the mains frequency. Periodic impulses synchronous with the mains are characterized by short durations and a PSD that decreases with increasing frequency.
- b) Periodic impulsive noise asynchronous with the mains frequency: It typically originates from switching (on and off) power supplies commonly found in various household appliances, and it has repetition rates between 50 kHz and 200 kHz [109].
- c) Asynchronous Impulsive Noise: the main cause of asynchronous impulsive noise is the transients that occur due to switching in different parts of the electrical network. According to the findings in [99] typical impulsive durations range from some microseconds to a few milliseconds. It is sporadic in nature, thus it can appear in bursts which signifies the severe impact it can have on high speed PLC communication systems. This also highlights the need for robust modulation schemes as well as powerful channel coding techniques.

Background noise is of time-variant nature, nonetheless, it can be considered stationary since it varies slowly over periods of seconds and minutes or at times hours [63], [70], [72]. On the other hand, the impulsive noise cannot be considered stationary. Typically, impulsive noise has short durations ranging from some microseconds up to a few milliseconds and are characterized by high amplitudes. During the occurrence of impulsive noise, the power spectral density (PSD) of this type of noise can be up to 50 dB above the background noise [76]. Therefore, the resultant noise scenario can be represented as the sum of the two major noise terms:



$$\eta(t) = n_b(t) + n_{imp}(t) \quad (3.1)$$

where the background and impulsive noise terms are denoted by the first and second components respectively.

At the present moment, the aforementioned noise terms still have many related unknowns. The probability distribution and instantaneous PSD of the background noise are usually determined inclusive of the impulsive noise terms as well as the narrow-band interferences. Accordingly, quite a peaky PSD is obtained as well as a non-Gaussian probability distribution [110], [72]. Regarding the impulsive noise, its determination has mainly been accomplished in the time domain using digital storage oscilloscopes triggered by a peak detection output. Statistical data such as inter-arrival time, pulse width, and pulse amplitude [70], [111] are computed from the stored data. However, this procedure has some drawbacks. The key one being that low-level impulses are typically dominated by those of high-level amplitudes, particularly narrow-band interferences. The masked noise components thus hardly contributes to the statistical derivations, making it difficult to identify its periodicity. This creates a bias in the estimation of statistical occurrence of the pulse widths as well as pulse amplitudes. In time domain, there is a possibility of discrimination against some impulsive noise terms from different components due to overlaps. As a consequence, computation of statistics from data obtained in this manner may be of little use towards the development of realistic PLC noise models.

We consider the time dependency of PLC channels. The major contribution to this effect is due to the unpredictable nature of the noise sources. It is from this time-variability that we derive confidence in the measured data, that there is adequate integrity in the collected data. Continuous data collection addresses two key issues: 1) over time, missed impulsive peaks either due to instrument resolution limitations (time domain) or overlaps will eventually be captured at some other time instant, 2) in the frequency domain, narrow-band interference caused by radio broadcasting occupy specific portions of the band and is dominant therein (see Figure 3.7). Thus, a mitigation technique employed to curb this noise should equally suppress any other noise in the same band. The measurement approach thus requires a reasonably large number of measurements taken repeatedly over a period of time to improve its integrity and usefulness.

The focus of this chapter is the characterisation of the numerous noise terms as found in PLC channels aimed at providing broadband services to the home. We have thus decided to classify noise macroscopically as either background (predictable) or impulsive in nature (unpredictable). A classification of the background noise is according to its power spectral density while the impulsive noise is presented according to its statistical characteristics.

### 3.2 Noise Measurements

In this section we describe the measurement procedure and instrumentation employed throughout the measurement process. PLC noise from actual indoor channels was measured both in time and frequency domain using Tektronix TDS 2024B digital storage oscilloscope and Rhode & Schwartz spectrum analyser respectively. A coupling circuit is used as an interface between the PLC channel and measurement devices. The broadband coupler not only facilitates reception of the noise signals, but also provides galvanic isolation between mains and measurement equipment. The coupler as shown in Figure 3.2 employs a broadband 1:1 transformer in combination with a capacitor yielding a high pass (LC) filter. On either side of the transformer are placed transient voltage surge suppressors (TVSS) with a metal oxide varistor (MOV) on the primary and back-to-back zener diodes on the secondary. Their purpose is to suppress any voltage spikes large enough to damage the sensitive measuring equipment. The coupler transfer characteristics exhibit a reasonably flat response in the 1-30 MHz band, with the worst case loss of 1.59 dB within this band. Nonetheless, a calibration is performed prior to measurements.

PLC network noise as reported in [107] is very complex. It is resultant from electrical appliances connected to the network as well as external noise coupled to the network either by radiation or conduction. This noise can be classified in terms of its periodicity, randomness and cyclic nature [70].

### 3.3 Impulsive Noise

Impulsive noise (synchronous and asynchronous) is one of the main challenges for high speed communications over power lines. It has been shown practically that this type of noise tends to carry large amounts of energy enough to cause significant degradation in the performance of a PLC system [71], [81]. It is thus a concern to both researchers and designers that impulsive noise may frequently sweep complete data symbols. In [82], practical measurements in power lines found that the typical strength of a single impulse is more than 10 dB above the background noise level and can on occasion

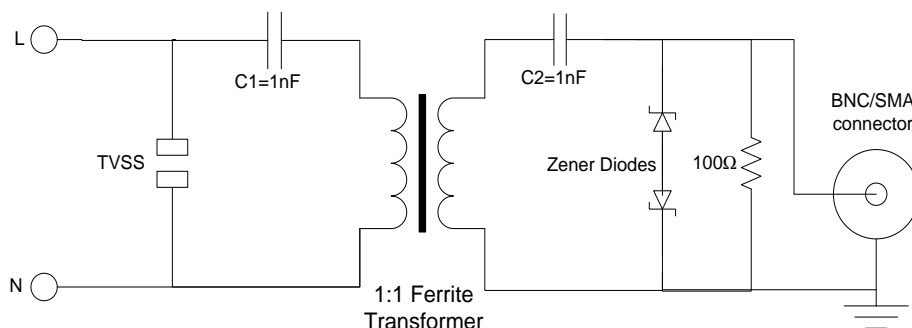


Figure 3.2: Coupling Circuit

exceed 40 dB. The same behaviour can be observed from our measurements where impulse strength rise well above the background noise.

### 3.4 Measurements Results

It is evident from figure 3.3 that there exists impulsive amplitudes that attains values well above background noise level, as high as 0.6V. For meaningful interpretation of the impulse energy, a threshold value needs to be defined that represents background noise. This is not always clear simply because, often times, there exists impulses of varying amplitudes between the dominant ones. The background noise is not always flat. A decision thus has to be made to define the appropriate level to be considered background noise. Any voltage level measured above this value shall be regarded as impulsive noise. In figure 3.3 however, it is less ambiguous to determine the level to consider background noise as compared to, say, that of figure 3.4. We determine the background noise level to be 0.05V. Using this value as the reference we now calculate the amount of increase in the noise level beyond this value as follows:

$$L_v = 20 * \log_{10} \left( \frac{V_i}{V_b} \right) \quad (3.2)$$

$$L_v = 20 * \log_{10} \left( \frac{0.6}{0.05} \right) = 21.58 \text{ dB}$$

where  $L_v$  is the voltage level in dB,  $V_i$  and  $V_b$  represents the impulsive and background noise voltage levels respectively. This is the highest value recorded for an impulse strength above background noise and the lowest recorded value is 8.32 dB. Impulsive noise measurements from other electrical outlets exhibit relatively high voltage levels e.g. figure 3.4 (~4V compared to 0.6V of figure 3.3, but at the same time the background threshold will be chosen correspondingly high.

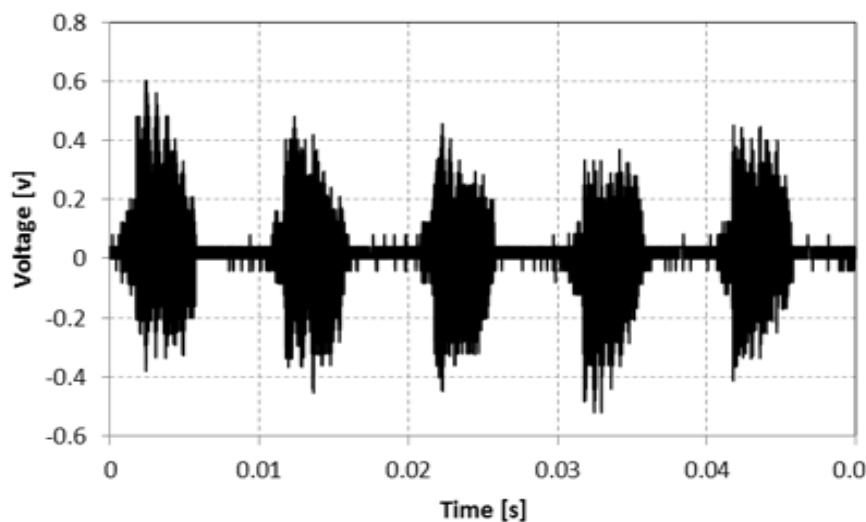


Figure 3.3: Synchronous Impulsive Noise showing the dominant 100 Hz components

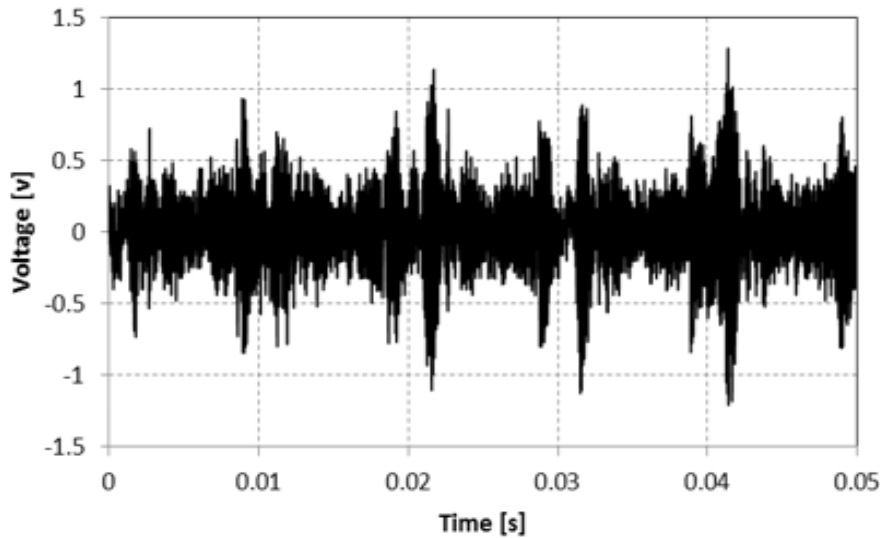


Figure 3.4: Asynchronous Impulsive Noise

### 3.4.1 Periodic Impulsive Noise Synchronous With the Mains

The noise components appears in the manner characterized by a series of impulses in isolation with significant duration and amplitude. Figure 3.3 shows impulsive noise synchronous with the mains' second harmonic (100 Hz) while the impulsive noise synchronous with the mains' frequency (50 Hz) is depicted in figure 3.6. Another property of this noise is that it has impulse trains in which the impulse number and the separation between them differs from one cycle to another. That is, for a given impulse train, the impulses are not always equally spaced. However, these terms always occur at the same instant of the mains' cycle with a repetition rate of 50 Hz or 100 Hz (in South Africa). This behaviour is shown in detail in figure 3.5 with an observation over two mains' cycles. The coloured dots (red, blue, green and brown) corresponds to four impulse trains all having a repetition rate of 100 Hz.

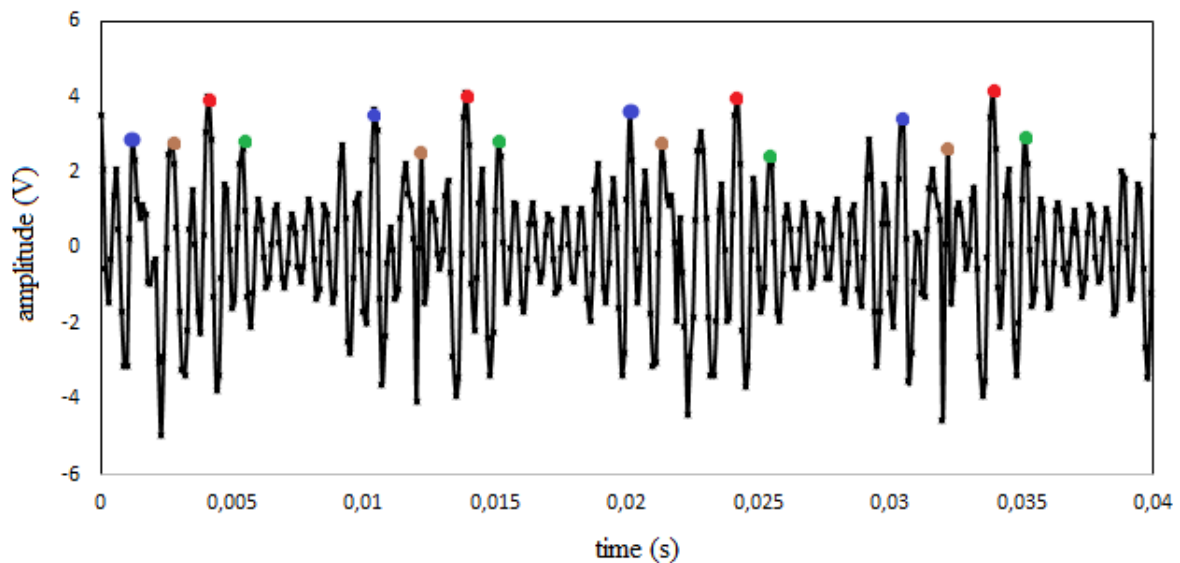


Figure 3.5: detailed synchronous impulsive noise over two mains cycles

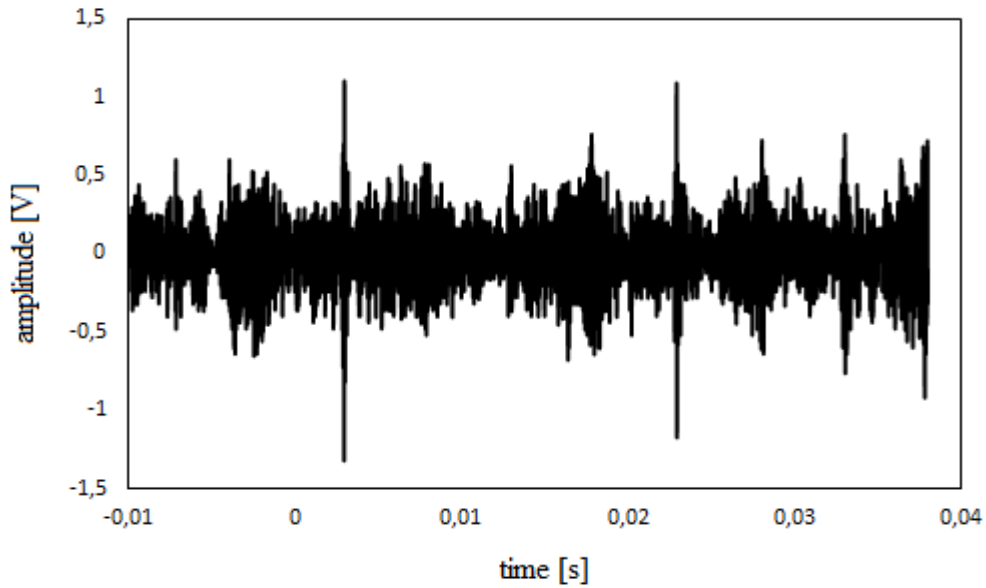


Figure 3.6: Impulsive noise captured in a laboratory with view of the dominant 50 Hz synchronous components

### 3.4.2 Periodic Impulsive Noise Asynchronous With the Mains

The impulse trains that describes this noise are composed of impulses whose repetition rates have no relation to the mains' frequency. It is for this reason that it has been formerly classified as asynchronous. However, recently, also shown here, it has been shown that these impulses in fact always appear at the same instants of the mains cycle [112], which validates their synchronous stature. We will continue to refer to this noise as asynchronous for consistency and to avoid confusion. The detailed view in figure 3.7 and figure 3.8 shows noise captured for half the mains' cycle and for 7 milliseconds respectively. They have repetition rates of 1.7 kHz and 17 kHz respectively.

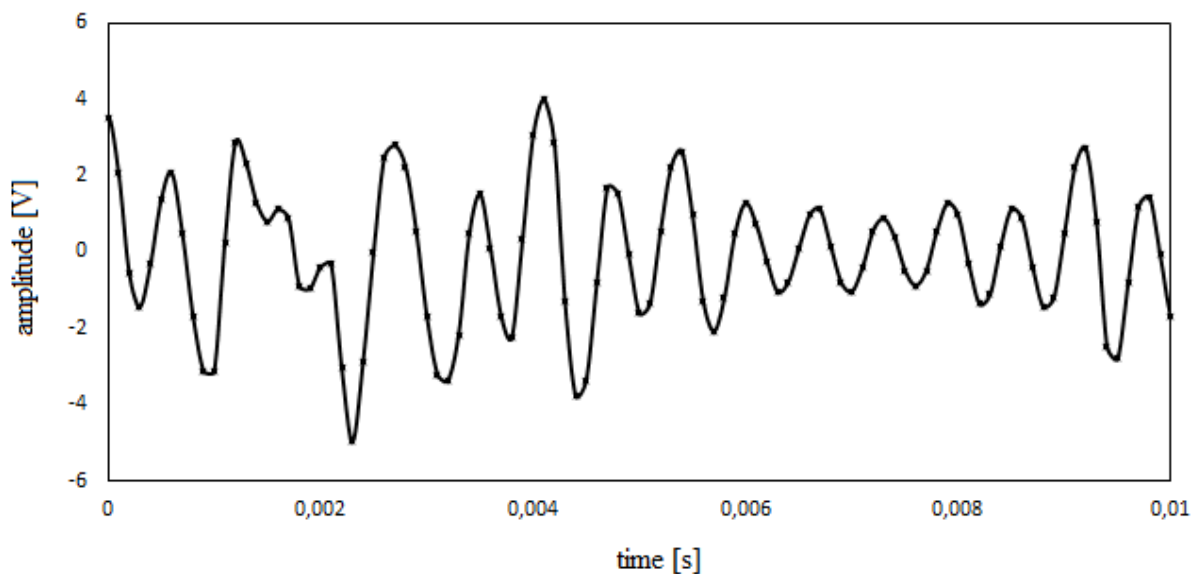


Figure 3.7: Detailed view of registered periodic impulsive noise for half mains cycle

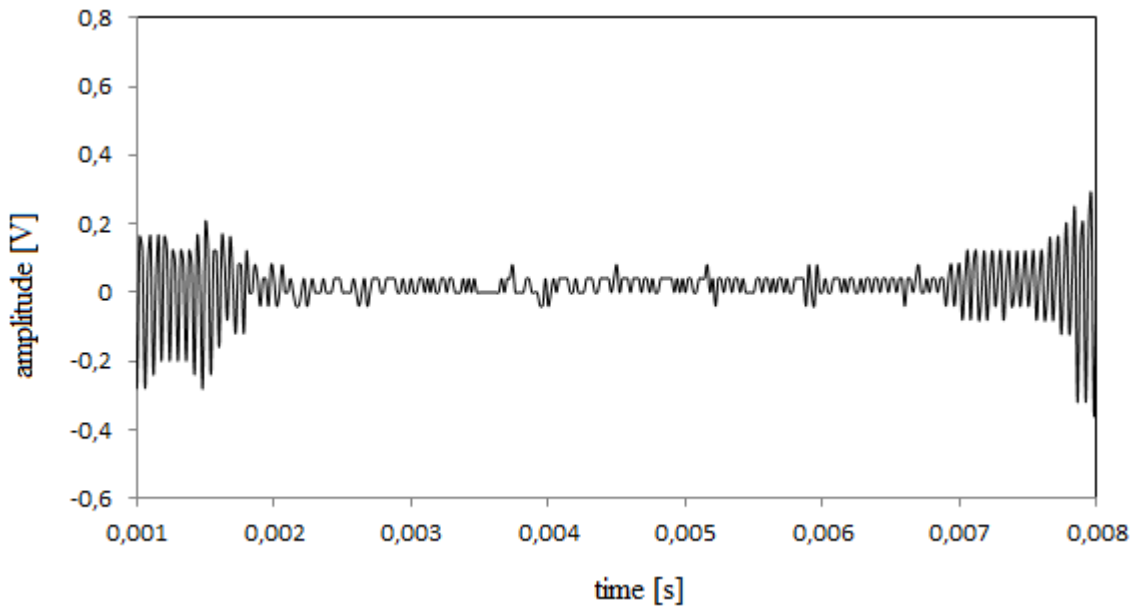


Figure 3.8: Detailed view of registered periodic asynchronous noise

### 3.5 Asynchronous Impulsive Noise

Impulsive noise can be either synchronous or asynchronous with the mains frequency. It is usually a result of switching transients peculiar with some electrical appliances in the electrical distribution network. Typical durations of impulses range from some microseconds up to a few milliseconds [113]. Typical synchronous impulsive noise is as shown in figure 3.3 while figure 3.4 depicts asynchronous impulsive noise. These are samples from a multitude of measurements performed in our University premises. In either case, the amplitude variability of the impulsive noise is observable. In actual PLC channels, components of both cases are present most of the time, hence in this chapter; we present the behavioural statistics of impulsive noise in terms of its amplitude, duration of occurrence and time-interval between impulses. We compare our results to that of E. Liu *et al* [113] which considered only the asynchronous impulsive noise. In our work, we have considered impulsive noise as that which has magnitude above a certain threshold (background noise) without cyclic classification. The results are presented in Table 3.1. Similar work has been done by T. Esmailian *et al* [114] which presented their parameters in terms of their probability distributions.

In comparison, the disparity concerning the inter-arrival times is quite significant. This can be attributed to varied environments under study. From Table 3.1, the average inter-arrival time of  $0.667ms$  correspond to 15 impulses per half-cycle of 50 Hz mains. In our measurements, roughly 180 impulses are recorded on average every half-cycle of the mains. This is expected considering that most of our measurements are taken in laboratories running numerous electrical equipment such as electrical machines, drills, measuring equipment etc. Also, the absence of the synchronous impulsive noise peaks in [113] reduces the peak count a great deal in their data collection.

Table 3.1: Statistical Parameters of Impulsive Noise

		Mean	Standard Deviation
Amplitude ( <i>mV</i> )	Our Measurements	391	198
	E. Liu <i>et al</i> [113]	229	121
Duration ( $\mu$ s)	Our Measurements	152	139
	E. Liu <i>et al</i> [113]	205	157
Interval time ( <i>ms</i> )	Our measurements	0.0558	0.0458
	E. Liu <i>et al</i> [113]	0.667	0.445

### 3.6 Background Noise

A power spectral density (PSD) model has been proposed by Esmalian *et al* [114] for background noise as shown below:

$$PSD_{noise}(f) = A + B \cdot f^C \quad [\text{dBm/Hz}] \quad (3.3)$$

Based on the results of [114], the background noise has variability in frequency and coloured. The parameter  $C$ , being less than zero, results in the background noise heavily present in lower frequencies than in higher frequencies. Guillet *et al* [115] applied the same model to their measurements and obtained parameters in the same order of magnitude as that of [114]. However, [115] proposed a different approach aimed at modifying the actual description of background noise to accommodate the fact that the noise decreases as the frequency goes higher. The motivation comes from the fact that narrowband interferences and disruptive transmissions inherent with the unshielded and vulnerable indoor power lines influence the estimated parameters [115]. They proposed an algorithm that performs a frequency sweep across the entire band with a view to determine the minimum noise level. Since their PSD is estimated from time domain data, this algorithm is embedded in their post-processing of the data. In this work, though we still use the model of [114] to describe the PSD of background noise, we consider the proposal in [115] by tracking the minimum noise spectrum during measurements in the frequency domain. However, instead of post-processing the measured data, we track the data values and sort them as they are captured. In our measurements, the new spectral magnitudes are compared to the previous data and if the new data is smaller, the new data is stored. Only the desired data is stored. The minimum spectral noise recorded is shown in Figure 3.9 with its mathematical model. Clearly the influence of narrowband interference and other effects are minimised, thus the background noise is not overestimated. It is also equally important to describe the worst case scenario of the PLC channel noise.

In-band spurious signals are unlikely to be intercepted even with spectrum analyzers of highest dynamic range and fast sweep capability. We apply the same algorithm to determine the minimum spectral noise, only this time the result is updated only when the new data value is larger than the previous data value. The maximum spectral noise recorded is shown in Figure 3.10 with its mathematical model. The model is not in good agreement with the measured results but rather presents a macroscopic capture of the measured data.

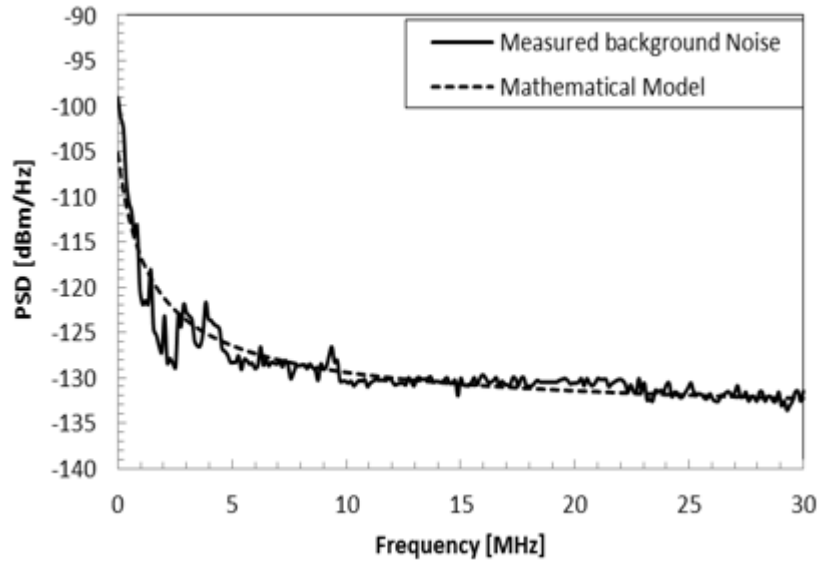


Figure 3.9: Minimum Spectral Noise

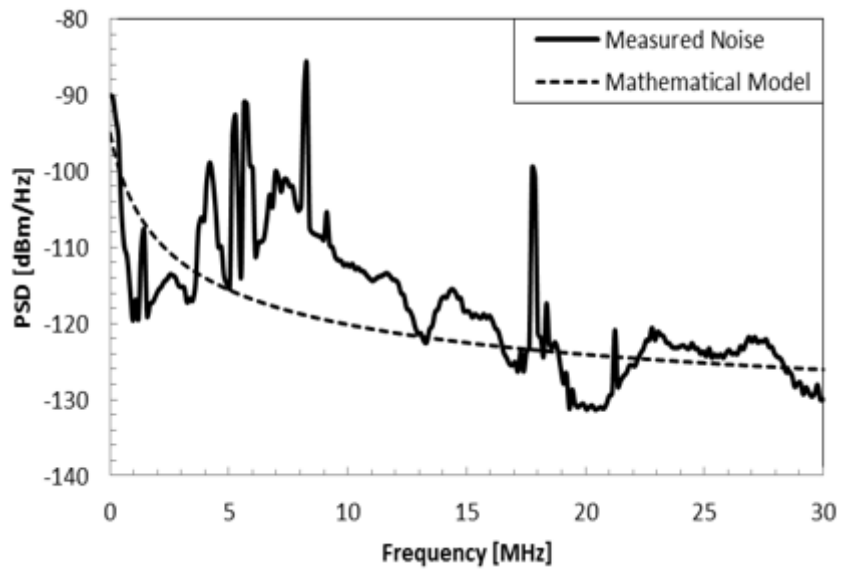


Figure 3.10: Maximum Spectral Noise



The results are compared with those of Esmalian *et al* [114] in Table 3.2 which also consider both the best and the worst case noise scenario. As discussed in section 3.1, narrowband interferences tend to occupy the same portion of the spectrum as clearly shown in Figure 3.11. Measurement results were obtained by taking readings during the day time (around 15:00 PM) and at night (around 10:00 PM). It should be noted that these results represents averages over several days/nights. It can be seen that during the night time the PLC channel is much “quieter” than it is during the day. This can easily be attributed to the lack of activity at night as the building occupants depart for home typically around 17:00 PM. However, the narrowband interference due to other radio services operating within the same band remains prominent irrespective of the time of the day. Accordingly, this behavior is expected to be the opposite in a home environment where the house is vacated for most of the day. The noise level will rise significantly in the evening as consumers plug in several appliances as they prepare their evening meals, watch their favorite TV shows, water heating, air-conditioning, personal computers etc.

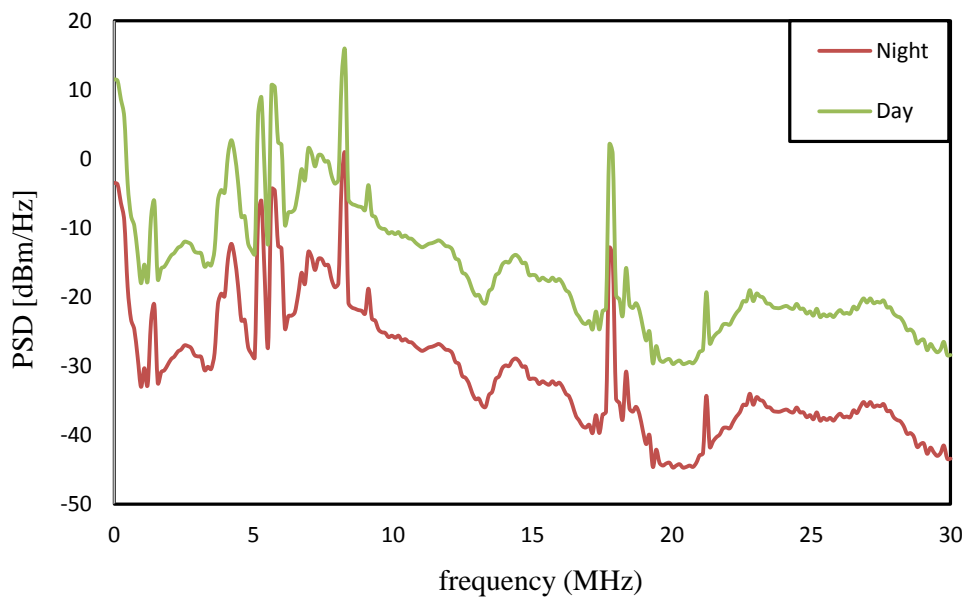


Figure 3.11: Time-of-the-day noise characteristics

Table 3.2: Background noise parameters

Statistics		Background Parameters		
		A	B	C
Best Case	Our Measurement	-135	30.71	-0.721
	Esmalian <i>et al</i> [114]	-140	38.75	-0.72
Worst case	Our Measurement	-140	45.26	-0.341
	Esmalian <i>et al</i> [114]	-145	53.23	-0.337

We use the parameters from Esmailian *et al* [114] to generate a graphical representation of the background noise up to 30 MHz as shown in Figure 3.12. We then compare, graphically, their findings with three of our measurements taken from a student laboratory, post-graduate office, and a research lab (measurement lab). We observe that though these results are derived from vastly different locations, their power spectral densities differ by not more than  $\sim 12$  dBm/Hz across the entire band. Although this model shows considerable variation with measured data, it has the ability to present simple bounds within which background noise lies. Moreover, the model exaggerate the noise PSD due to narrowband interference which effectively results in increased disparities between modelled data.

Considering the results of Table 3.2, where the best and worst case noise scenarios are studied, it is easy to see that bounds for this noise could be defined regardless of the different environments. This is with reference to the fact that in [114], the power signal specification is different from that used in South Africa. Their power grid uses 110 V at 60 Hz while we use 220 V at 50 Hz. This also implies that the cabling is different. Despite this adverse differences, there is no evidence of their impact on the background noise. It is highly possible that the main contributing factor is simply the network topology and loading.

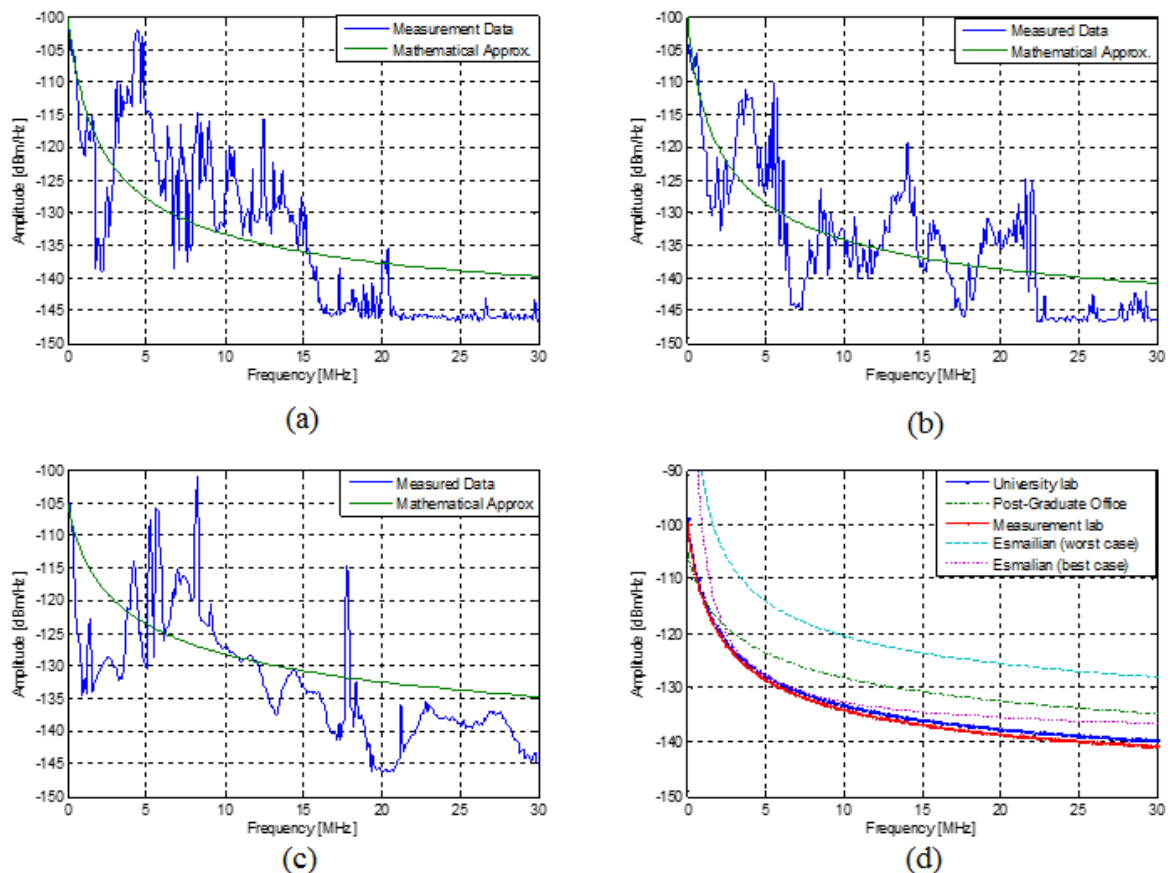


Figure 3.12: Sample noise measurements and their models (a) University lab (b) measurement lab (c) post-graduate office, and (d) comparison of models with those of Esmailian *et al* [114]

### 3.7 Chapter Summary

Noise characteristics of an indoor power line network strongly influence the link capability to achieve high data rates. The appliances shared with PLC modems in the same power line network generate different types of noises, among them the impulsive noises are the main source of interference resulting in signal distortions and bit errors during data transmission. In broadband communications applications, some portions of the spectrum is shared with other broadcasting radio services leading to channel interference. The influence of this narrowband interference on background noise has been evaluated and eliminated.

In this chapter, based on the measurements carried out in typical indoor power line channels, the noise characteristics were investigated. The noise studies were summarised by finding the parameters of the impulsive noise statistics in terms of its amplitude, duration and interval time in time domain. The impulsive noise is the main cause of packet errors in power line communication networks. Additive cyclostationary impulsive noise (figure 3.3 and 3.6) limits communication performance in OFDM power line communication systems. Conventional OFDM receivers assume additive white Gaussian noise and hence experience degradation in communication performance under impulsive noise. Further studies were undertaken in the frequency domain with a simple three parameter model used to capture its behaviour. The parameters of this model are presented. For both time and frequency domain, the parameters are compared with those of other campaigns elsewhere, with the understanding that different environments will present different challenges. Nonetheless, the nature of the noise can be described without loss of generality. Results presented in this chapter are especially useful in the development of noise models towards the design, optimization and implementation of digital communications systems. This is particularly applicable to coding schemes which need to be matched to the characteristics of the anticipated noise. Moreover, with a good knowledge of some of the noise components that are predictable in character such as periodic synchronous impulsive terms, optimization of modulation parameters and receiver structures can be achieved by employing these terms [116].

## CHAPTER 4

### DISPERSIVE CHARACTERISTICS FOR BROADBAND INDOOR POWER-LINE COMMUNICATION CHANNELS

#### 4.1 Introduction

The dramatic increase in the number of digital radio communication systems within indoor environments has raised the demand for broadband characterization of indoor PLC channels. Signal time dispersion remains the core study issue owing to its limitation of the achievable maximum symbol rate without inter-symbol interference (ISI) [117]. The impulse response (IR) of the PLC channel along with other parameters such as the mean delay ( $\tau_e$ ) and the root mean square (rms) delay spread ( $\tau_{rms}$ ) [118], [119], are usually used to characterize the channel's time dispersion. The frequency selectivity nature of the PLC channel can also be described by the coherence bandwidth ( $B_c$ ), a parameter with a close relation to  $\tau_{rms}$  [120].

Previous works have investigated the time delay spread parameters for indoor PLC channels in different parts of the world and for different frequency bands [121], [111], [110], [122]. Nonetheless, few experimental results exist that describe these parameters. A study of time dispersion of multitudes of indoor power line communications (PLC) channels in the 1-30 MHz band is presented in this chapter. The dispersive characteristics of the PLC channel are derived from the measured complex channel transfer function (CTF) by evaluating its impulse response (IR). The impulse response provides a wideband characterization of the propagation channel and provides the basis for which the channel power-delay profile (PDP) is determined. The expected degree of dispersion is derived from the PDP of the channel, hence time-delay spread parameters such as the root mean square (*rms*) delay spread, mean excess delay, maximum excess delay and the first arrival delay are obtained. This chapter thus presents the time delay parameters statistically for the measured PLC channels. Finally, the chapter presents the coherence bandwidth at 0.9 correlation level and evaluates its dependence on the *rms* delay spread. Results show that the two parameters have an inverse relationship. The delay parameters are given statistically including their 90<sup>th</sup> percentiles.

#### 4.2 Measurement Setup & fundamentals

A Rhode & Schwartz ZVL13 VNA was used to measure the channel complex frequency response in the 1-30 MHz frequency band. The measurement setup is as shown in figure 4.1. It is necessary to use coupling circuits to protect the measurement equipment from damage when connecting it to the electrical network to launch or receive the information signal. The measured results represents the frequency response of all the devices connected between the two ports of the VNA, comprising the channel, measurement cables, coupling circuitry, and the frequency response of the VNA itself. The

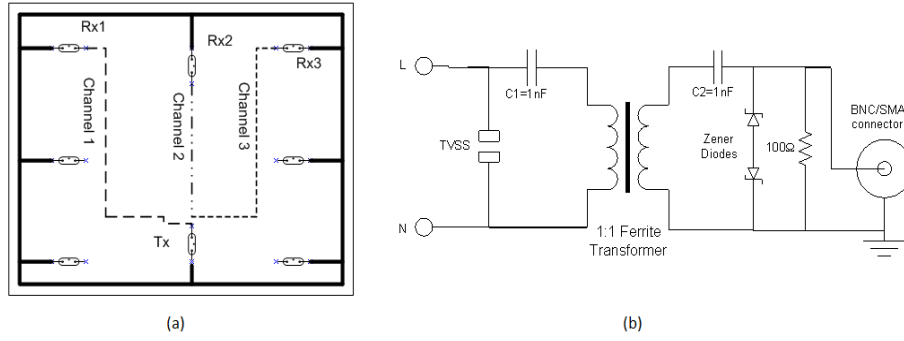


Figure 4.1: (a) Channel determination setup In-Building and (b) Coupling Circuitry

effect of the measuring system on measurements needs to be eliminated; thus a calibration is required to be carried out prior to channel measurements. With this purpose, the couplers were connected directly between the two ports of the VNA, with the frequency response  $H(f, t)_{system}$  being measured. This result was automatically subtracted from all subsequent channel measurements, minimizing the effects of the measuring system on channel transfer characteristics. The true channel frequency response takes the following form [120]:

$$H(f, t)_{channel} = \frac{H(f, t)_{measured}}{H(f)_{system}} \quad (4.1)$$

### 4.3 Channel Impulse Response (CIR)

The random and complex nature of the PLC channel can be characterized using the impulse response approach. The channel impulse response  $h(t)$  can be determined by means of inverse Fourier transform (IFT) derived from the magnitude and phase of the measured channel transfer characteristics [123]. It provides a broadband characterization of the propagating channel, and provides necessary information for the analysis of radio transmission through the channel. Thus the time domain channel impulse response including cable losses is [124]:

$$h(t) = \sum_{i=1}^N I_i \cdot [A_t(t, vT_i) \otimes \delta(t - T_i)] \quad (4.2)$$

where  $I_i$ , and  $T_i$  are magnitude and delay of the  $i$ th path respectively.  $v$  is the TEM wave propagation speed in the cable which can be calculated according to the permittivity of the insulating material of the cable ( $v = c/\sqrt{\epsilon_r}$ ).  $A_t(t, vT_i)$  is the cable loss effect in the time domain evaluated as the inverse Fourier transform of the cable attenuation [124]. A sample channel obtained through the IFFT of the channel transfer function (CTF) is shown in figure 4.2. Due to multiple reflections experienced by the signal as it propagates through the network, echoes appear at the receiver. Thus, multiple delayed

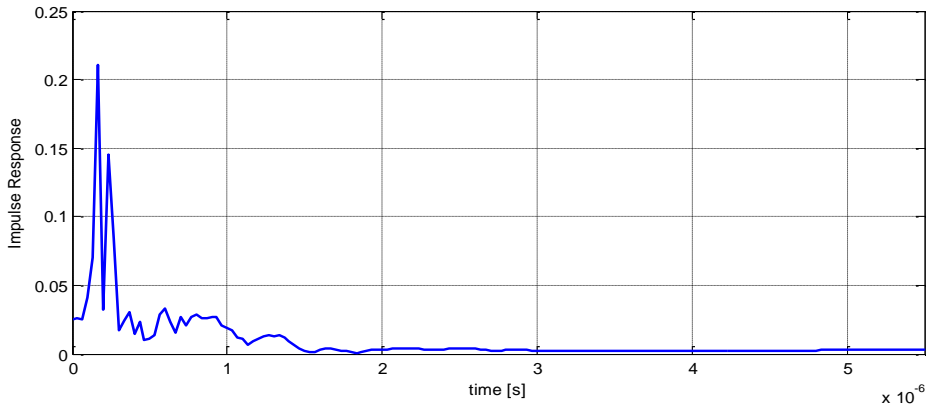


Figure 4.2: Sample Channel IR (absolute)

versions of the transmitted signal appear at the receiver with reduced amplitudes as shown in figure 4.2.

#### 4.4 Power Delay Profile (PDP)

Multipath propagation causes severe dispersion of the transmitted signal [125]. The severity of the dispersion is determined through the channel power delay profile (PDP). The PDP provides an indication of the distribution of the transmitted power over various paths in a multipath environment. The channel PDP is considered as the spatial average of  $|h(t)|^2$ , a density function such that [123]:

$$p(\tau) = \frac{|h(\tau)|^2}{\int_{-\infty}^{\infty} |h(\tau)|^2 d\tau} \quad (4.3)$$

A typical plot of the power delay profile is shown in figure 4.3, corresponding to the IR of figure 4.2.

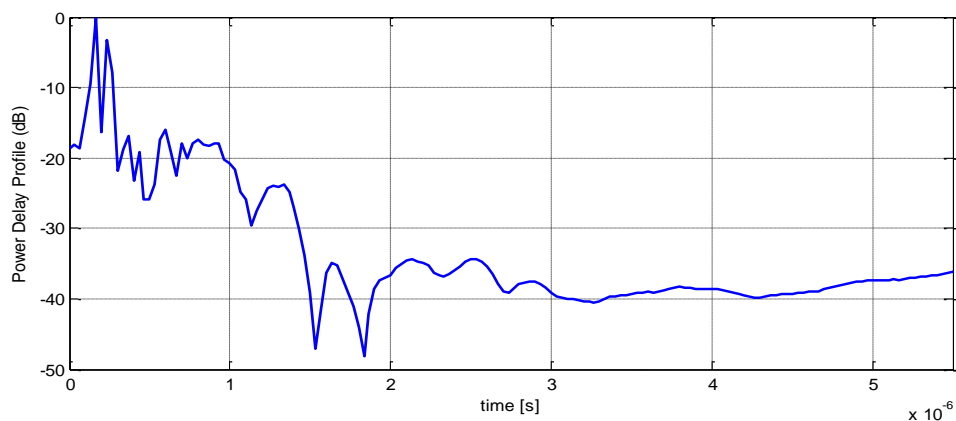


Figure 4.3: A typical PDP plot

An ensemble of PDPs is built each representing a multipath propagation PLC channel. Time delay multi-path channel parameters are derived from the PDP. Time dispersion varies widely in a PLC channel due to the multiple reflections in the power network and random loading profiles; resulting in random channel responses.

#### 4.5 Time-Delay Spread Parameters

Since time dispersion is dependent on factors such as the network topology, loading characteristics, transmitter-receiver distance, just to name a few; some parameters that can be used to grossly quantify the PLC multipath channel are described [125].

##### 4.5.1 First-Arrival Delay ( $\tau_A$ )

This is the first arrival delay. This delay corresponds to the arrival of the first transmitted signal at the receiver. It translates to the minimum possible propagation path delay from transmitter to receiver. This parameter serves as a reference i.e. all other delay parameters are measured relative to it. Any delay measured beyond this reference is considered excess delay.

##### 4.5.2 Mean Excess Delay ( $\tau_e$ )

The mean excess delay represents the first moment of the power-delay profile with respect to the first arrival delay. It can be computed as follows:

$$\tau_e = \int (\tau - \tau_A)P(\tau)d(\tau) \quad (4.4)$$

##### 4.5.3 RMS Delay Spread ( $\tau_{rms}$ )

This is the square root of the second central moment of the power-delay profile. It is the standard deviation about the mean excess delay and is expressed as follows:

$$\tau_{rms} = \left[ \int (\tau - \tau_e - \tau_A)^2 p(\tau) d\tau \right]^{1/2} \quad (4.5)$$

The RMS delay spread indicates the severity of the multipath spread. The possibility of inter-symbol interference (ISI) is determined through this parameter. Propagation through a dispersive channel is a major concern in the design of high-speed data networks. The RMS delay spread is a commonly used practical measure of the extent of time dispersion introduced by multipath channels. Signal delays of high magnitude (relative to the shortest path) with long delay time contribute immensely to the  $\tau_{rms}$  [125]. Regardless of the shape of the PDP, the dispersion effects on digital receiver performance

are related only to the RMS delay spread. ISI will be avoided as long as the RMS delay spread is smaller compared to the symbol period ( $T$ ) of the digital modulation. Data rates for transmission can also be estimated using this parameter.

#### 4.5.4 Maximum Excess Delay ( $\tau_m$ )

The maximum excess delay is specified as the excess delay for which  $p(\tau)$  falls below a specified threshold of the signal. Researchers have considered different threshold levels, but mostly consider -30dB with respect to the maximum value as such it is adopted in this work. The signal levels below the threshold are then processed as noise. Accordingly, the mean excess delay ( $\tau_e$ ) and the RMS delay spread ( $\tau_{rms}$ ) are calculated based on channel time coefficients lower than  $\tau_m$ .

### 4.6 Results Analysis

The time dispersion characteristics of PLC channels are presented statistically in Table 4.1. The analysis evaluates the minimum, maximum, mean, standard deviation and the 90<sup>th</sup> percentiles of each time-delay parameter. Alongside our results is that of an extensive measurement campaign carried out in France for comparison (here shown with a subscript (1)). It should be noted that their measurements extends to frequencies up to 100 MHz, though for the same threshold signal level, similar delay characteristics are expected and it is macroscopically the case here.

In our study, the first arrival delay ( $\tau_A$ ) was observed to have a minimum value of 0.033 $\mu$ s, standard deviation of 0.143 $\mu$ s, and a mean value of 0.179 $\mu$ s. For 90% of the time, the value of  $\tau_A$  was found to be less than 0.37 $\mu$ s and above 0.067 $\mu$ s. On the other hand, the mean excess delay ( $\tau_e$ ) has a mean value of 0.163 $\mu$ s, and a standard deviation of 0.216 $\mu$ s. Though  $\tau_e$  is confined between 0.00082 $\mu$ s and 0.97 $\mu$ s, it is found that for 90% of the time, its values are between 0.025 $\mu$ s and 0.40 $\mu$ s.

Table 4.1: Time delay parameters

$\tau$ (us)	Min (us)	Max (us)	Mean (us)	STDev (us)	90% above	90% below
$\tau_A$	0.033	0.534	0.179	0.143	0.067	0.37
$\tau_{A1}$	0.010	0.410	0.152	0.097	0.050	0.30
$\tau_e$	0.00082	0.97	0.163	0.216	0.020	0.40
$\tau_{e1}$	0.00030	0.88	0.182	0.157	0.025	0.36
$\tau_{rms}$	0.0215	1.16	0.287	0.222	0.04	0.55
$\tau_{rms1}$	0.026	1.039	0.309	0.212	0.06	0.60
$\tau_m$	0.534	4.535	1.749	0.867	0.83	3.27
$\tau_{m1}$	0.18	6.26	2.228	1.327	0.55	3.81



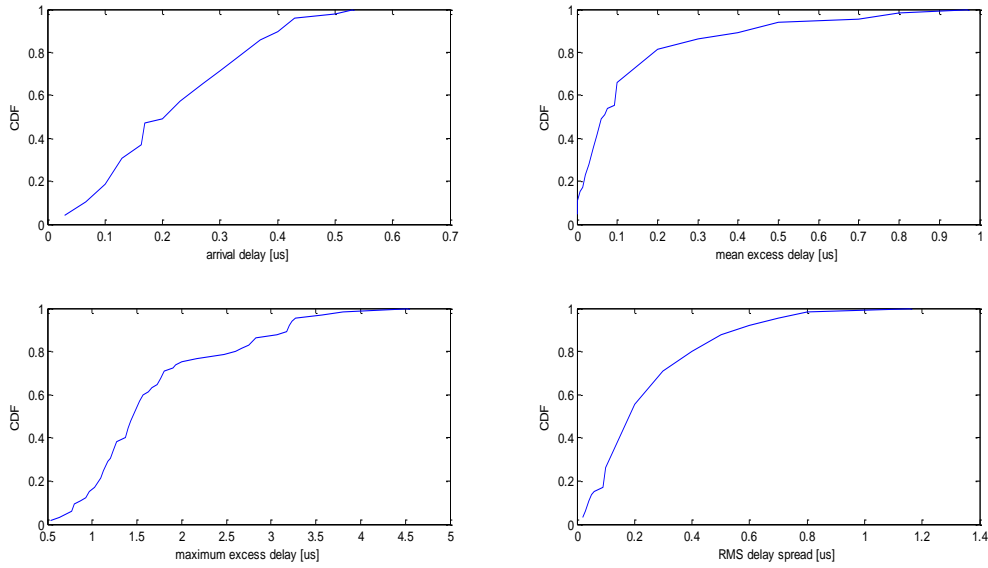


Figure 4.4: Cumulative distributions (CDFs) of the time delay parameters

With regards to the maximum excess delay ( $\tau_m$ ) 90% of the measured channels were observed to lie between  $0.83\mu\text{s}$  and  $3.27\mu\text{s}$ . Its mean and standard deviation were found to be  $1.749\mu\text{s}$  and  $0.867\mu\text{s}$  respectively. Of the measured channels, 90% of them exhibit an RMS delay spread between  $0.04\mu\text{s}$  and  $0.55\mu\text{s}$ . The percentiles for the time delay parameters are displayed in figure 4.4 in the form of cumulative distributions (CDFs). Other percentiles not discussed in this paper can easily be estimated from the CDFs.

#### 4.7 Coherence Bandwidth

An important parameter in characterizing radio communication channels is the coherence bandwidth. In this paper, we present an analysis of the coherence bandwidth in PLC networks. When designing robust and reliable communication systems, a significant amount of effort is placed on choosing modulation, coding and receiver architecture schemes that mitigates the deleterious effects of the propagating channel [126]. The PLC propagation environment is characterized by multipath effects which results in significant nulls in the amplitude frequency response. One measure of the varying frequency response is the coherence bandwidth ( $B_c$ ).

In the frequency domain, the magnitude spectrum has spectral peaks that are quasi-constant over a minimum band that is the inverse of the maximum delay spread, the same for the phase spectrum where it is linear only in such a band. The coherence bandwidth statistically quantifies this band and is therefore a function of the RMS delay spread. It is the measure of the magnitude correlation between the channel responses at two spaced frequencies, thus, it statistically quantifies the frequency range

within which the frequency correlation function (FCF) can be considered uniform [123]. The frequency selective nature of the PLC channel can be described in terms of the auto-correlation function for a wide sense stationary uncorrelated scattering (WSSUS) channel. The frequency correlation function is given by [123]:

$$R(\Delta f) = \int_{-\infty}^{\infty} H(f)H^*(f + \Delta f)df \quad (4.6)$$

where  $H(f)$  is the complex transfer function of the channel,  $\Delta f$  is the frequency shift and  $*$  denotes the complex conjugate.

Frequency correlation functions obtained for five sample transmitter-receiver scenarios are shown in figure 4.5. We observe the rapid degradation of the FCF with respect to frequency separation. There is no definitive value of correlation that has been put forward for specification, but generally accepted coefficients are 0.5, 0.7, and 0.9. In this work we have considered the latter, which will further be referred to as  $B_{0.9}$ . Due to the presence of multiple replicas at the receiver in PLC channels; the decrease of FCF with increasing frequency is non-monotonic.

In figure 4.5, the upper graph (blue) represents a good channel due to its high coherence bandwidth for a given RMS delay spread. The worst channel would be the lower-most graph (green) as it exhibits the lowest coherence bandwidth for a given RMS delay spread. A good channel can be assumed to have the least multipath contributions. The correlation coefficient was computed using the smallest frequency separation, 150 kHz in this work. The estimate of the coherence bandwidth is derived from the FCF graph.

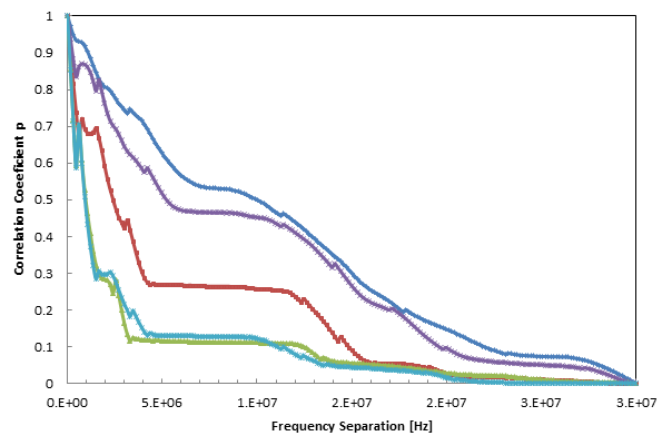


Figure 4.5: FCFs of sample measured channels

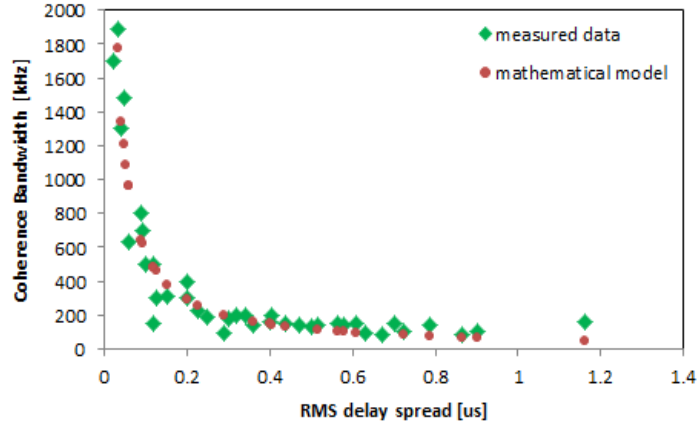


Figure 4.6: Scatter plot of coherence bandwidth against RMS delay spread

Figure 4.6 shows the scatter plot of the RMS delay spread against the coherence bandwidth  $B_{0.9}$  for the measured PLC channels. An approximation of their relationship (shown in red) was determined to be:

$$B_{0.9}(kHz) = \frac{60}{\tau_{rms}(\mu s)} \quad (4.7)$$

The results show that RMS delay spread values less than  $0.09\mu s$  achieve a coherence bandwidth of at least 600 kHz. On the other hand, in the range  $0.09\mu s - 1.16\mu s$ , the coherence bandwidth is between 80 kHz and 600 kHz. In terms of system design, desired values of  $\tau_{rms}$  are those that result in high coherence bandwidth as this translates to faster symbol transmission rates [127]. The coherence bandwidth of the channel is particularly relevant to frequency-hopping spread spectrum (FHSS) systems [128] and other multi-carrier systems such as OFDM.

#### 4.8 Chapter Summary

An indoor PLC channel measurement campaign has been established to determine the time dispersive characteristics of these channels. This chapter includes the statistics of time delay parameters as well as coherence bandwidth and its relation to RMS delay spread in the frequency range up to 30 MHz. We have observed the inverse relationship between coherence bandwidth and RMS delay spread as given in equation (4.7). The frequency correlation function is also found to decrease rapidly with frequency separation. The 90<sup>th</sup> percentile of the RMS delay spread was found to be between  $0.04\mu s$  and  $0.55\mu s$  with a mean of  $0.287\mu s$  and standard deviation of  $0.222\mu s$ . The results show that RMS delay spread values less than  $0.09\mu s$  achieve a coherence bandwidth of at least 600 kHz. On the other hand, in the range  $0.09\mu s - 1.16\mu s$ , the coherence bandwidth is between 80 kHz and 600 kHz. In terms of system design, desired values of  $\tau_{rms}$  are those that result in high coherence bandwidth as this translates to faster symbol transmission rates [127]. The coherence bandwidth of the channel is particularly relevant

to frequency-hopping spread spectrum (FHSS) systems [128] and other multicarrier systems such as OFDM. Coherence bandwidth is one of the key parameters which provides a good indication towards the possibility for achieving the PLC wideband performance as envisaged for PLC networks. In this frequency range, the transmission rates of 200Mbps are expected at the physical layer with about 80Mbps at the MAC layer [35]. We thus, however, take note that for improved accuracy and consistency a lot more data still needs to be captured and incorporated into our analysis. Also, for improved coherence bandwidth estimation, smaller frequency steps are required for increased data points within the band of interest.

Comparatively, the relationship between coherence bandwidth and RMS delay spread as shown in equation (4.7) is very close to that obtained by [123]. The constant in the numerator (60 in this case and 55 in [123]) is expected to differ from site to site but with more measurement campaigns, this number could be defined as bound within a reasonable range just like it is the case with wireless networks. The comparisons in Table 4.1 also show closeness in terms of bounds for other time delay parameters for indoor PLC channels. We also take note of the difference in bandwidth consideration in our case and that of [123], which considers frequencies up to 100 Mhz.

## CHAPTER FIVE

### BROADBAND CHARACTERISTICS FOR MULTI-PATH POWER LINE COMMUNICATION CHANNELS: INDOOR ENVIRONMENTS

#### 5.1 Introduction

The idea of utilizing power lines as a communication medium dates back to the 1900's [129]. However, until recently, their use has been restricted to narrowband applications. In Europe, the indoor network was almost restricted to home automation [130], [131], exploiting the CENELEC band [132] and using rather simple modulation schemes. The main reason for dismissing usage of power lines for broadband applications was simply because the channel was considered too noisy and unpredictable [133]. However, the advances in digital transmission techniques have provided a different perspective on the possibility to employ power line communication (PLC) for broadband applications. Thus, the PLC local area networks (LAN) would not be restricted to computer connections, but is also extended to peripherals and multimedia equipment. PLC has a promising future in developing countries, as opposed to developed countries where there is a plausible rivalry from digital subscriber lines (DSL), wireless networks as well as cable services [133], [134]. Telecom operators are currently offering triple play solutions (telephony, video, and internet access) and PLC is a viable option to deliver broadband data to the residential gateway, to the television set top box and the computer [133].

PLC channels have variable physical characteristics and network topologies vary from country to country [135]. The provision of the service is still deterred by the lack of standards, simply because PLC channels are not standard and their characterisation is not repeatable even though efforts are in place. Another factor in question is as to whether PLC systems are capable of rivalling their counterparts in terms of providing high data bit rates. In this chapter we show the variability of channel transfer characteristics in different types of indoor environments. It is this variability that leads to numerous channel modelling approaches and consequently lack of a common agreement on the most suitable channel model. A series of standards such as IEEE P1901/1901.2 and ITU-T G.hn/G.cx/G.hnem have been released owing to the increasing market demand for indoor broadband communications, smart grid applications, and in-home energy management [136]. Thus, the quest to develop accurate models to facilitate these technologies remains an on-going process. The existing models proposed in literature can be classified into two main categories [124]: the multipath approach [75], [137], [138] and the transmission line theory approach [139], [140]. The multipath model considers the reflected signals due to impedance discontinuities at branches and its accuracy is reliant on the proper selection of the parameters of the signal propagation properties [124]. The effect of multiple paths is based on the actual measurements of channel transfer functions; thus it is not rewarding to evaluate the propagation

properties of each individual path. On the other hand, transmission line theory based models considers a PLC network as a series of cascaded two port networks and can thus be adapted to different network topologies using popular transmission matrices [124]. This model is rather computation intensive especially when dealing with complex networks. The other drawback is its dependency on the availability of the line parameters to generate matrices, thus its applicability to real networks of unknown cable types and topology is limited. We consider a multipath approach in this work and treat the network under consideration as a “black box” of unknown parameters and describe its frequency response  $H(f)$  in the frequency range 1-30 MHz. The key parameters of this model are: cable attenuation  $A(f, d_i)$ , weighted transmission/ reflection factor  $g_i$ , path length  $d_i$ , and the number of significant paths  $N_i$ .

We employ a top-down strategy where the channel is considered a multipath propagation environment with frequency-selective fading. The model is based on the physical signal propagation effects of numerous PLC architectures which comprise unknown number of branches and load conditions. We further consider the attenuation of a typical power-line to be increasing with length as well as frequency. The applicability of the model is verified with measurements from practical indoor channels from our laboratories and offices within the 1-30 MHz frequency band. The generated channel frequency response (CFR) has a fairly good agreement with measurements results from actual PLC channels. Furthermore, we study the dispersive nature of these channels through their impulse responses (IR) in order to derive some of the relevant parameters required by the proposed model.

This chapter is organized such that it provides a description of the measurements procedure as well as the instrumentation used throughout the process. We then present measurement results for three sample channels with several measurements for each and finally the frequency-averaged channel. The channel impulse response (CIR) is studied and presented as it provides some of the parameters required for the proposed model and the dispersive nature of PLC networks are discussed briefly. Finally, we present the proposed model, its parameter extraction and then its validation on real PLC networks including the model parameters for the sample channels mentioned above.

## **5.2 Measurement Description & Instrumentation**

The measurements have been performed in three different in-building scenarios in the Electrical Engineering building in Howard College Campus, Durban, South Africa: small office, large office, and some laboratories. Measurements were acquired in the frequency domain. The measurement setup is as shown in Figure 5.1, with channel definition described in Figure 5.2(a). The frequency domain measurements were performed using the Rhode & Schwartz ZVL13 vector network analyser with full 2-port calibration for the channel frequency response (CFR) in the 1 – 30 MHz band; it has specifications as shown in [141].

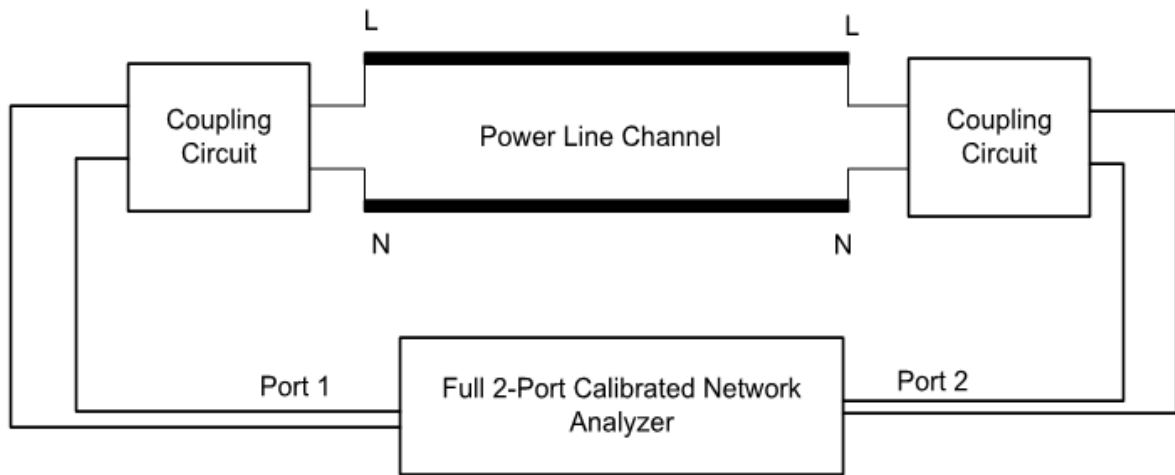


Figure 5.1: Measurement setup

The measuring instrument was coupled to and from the power network through broadband couplers to provide the necessary protection and galvanic isolation from the mains. The couplers, which are of differential type, are employed primarily to relay the communication signal to and from the power line channel. The coupler shown in Figure 5.2 (b) has transfer characteristics showing a reasonably flat response, as shown in Figure 5.3, for frequencies up to 30 MHz, with an average loss of 1.59 dB in this band. This response is taken into consideration in all subsequent measurements. The coupler is ideally a high pass filter employed to block the 220 V power line voltage with a -3dB cut-off frequency of ~200 kHz and presents an attenuation of 46.3 dB at 9 kHz (instrument lower limit, see [141]) - hence the attenuation is expected to be even much lower at the mains frequency (50 Hz), thus providing reasonable measurement integrity, protection of measurement instrumentation and reliability in the band of interest. To avoid distortion of the coupler performance, measurement cables of length ~ 10 cm were used for connections.

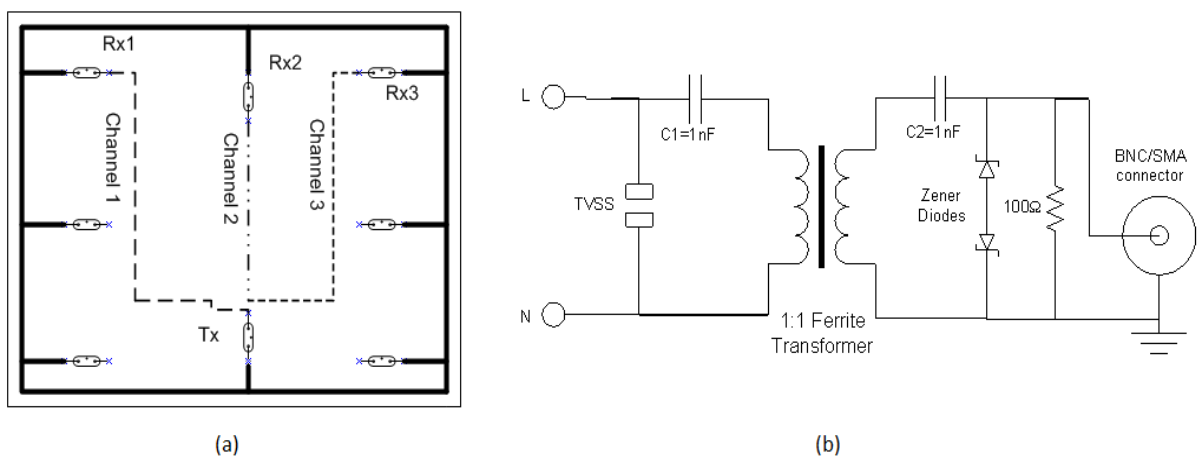


Figure 5.2: (a) Channel determination setup In-Building and (b) Coupling Circuitry

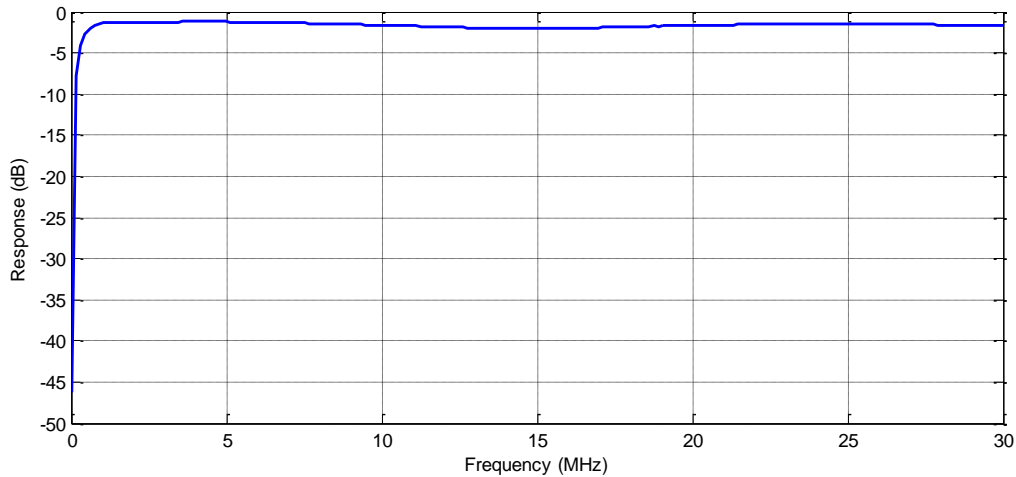


Figure 5.3: Coupler Characteristics

### 5.3 Channel Frequency Response (CFR) Measurements

Channel frequency response measurements were carried out in in-building environments in the Electrical Engineering building. Small post-graduate offices, a research laboratory, a large post-graduate office, and a student laboratory formed three scenarios under consideration for the campaign. The post-graduate offices house several computers and two medium-sized air conditioning units, while the research laboratory comprise of three microwave measuring units and three data logging PCs along with a medium-sized air conditioning unit. The student laboratory, used as a second-year Bachelor of Engineering practical laboratory, is capable of accommodating up to 100 students sharing 50 stations during a practical session; it comprises of measuring instruments in the form of oscilloscopes, signal generators, power supplies, spectrum analysers, and other devices including PCs as well as motor-generator (M-G) units. Typical channels are as described in Figure 5.2(a) and chosen at random within each scenario. All the loads connected throughout the building were running as usual, and to anticipate worst case channel conditions, all measurements were performed during the day. Three channels were considered in each scenario and presented, with a total of twenty (20) acquisitions taken for each individual channel as shown in Figure 5.4. This allows for a fair average characterization, considering the unpredictable nature of the channel due to noise and loading. As the signal traverses the network, it experiences multiple reflections due to impedance mismatches and branching. Delayed signals thus show up at the receiver as multiple echoes, creating notches (nulls) throughout the frequency band. The concentration of notches translates into the population of branches and loading conditions in a given network. The state of the channel depends not only on its architecture, but also on the loading conditions. This characterises a PLC channel as time-variant and unpredictable due to the arbitrary loading profile the network is subjected to. To accommodate the time-dependence of channel variability, an average channel response is considered in order to capture its behaviour as shown in Figure 5.4 (bottom right corner).



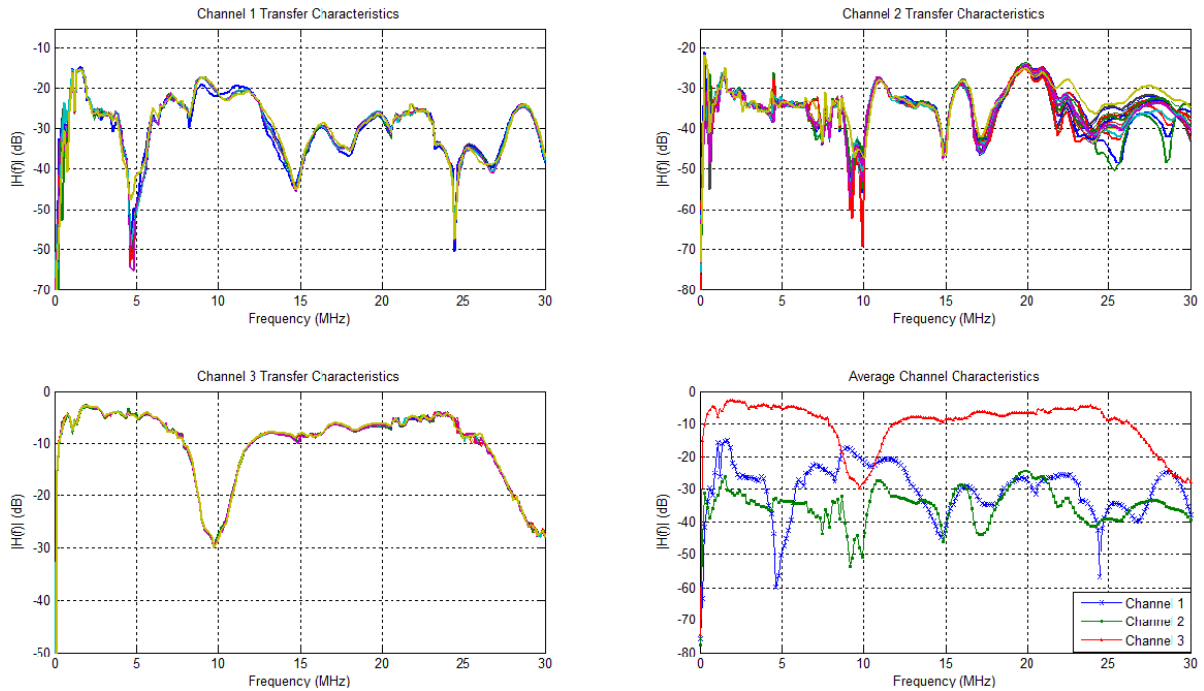


Figure 5.4: Channel Response of Real In-door Channels and their Average Responses (bottom right corner)

Channel 1 and 2 (student laboratory and a large post-graduate office, respectively) are characterized by a series of deep notches distributed across the band, while channel 3 (research laboratory) consists of a single deep notch at 10 MHz. In general, we can assume channel 1 and 2 to be heavily branched and loaded and thus expect longer impulse responses as opposed to channel 3 [136].

## 5.4 Practical PLC Channel Modelling

### 5.4.1 Channel Response Characteristics

We consider a PLC channel to be a frequency-selective multipath propagation medium. This arises from the fact that in power-line communication channels, transmitted signals do not only propagate along a direct “line-of-sight” (LOS) path between the transmitter and the receiver but also suffers multiple reflections (echoes) due to additional paths [142]. The multipath behaviour is caused by the presence of power cable joints (nodes), consumer loads, connection boxes and in some cases the heterogeneity of the network resulting in impedance mismatches.

In this work, we employ a top-down approach to model the power line channel as a ‘black box’ and describe its transfer characteristics within the of 1-30 MHz frequency band. We propose the model of Zimmermann & Dostert [75], structured based on the fundamental physical effects analysed over a great number of measurements. The basis of this model was first brought forward in [79] while a simpler but less accurate multipath approach was given in [143]. As pointed out in [75], only when considering simpler topologies such as single-branched cables, can one easily attribute portions of the observed

results to specific physical effects (cable attenuation, reflection, and propagation factors). Thus, in practical networks, back-tracing of measurements results to physical effects will prove generally impossible due to the complexity of the network topology. Regardless of this short-coming, the proposed model describes the frequency response of real networks with sufficient precision. The proposed band-pass PLC model takes into account the multipath effects, and the frequency response can be synthesized as follows [75]:

$$H(f) = \sum_{i=1}^{N_i} g_i \cdot (f) e^{-j\frac{2\pi d_i}{v} f} \cdot A(f, d_i), \quad 0 \leq B_1 \leq f \leq B_2 \quad (5.1)$$

where  $N_i$  is the number of paths,  $g_i(f)$  represents the complex and frequency-dependent transmission/reflection factor for path  $i$ . The path length is represented by  $d_i$  while  $v = c/\sqrt{\epsilon_r}$ , with  $c$  the speed of light and  $\epsilon_r$  the cable's dielectric constant. The lossy cables cause an attenuation given by  $A(f, d_i)$  which increases with frequency and distance. In [75], it is suggested that it is possible to simplify the specification of the weighting factors  $g_i$  to being complex but not frequency-dependent. Furthermore, considering practical interests,  $g_i$  can even be considered real-valued [75]. We therefore simplify equation (5.1) as follows:

The attenuation of a power line cable can be characterized as:

$$A(f, d_i) = e^{-\alpha(f) \cdot d_i} = e^{-(a_0 + a_1 f^K) \cdot d_i} \quad (5.2)$$

The PLC channel transfer function then reduces to:

$$H(f) = A \sum_{i=1}^{N_i} g_i \cdot e^{-j\frac{2\pi d_i}{v} f} \cdot e^{-(a_0 + a_1 f^K) d_i}, \quad 0 \leq B_1 \leq f \leq B_2 \quad (5.3)$$

where the parameters  $a_0, a_1, K$ , and  $N_i$  are chosen to adapt the model to a specific PLC network. Parameter  $A$  is brought in to adjust the attenuation of the final result. Appropriate parameter fitting enables the model to realistically capture the channel frequency response. Equation (5.3) covers all the relevant propagation effects of the transfer characteristics of a typical power-line channel. However this parametric model should be used to fit measured frequency responses [75]. To further enhance the usability of the model, we consider the approach of [144], which evaluates performance with a statistical model that allows for capture of the ensemble of power-line grid topologies. We consider the parameters in (5.3) to be random variables. This allows us to model the channel transfer characteristics through a realisation of these parameters [144]. The resultant multiple paths are assumed to be caused by reflectors placed over a finite distance interval with the first reflector placed at distance  $d_1$  ( $i=1$ ). The remaining

reflectors are distributed according to a Poisson arrival process with intensity  $\Lambda[m^{-1}]$ . As mentioned before, the reflection factors  $g_i$  are considered real-valued and we further characterize them as independent and uniformly distributed in  $[-1, +1]$ . The values of  $a_0$ ,  $a_1$  and  $K$  are then appropriately chosen to a fixed value.

The structure of (5.2) is derived from cable physical effects; however, the parameters  $a_0$ ,  $a_1$ , and  $K$  cannot be easily determined from previously known cable parameters. Nonetheless, the value of the model in practice is not limited since it is generally impossible to obtain all the required cable geometry data for real networks [75]. To estimate the attenuation parameters, we consider the attenuation profile of a single-path cable link as shown in Figure 5.5. The red line represent a linear function for  $k = 1$ . The attenuation coefficient from (5.2) is given as:

$$\alpha(f) = a_0 + a_1 f^K \quad (5.4)$$

The plot of  $\alpha(f)$  versus frequency is fairly linear in the frequency range 0 - 30 MHz, allowing us to estimate the value of  $K$  to be  $\sim 1$ . The intercept and slope of the graph gives us an estimate of  $a_0$  and  $a_1$  respectively. Initial estimates were obtained through tests of two types of cables commonly used by the local power utility. We have used the  $2.5 \text{ mm}^2$  and  $4 \text{ mm}^2$  cables of both VVF and NYM types. The parameters do not vary much with cable diameter but rather significantly with cable type as frequency increases. The value for  $a_0 = 1 \times 10^{-3} (m^{-1})$  is recorded for the two cable types while  $a_1 = 1.16 \times 10^{-9} (s/m)$  and  $6.6 \times 10^{-10} (s/m)$  for NYM and VVF cable types, respectively. We will settle

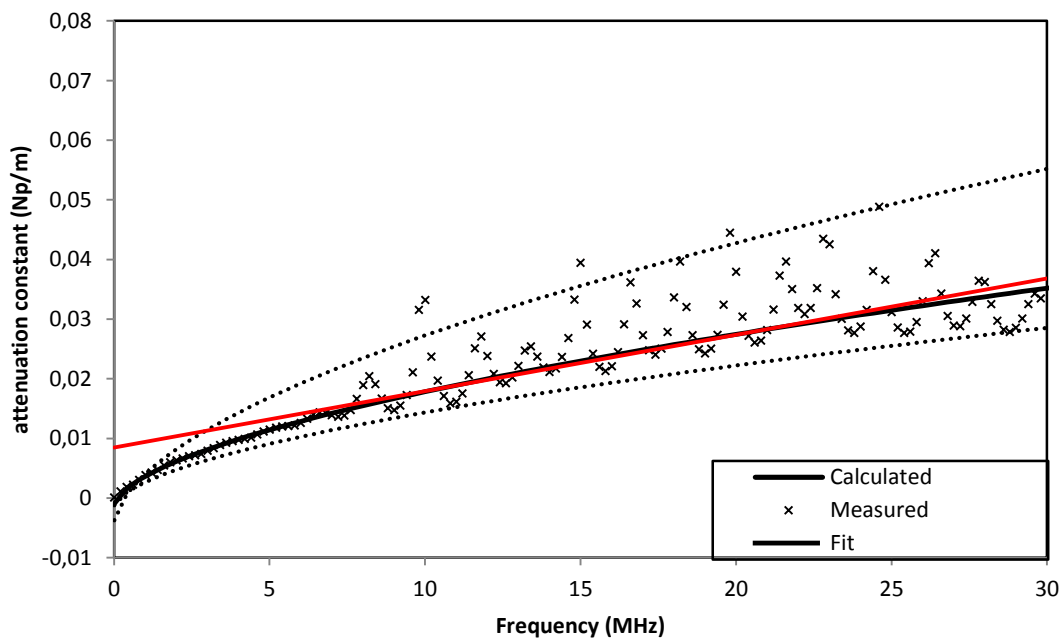


Figure 5.5: Attenuation parameters estimation

for an average value of  $\alpha_1 = 1 \times 10^{-9}(s/m)$  since neither the cable diameter nor the cable type is known. This does not exclude the fact that the network could also be heterogeneous. These parameters are our starting point in the parameter estimation technique. They can further be tuned to adapt to the particular network under study.

#### 5.4.2 Channel Impulse Response (CIR)

The channel impulsive response  $h(t)$  can be determined by means of the inverse Fourier transform (IFT) derived from the absolute value and phase of a measured transfer function [123]. Thus the time domain channel impulse response including cable loss is [124]:

$$h(t) = \sum_{i=1}^N I_i \cdot [A_t(t, vT_i) \otimes \delta(t - T_i)] \quad (5.5)$$

where  $I_i$ , and  $T_i$  are magnitude and delay of the  $i$ th path respectively;  $v$  is the TEM wave propagation speed in the cable which can be calculated according to the permittivity of the insulating material of the cable ( $v = c/\sqrt{\epsilon_r}$ ).  $A_t(t, vT_i)$  is the cable loss effect in the time domain evaluated as the inverse Fourier transform of (5.2) [124]. The results of Figure 5.6 show the impulse responses of three sample channels of Figure 5.4 as well as the associated group delays. The impulse responses depicted in Figure 5.6 shows some peaks which confirm the multipath characteristics of PLC channels. The main peak is followed by several consecutive peaks with descending magnitudes. The characteristic summary of the impulse responses is populated in Table 5.1. We consider the dominant peaks in each channel and record their time of occurrence as peak time ( $s$ ). The time interval between the peaks is calculated as  $Peak_i - Peak_{i-1}$  which can be translated into the difference in path lengths using  $d = c \times \Delta t$ . Considering a fairly linear phase characteristic, the group delay is determined as follows [145]:

$$\tau_g = -\frac{1}{2\pi} \cdot \frac{d\vartheta(f, t, l)}{df} \quad (5.6)$$

The impulse response of PLC transmission channels can be described by various time-domain parameters. There have been some thorough studies on PLC channels undertaken in the frequency range 1-30 MHz by [110], [111]. They observed that for 90% of the channels studied, an *rms* delay spread was below  $0.5 \mu s$ . In [122], considering the transmission frequency band 0.5-15 MHz, the maximum excess delay was found to be below  $3 \mu s$ . In the frequency range up to 30 MHz, it is found that, for 95% of the channels studied, the mean delay spread is between  $0.16 \mu s$  and  $3.2 \mu s$  and the same percentage of channels exhibit a delay spread between  $0.24 \mu s$  and  $2.5 \mu s$  [121].

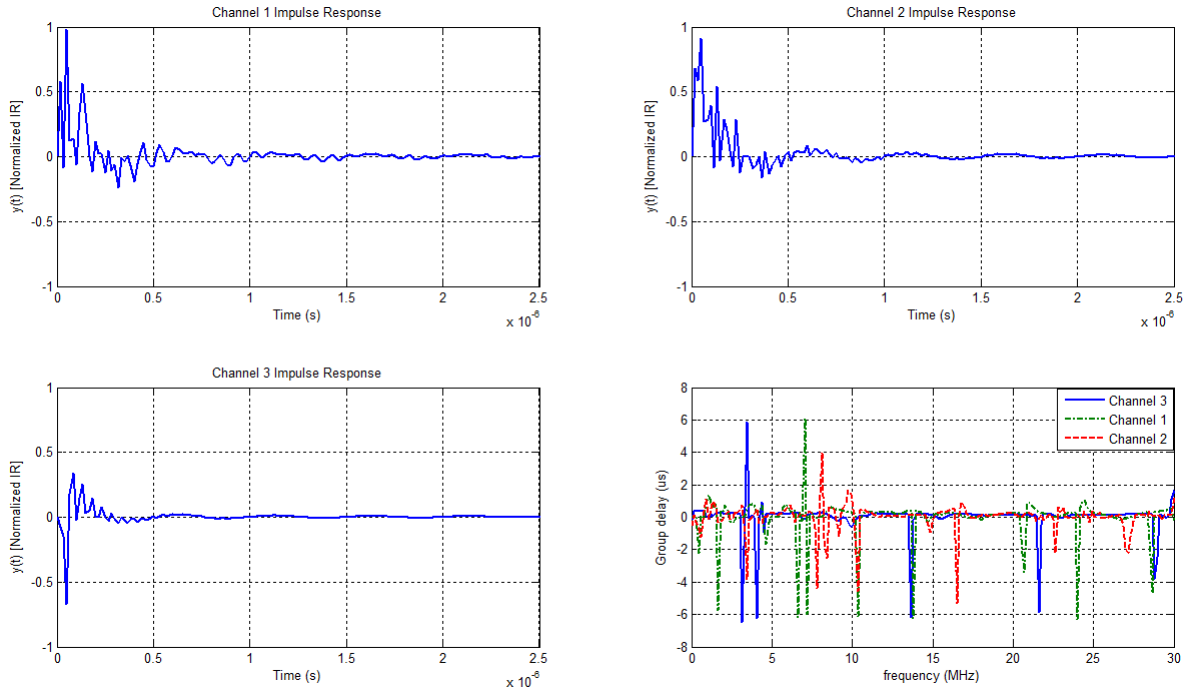


Figure 5.6: Impulse Response of figure (3) Channels and their corresponding group delays

Table 5.1: Impulse response summary of eight sample channels

Channel #	Peak #	$\tau_A (s)$	$Peak_i - Peak_{i-1}$	$d (m)$	$\tau_m (\mu s)$	$m_\tau (\mu s)$	$\sigma_\tau (\mu s)$
1	1	$5.00 \times 10^{-8}$		7.5	1.95	0.196	1.08
	2	$1.33 \times 10^{-7}$	$8.33 \times 10^{-8}$	12.5			
2	1	$5.00 \times 10^{-8}$		7.5	1.71	0.144	0.84
	2	$1.00 \times 10^{-7}$	$5.00 \times 10^{-8}$	7.5			
	3	$1.33 \times 10^{-7}$	$3.33 \times 10^{-8}$	5.0			
	4	$1.66 \times 10^{-7}$	$3.33 \times 10^{-8}$	5.0			
3	1	$5.00 \times 10^{-8}$		7.5	1.22	0.136	0.89
	2	$6.67 \times 10^{-8}$	$1.67 \times 10^{-8}$	2.5			
4	1	$1.00 \times 10^{-7}$	$3.33 \times 10^{-8}$	5.0	1.56	0.128	0.77
	2	$1.67 \times 10^{-7}$	$6.70 \times 10^{-8}$	10			
	3	$1.98 \times 10^{-7}$	$3.10 \times 10^{-8}$	4.7			
	4	$2.33 \times 10^{-7}$	$3.50 \times 10^{-8}$	5.3			
5	1	$5.00 \times 10^{-8}$		7.5	1.82	0.177	0.82
	2	$8.33 \times 10^{-8}$	$3.33 \times 10^{-8}$	5.0			
	3	$1.33 \times 10^{-7}$	$4.97 \times 10^{-8}$	7.5			
6	1	$5.00 \times 10^{-8}$		7.5	1.75	0.189	1.02
	2	$6.67 \times 10^{-8}$	$1.67 \times 10^{-8}$	2.5			
	3	$1.00 \times 10^{-7}$	$3.33 \times 10^{-8}$	5.0			
	4	$1.42 \times 10^{-7}$	$4.20 \times 10^{-8}$	6.3			
	5	$1.67 \times 10^{-7}$	$2.50 \times 10^{-8}$	3.8			
7	1	$5.00 \times 10^{-8}$		7.5	1.18	0.167	0.95
	2	$7.45 \times 10^{-8}$	$2.45 \times 10^{-8}$	3.7			
	3	$8.33 \times 10^{-8}$	$8.80 \times 10^{-9}$	1.32			
	4	$1.00 \times 10^{-7}$	$1.67 \times 10^{-8}$	2.5			

The three channels under study are successfully modelled as shown in Figure 5.7 using (5.3) and the notches are not underestimated or exaggerated in all the cases.

It is not realistic to expect a perfect fit since the model is constructed without any knowledge of the actual network topology and condition. Nonetheless, the ability of the model to capture unknown real PLC channels is demonstrated. The measured phase is also shown in the same figure to outline its non-linearity at notch frequencies. Between these notches, there exist frequency bands with linear phase details, and such bands could be combined for reliable transmission [136].

Since the impulse response (IR) and the transfer characteristics of a channel have a relationship based on the Fourier transform, intuitively one would deduce that if the transfer magnitude is characterized by more fades per bandwidth, a longer IR is expected. This can be quantified in terms of maximum excess delay of the channel. The results in Table 5.1 show that channel 1 and 2 have longer maximum excess delays (1.95 and 1.71  $\mu\text{s}$  respectively) compared to channel 3 with 1.22  $\mu\text{s}$ . This correlates with the results of Figure 5.4 where channel 1 and 2 are dominated by deep fades throughout the bandwidth. Channel 3, however, comprises of a single deep fade at 10 MHz. We further investigate the dispersive nature of the PLC channel derived from an ensemble of measurements performed as described in section 5.3 and present some of the data in Table 5.1. These also gives a clear picture of the PLC environment. The fifth column of Table 5.1,  $d(m)$ , represents the separation between the dominant reflectors in the power line network. Alternatively, this could be thought to represents the length of branches in the

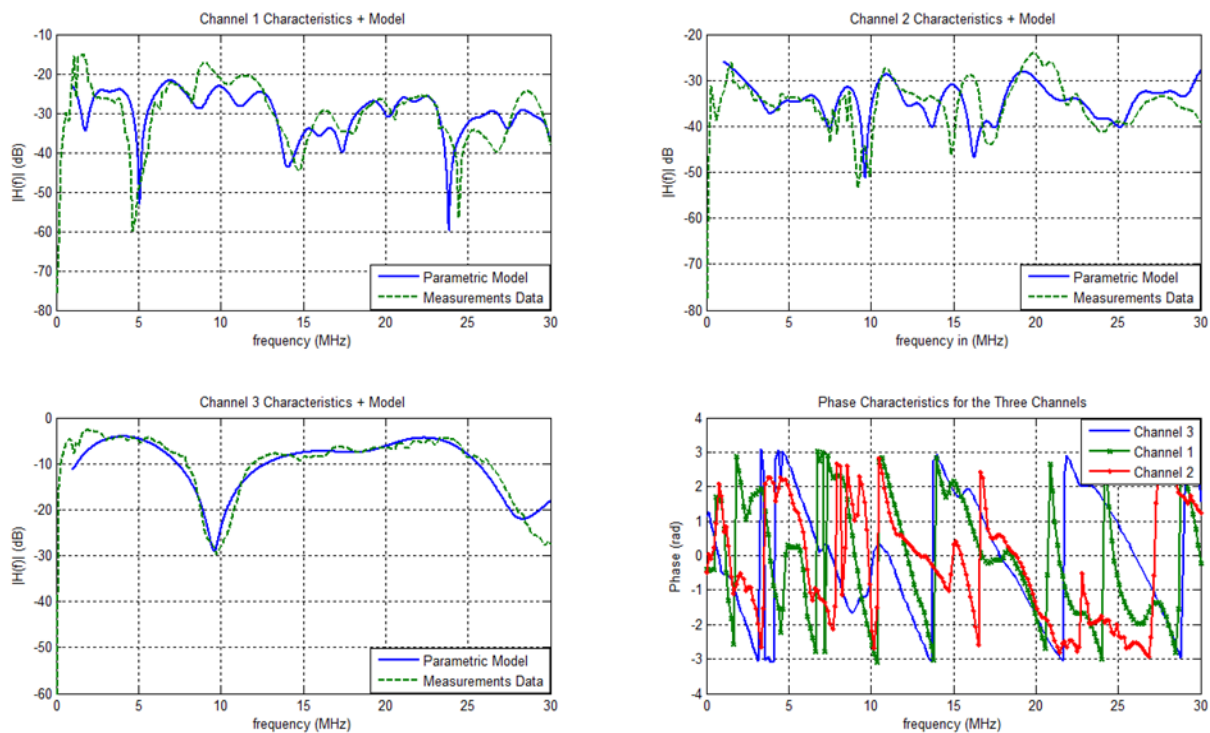


Figure 5.7: Modelled real CTFs and Their Phase Characteristics

network. It is noticeable from Table 1 that the first dominant reflection occurs after the same amount of time ( $5.0 \times 10^{-8} \text{s}$ ) for all measured channels which corresponds to a cable length of roughly 7.5 m. This tallies well with our measurement setup. A 7.5 m long power cable was consistently hooked to one of the network analyzer ports (specifically the transmitting end), simply to provide flexibility and reach during measurements. The network analyzer serves as both the transmitter and receiver simultaneously, thus, the two cannot be separated to accommodate long communication links within the building. This extension cable is generally regarded as part of the channel under investigation. Nonetheless, it can easily be calibrated out of the measurements since we know that it will cause the first reflection at the point of connection. Therefore, we consider it our reference point in the measurements and measure every other reflection off it. For our model, as given by (5.3), we need to establish the distribution of branches in typical indoor power line networks in order to be able to estimate the associated behavior. As presented in Table 5.1, different path lengths exist within the PLC network. By taking the average of an ensemble of these lengths from all the impulse responses derived from the CTFs measured, we determine that typically there exist a branch every 4.5 m in the network. Considering other factors such as propagation velocity, measurement resolution, network heterogeneity and other factors involved in the computation of the relevant parameters leading to the determination of this cable lengths, it is advisable to rather use a value less than 4.5 m in the model. This exaggerates the population of branches per unit transmitter-receiver separation distance.

### 5.4.3 Channel Model Parameters

Utilizing the model discussed in sub-section 5.4.1, we generated channel models based on the parameters in Table 5.2. We consider the fact that indoor propagation involves a significantly high number of short paths, and thus we chose the Poisson arrival process intensity  $\Lambda = 1/3[\text{m}^{-1}]$ . This corresponds to an average of a single reflector (branch) every 3 m. This is simply because our measurements were taken in laboratories, environments populated with multiple power outlets (roughly within 3 m of each other) for multiple users as seen in Table 5.1. The same goes for a post-graduate office which houses 6-7 post-graduates. The first ray is set at  $d_1$  with exponential distribution and the maximum path length is taken to be 200 m.

Table 5.2: Model parameters for three simulated channels of Figure 3.

Channel #	$a_0(\text{m}^{-1})$	$a_1(\text{s/m})$	$N_i$	$K$
1	5E-3	4.5E-9	50	0.8
2	2.5E-3	5.5E-9	40	0.8
3	4E-3	2E-11	15	0.8

Frequency parameters  $B_1$  and  $B_2$  were set to 1 MHz and 30 MHz respectively and the value of  $K=0.8$  was used in all the cases.

Our initial estimates of  $a_0 = 1 \times 10^{-3}(m^{-1})$ ,  $a_1 = 1 \times 10^{-9}(s/m)$ , and  $K=1$  were not too far from the final values, though further tuning of these parameters was required as we see in Table 5.2. We also notice that it took a considerably smaller number of paths to model channel 3 as compared to both Channel 1 and 2. This is foreseeable from the CTFs of Figure 5.4 given the spread of notches within the band considered. Thus, channel 1 and 2 have many significant signal paths leading to the receiving end. The parameter  $N_i$  thus acts as the accuracy controller for the model, with certain channels requiring consideration of more number of paths than others for the same accuracy.

## 5.5 Chapter Summary

In this chapter, we have modeled the complex frequency response of real-world PLC channels using multipath signal propagation technique in the 1-30 MHz frequency range. The time-domain technique allows us to capture the response of any power line topology by describing the model parameters as random variables. The number of paths are described to follow a Poisson arrival process while the path lengths follows an exponential distribution. The model accuracy is controlled by the number of dominant paths considered and by altering other feed parameters, the model can successfully be tuned to describe respective PLC channels. The applicability of the model to complex networks with unknown parameters is demonstrated with good agreement between simulation and measurement results as shown in Figure 5.7. The motivation for this approach derives from the desire to utilize existing indoor power networks to establish high speed communication links. In most cases the architecture of the network is not readily available; hence we sought for solutions that require little knowledge about the network.

To compare different multipath channels in the quest to develop some general guidelines for PLC systems, we have used parameters which grossly quantify the multipath channel. These are in the form of maximum excess delay  $\tau_m$ , mean excess delay  $m_\tau$ , and *rms* delay spread  $\sigma_\tau$ . It has been found that typical values of *rms* delay spread are in the order of  $\mu s$  in real PLC channels, comparable to outdoor mobile radio channels. The *rms* delay spread provides a good indication of the multipath spread. In digital communications, the *rms* delay spread in comparison with the symbol duration gives an indication as to whether the channel requires equalization to avoid inter-symbol interference (ISI) or not. This is popular in OFDM and CDMA communication systems. The most significant contribution to *rms* delay spread is due to strong reflections with long delays [123].

The general conclusion derived from our results is that heavily branched PLC channels will require a consideration of a high number of paths in the solution process due to increased path significance as compared to channels with relatively low branch density as shown in Table 5.2. Our test environment consists of such short paths through which the reflected signals arrives at the receiver end with high energies.



## CHAPTER SIX

### CONCLUSIONS AND FUTURE DIRECTIONS

The future smart grid systems will autonomously monitor and control energy systems to improve their efficiency and reliability. Intelligent control and monitoring requires low delays, highly reliable and two-way communication between customers, local utilities and regional utilities. In the present age of information technology, the current focus is on creation as well as dispersion of information. In order to be able to reach end users for the provision of information, alternative delivery mechanisms are required. Conventional technologies currently being employed include telephone loops, Ethernet cables, fibre optics, wireless and satellite technologies. Nonetheless, each technology has its own limitations in terms of cost and availability to reach the maximum number of consumers.

Despite its potential to become a successful and widespread technology enabling high speed broadband internet and numerous network applications, PLC technology suffers from serious challenges from noise and channel attenuation which are the main channel impairments. These challenges result from the fact that the power line network was not originally intended for data transport, therefore PLC systems inherit the harsh intrinsic attributes of the power line. In this dissertation, the behaviour of noise is studied through measurements and presented. The multipath propagation behaviour of power line networks is studied by determining its dispersive characteristics through time-delay parameters, and finally a multipath model is proposed and implemented to capture the transfer characteristics of practical power lines. The studies conducted during the author's MSc candidature resulted in the publication of two internationally refereed conference papers and the submission of a journal paper.

#### 6.1 Summary of Results

- Through measurements carried out in practical indoor power line networks, the noise characteristics were investigated. We found that impulsive noise is the most dominant in PLC channels, especially cyclostationary impulsive noise. This is highly influenced by the devices connected to the electrical network, switching at every zero-crossing of the mains signal. However, there's still a strong presence of asynchronous impulsive noise and we collectively characterize them as simply impulsive noise to determine its statistics. It is from these statistics that reliable noise models are derived. Background noise is also captured by a simple three parameter model. The model performs well when the effects of narrowband interference are eliminated, validating its suitability (see Figure 3.8). The strong presence of narrowband interference within the 1 – 30 MHz band affects the accuracy of the model (see Figure 3.9),

leading to exaggerated noise levels. However, its simplicity and ability to capture background noise macroscopically remains an attractive feature.

- An indoor PLC channel measurement campaign has been established to determine the time dispersive characteristics of these channels through time-delay parameters. The statistics of the time-delay parameters as well as coherence bandwidth and its relation to RMS delay spread in the frequency range up to 30 MHz are provided. We have observed the inverse relationship between coherence bandwidth and RMS delay spread as given by (4.7). The frequency correlation function is also found to decrease rapidly with frequency separation. This is expected given the nature of the channel. Between any two neighbouring frequencies it is difficult to find a flat response as their separation is increased. The 90<sup>th</sup> percentile of the RMS delay spread was found to be between 0.04 $\mu$ s and 0.55 $\mu$ s with a mean of 0.287 $\mu$ s and standard deviation of 0.222 $\mu$ s. 80% of the measured channels exhibit estimated values of coherence bandwidth between 600 kHz and 90 kHz. We thus, however, take note that for improved accuracy and consistency a lot more data still needs to be captured and incorporated into our analysis. Also, for improved coherence bandwidth estimation, smaller frequency steps are required for increased data points within the band of interest.

Comparatively, the relationship between coherence bandwidth and RMS delay spread as shown in (4.7) is very close to that obtained by [123]. The comparisons in Table 4.1 also show closeness in terms of bounds for other time delay parameters for indoor PLC channels. We also take note of the difference in bandwidth consideration in our case and that of [123], which considers frequencies up to 100 MHz. In terms of system design, desired values of  $\tau_{rms}$  are those that result in high coherence bandwidth as this translates to faster symbol transmission rate, and the coherence bandwidth of the channel is particularly relevant to frequency-hopping spread spectrum (FHSS) systems [128] and other multi-carrier systems such as OFDM. In digital transmission, inter-symbol interference (ISI) will be avoided as long as the RMS delay spread is smaller compared to the symbol period ( $T$ ) of the digital modulation. Should this not be the case, channel equalization will be required.

- Finally, we have modeled the complex frequency response of practical PLC channels using a multipath signal propagation technique in the 1-30 MHz frequency range. The applicability of the model to complex networks with unknown parameters is demonstrated with good agreement between simulation and measurement results as shown in Figure 5.7. The motivation for this approach derives from the desire to utilize existing indoor power networks to establish high speed communication links. In most cases the architecture of the network is not readily available; hence we sought for solutions that require little knowledge about the network. The

model parameters were derived from the measured data through cable attenuation profiles and channel impulse responses. From the channel IR we are able to derive the topology of the network in terms of the energy carried by the most significant paths from transmitter to receiver. This difference in the path lengths provides useful information in terms of the arrival delay distribution of the reflected signals.

## 6.2 Possible Future Work

There are several aspects of power line communications in this dissertation that can be extended through further research as follows:

- In chapter 3 we studied the characteristics of noise in power line networks. The analysis of both time and frequency domain measurements enabled us to study impulsive and background noise respectively. Whilst the signal processing algorithms employed in each case depends on the individual circumstance of the noise component under analysis, a high-resolution spectral analysis is required. An alternative solution is to design a custom data acquisition (DAQ) board with a much higher resolution than 8 bits (currently used-instrument limitation). This would greatly improve the capturing of noise terms and ultimately more accurate models can be developed.
- The multipath propagation PLC channel model presented in chapter 5 can be optimized to intelligently consider only the optimum paths in its calculations. This obviously requires a threshold constraint. In chapter 4, we determined the dispersive characteristics of a power line in terms of its time-delay spread parameters where a power threshold was set (-30 dB) and these parameters defined within this threshold. An intelligent model can be built such that it evaluates only the paths,  $N$ , which satisfies this threshold. All the other paths carrying energy less than the threshold will be regarded as noise. The significance of this modification is in its computational efficiency.
- In this work, statistical analysis of impulsive noise components from data collected has been studied and presented. This provides the starting point towards the development of realistic and consistent noise models with more measurements and data collection coupled with accuracy enhancements as suggested in the first bullet.

## REFERENCES

1. Owen Rubin, "Plug Into Home Networks", *IEEE Spectrum*, pp. 60-62, June 2002.
2. H.-K Podszcek, *Carrier Communication over Power Lines*, 4th Edition, New York: Springer-Verlag, 1972.
3. K. Dostert, *Powerline Communications*, Englewood Cliffs, NJ: Prentice-Hall, 2001.
4. O. Hooijen, *Aspects of Residential Power Line Communications*, Aachen: Shaker Verlag, 1998.
5. A. J. Baggot, B. E. Eyre, G. Fielding, F. M. Gray, "Use of London's electricity supply system for centralized control," *Proceedings of the IEE*, vol. 125(4), April 1978, pp. 311-327.
6. A. Forrest, F. M. Gray, "Maximum demand limitation by the automatic and remote control of nonessential loads using the supply network as the communications medium," *Proceedings of the 3rd International Conference on Metering Apparatus and Tariffs for Electricity Supply, (MATES '77)*, London, UK, 15-17 November 1977, pp.112-116.
7. D. Radford, "Spread-spectrum data leap through ac power wiring," *IEEE Spectrum*, Nov. 1996, pp. 48-53.
8. P. A. Brown, "Power line communications - past, present, and future," *Proceedings of the 3rd International Symposium on Power-Line Communications and its Applications (ISPLC'99)*, Lancaster, UK, 30 March - 1 April 1999, pp. 1-8.
9. K. H. Afkhamie, S. Katar, L. Yonge, and R. Newman, "An Overview of the upcoming HomePlug AV Standard," *Proceedings of the 9th International Symposium on Power-Line Communications and its Applications (ISPLC'05)*, Vancouver, Canada, 6-8 April 2005, pp. 400-404.
10. IEEE Guide for Power-Line Carrier Applications, IEEE Standard 643-1980.
11. A. J. Snyders, H. C. Ferreira, P. A. Janse van Rensburg, "Carrier gain adjustment for improved power-line signal-to-noise ratios," *Proceedings of the 10th International Symposium on Power-Line Communications and its Applications (ISPLC'06)*, Orlando, USA, 26-29 March 2006, pp. 39-43.
12. Anatory, N. Theethayi, M. Kissaka, N. Mvungi, "Broadband power line communications: the factors influencing wave propagations in the medium voltage lines," *Proceedings of the 11th International Symposium on Power-Line Communications and its Applications (ISPLC'07)*, Pisa, Italy, 26-28 March 2007, pp. 127-132.

13. H. C. Ferreira, H. M. Grové, O. Hooijen, and A. J. H. Vink, *Power Line Communication* (in Wiley Encyclopedia of Electrical and Electronics Engineering), New York: John Wiley & Sons, 1999, pp. 706-716.
14. H. C. Ferreira, "PLC issues in emerging countries: technical and economical factors for the developments of potential PLC markets" ISPLC 07 Panel Session II in Proceedings of the 11th International Symposium on Power-Line Communications and its Applications (ISPLC'07), Pisa, Italy, 26-28 March 2007.
15. F. Zwane and T. J. O. Afullo, "An alternative Approach in Power Line Communication Channel Modelling," *Progress in Electromagnetics Research C (PIERC)*, vol. 47, pp. 85-93, 2014.
16. M. Mosalaosi, Thomas J. O. Afullo, "Broadband Analysis and Characterization of Noise for In-Door Power-Line Communication Channels", *Progress In Electromagnetics Research Symposium Proceedings (PIERS)*, Guangzhou, China, Aug. 25-28, 2014, pp. 719-723.
17. M. Mosalaosi, T. J. O. Afullo, "Dispersive Characteristics for Broadband Indoor Power-Line Communication Channels", *Southern Africa Telecommunication Networks and Applications Conference (SATNAC)*, pp. 313-317, 30 Aug.-03 Sep., 2014
18. J. Newel, "History and theory of ripple communication systems," *Conference Record of the 1976 National Telecommunications Conference (NTC'76)*, Dallas, USA, 29 November - 1 December 1976, pp. 2.3.1-2.3.6.
19. G. Lokken, N. Jagoda, R. J. D'Autenil, "The proposed Winconsin Electrical Power Company load management system using power line carrier over distribution lines," *Conference Record of the 1976 National Telecommunications Conference (NTC'76)*, Dallas, USA, 29 November - 1 December 1976, pp. 2.2.1-2.2.3.
20. G. Kaplan, "Two-way communication for load management," *IEEE Spectrum*, vol. 14(8), August 1977, pp.47-50.
21. B. E. Eyre, "Results of a comprehensive field trial of a United Kingdom customer telemetry system using mainsborne signaling," *Proceedings of the 5th International Conference on Metering Apparatus and Tariffs for Electricity Supply (MATES '87)*, London, UK, 13-16 April 1987, pp. 252-256.
22. M. C. King, "Experimental systems for tele-reading over the low-voltage network," *Proceedings of the 6<sup>th</sup> International Conference on Metering Apparatus and Tariffs for Electricity Supply, (MATES '90)*, London, UK, 3-5 April 1990, pp. 154-157.

23. C. Nunn, P. M. Moore, P. N. Williams, "Remote meter reading and control using high-performance PLC communications over the low voltage and medium voltage distribution networks," *Proceedings of the 7<sup>th</sup> International Conference on Metering Apparatus and Tariffs for Electricity Supply, (MATES '92)*, London, UK, 17-19 November 1992, pp. 304-308.
24. W. Downey, "Central control and monitoring in commercial buildings using power line communications," *Proceedings of the 1st International Symposium on Power-Line Communications and its Applications (ISPLC'97)*, Essen, Germany, 2-4 April 1997, pp.115-119.
25. N.-H. Ahn, T.-G. Chang, H. Kim, "A systematic method of probing channel characteristics of home powerline communication network," *Digest of Technical Papers: 21st International Conference on Consumer Electronics (ICCE'02)*, Atlanta, USA, 18-20 June 2002, pp. 378-379.
26. J. O. Onunga, R. W. Donaldson, "Personal computer communications on intrabuilding power line LAN's using CSMA with priority acknowledgements," *IEEE Journal on Selected Areas of Communication*, vol. 7(2),February 1989, pp. 180-191.
27. D. Tuite, "Power line spread-spectrum saves copper in LAN's and control systems," *Computer Design*, November 1992, pp. 50-53.
28. R. Dettmer, "The net effect," *IEE Review*, March 1995, pp. 67-71.
29. <http://www.echelon.com/applications> (05 December 2014)
30. <http://www.yitran.com/index.aspx?id=3327> (05 December 2014)
31. <http://www.advanced.com/about/quality-compliance/> (05 December 2014)
32. <http://www.cogency.com> (05 December 2014)
33. <http://www.intellon.com> (05 December 2014)
34. <http://www.powerlinecommunications.net> (05 December 2014)
35. <http://www.homeplug.org> (05 December 2014)
36. J. Auvray, M. Fourrier, *Problems in Electronics, including lumped constants, transmission lines and high frequencies*, ISBN 0-08-016982-1, Oxford: Pergamon Press, 1973.
37. C. Bowick, *RF Circuit Design*, Carmel: Howard W. Sams & Co, 1991.

38. P. Sutterlin, "A power line communication tutorial – challenges and technologies," *Proceedings of the 2<sup>nd</sup> International Symposium on Power-Line Communications and its Applications (ISPLC'98)*, Tokyo, Japan, 24-26 March 1998, pp. 15-20.
39. R. M. Vines, H. J. Trussel, K. C. Shuey, J. B. O'Neal, Jr., "Impedance of the residential power-distribution circuit," *IEEE Transactions on Electromagnetic Compatibility*, vol. EMC-27(1), February 1985, pp. 6-12.
40. O.G. Hooijen, "On the relation between network-topology and power line signal attenuation," *Proceedings of the 2nd International Symposium on Power-Line Communications and its Applications (ISPLC'98)*, Tokyo, Japan, 24-26 March 1998, pp. 45-56.
41. C. R. Perez, "An automatic impedance adapter for medium-voltage communications equipment," *Proceedings of the 4th International Symposium on Power-Line Communications and its Applications (ISPLC'00)*, Limerick, Ireland, 5-7 April 2000, pp. 218-224.
42. D. Chaffanjon, "A real knowledge of propagation: the way of efficiency and reliability making PLC generalization feasible," *Proceedings of the 2nd International Symposium on Power-Line Communications and its Applications (ISPLC'98)*, Tokyo, Japan, 24-26 March 1998, pp. 57-66.
43. M. H. L. Chan, R. W. Donaldson, "Attenuation of communication signals on residential and commercial intrabuilding power-distribution circuits," *IEEE Transactions on Electromagnetic Compatibility*, vol. EMC-28(4), November 1986, pp. 220-230.
44. H. Dalichau, "Evaluation of different frequency bands regarding their qualification for in-house powerline communication," *Proceedings of the 5th International Symposium on Power-Line Communications and its Applications (ISPLC'01)*, Malmö, Sweden, 4 -6 April 2001, pp. 203-210.
45. P. Favre et al, "Common mode current and radiations mechanisms in PLC networks," *Proceedings of the 11<sup>th</sup> International Symposium on Power-Line Communications and its Applications (ISPLC'07)*, Pisa, Italy, 26-28 March 2007, pp. 348-354.
46. H. Dalichau, "EMC aspects of inhome-PLC: crosstalk between neighbouring apartments...", *Proceedings of the 6th International Symposium on Power-Line Communications and its Applications (ISPLC'02)*, Athens, Greece, 27-29 March 2002, pp. 218-224.
47. P. A. Jansen Van Rensburg, "Effective Coupling for Power Line Communications", *Doctoral Thesis*, University of Johannesburg, 2008.

48. K. Dostert, "New PLC approaches for high speed indoor digital networks," *Proceedings of the 5th International Symposium on Power-Line Communications and its Applications (ISPLC'01)*, Malmö, Sweden, 4 -6 April 2001, pp.253-258.
49. A. Klip, "A short overview of the possibilities in PLC, inside and outside the private house," *Proceedings of the 1st International Symposium on Power-Line Communications and its Applications (ISPLC'97)*, Essen, Germany, 2-4 April 1997, pp. 120-126.
50. P. A. Brown, "Directional coupling of high frequency signals onto power networks," *Proceedings of the 1<sup>st</sup> International Symposium on Power-Line Communications and its Applications (ISPLC'97)*, Essen, Germany, 2-4 April 1997, pp. 121-126.
51. L. M. Milanta, M. M. Forti, "A classification of the power-line voltage disturbances for an exhaustive description and measurement," *Symposium Record of the 1989 IEEE International Symposium on Electromagnetic Compatibility (EMC'89)*, 8-10 September 1989, pp. 332-336.
52. R. M. Vines, H. J. Trussel, L. J. Gales, J. B. O'Neal Jr., "Noise on residential power distribution circuits," *IEEE Transactions on Electromagnetic Compatibility*, vol. EMC-26(4), November 1984, pp. 161-168.
53. S. N. Talukdar, J.C Dangelo, "Uncertainty in distribution PLC attenuation models," *IEEE Transactions on Power Apparatus and Systems*, vol. PAS-99(1), January / February 1980, pp. 328-334.
54. A. Schiffer, "Statistical channel and noise modeling of vehicular dc-lines for data communication," *Proceedings of the 51st IEEE Vehicular Technology Conference (VTC 2000 - Spring)*, Tokyo, Japan, 15-18 May 2000, pp. 158-162.
55. J. C. Dangelo, S. N. Talukdar, "A stochastic model for PLC systems," *IEEE Transactions on Power Apparatus and Systems*, vol. PAS-100(11), November 1981, pp. 4464-4472.
56. A. Voglsgang, T. Langguth, G. Korner, H. Steckenbiller, R. Knorr, "Measurement, characterization and simulation of noise on powerline channels," *Proceedings of the 4th International Symposium on Power-Line Communications and its Applications (ISPLC'00)*, Limerick, Ireland, 5-7 April 2000, pp. 139-146.
57. D. Benyoucef, "A New Statistical Model of the Noise Power Density Spectrum for Powerline Communication," *Proceedings of the 7th International Symposium on Power-Line Communications and its Applications (ISPLC'03)*, Kyoto, Japan, 26-28 March 2003, pp. 136-141.



58. G. Marubayashi, "Noise measurements of the residential powerline," *Proceedings of the 1st International Symposium on Power-Line Communications and its Applications (ISPLC'97)*, Essen, Germany, 2-4 April 1997, pp.104-108.
59. Carcelle Xavier, "Power Line Communications in Practice", *Artech House Publishers*, 2009
60. M. Harris, "Power-line communications – a regulatory perspective," *Proceedings of the 3rd International Symposium on Power-Line Communications and its Applications (ISPLC'99)*, Lancaster, UK, 30 March - 1 April 1999, pp. 131-138
61. J. Newbury, "Regulatory requirements for power-line communications systems operating in the high frequency band," *Proceedings of the 5th International Symposium on Power-Line Communications and its Applications (ISPLC'01)*, Malmö, Sweden, 4 -6 April 2001, pp. 305-310.
62. P. Strong, "Regulatory & consumer acceptance of powerline products," *Proceedings of the 5th International Symposium on Power-Line Communications and its Applications (ISPLC'01)*, Malmö, Sweden, 4 -6 April 2001, pp.175-184.
63. K. Dostert, "Power line Communications", Prentice-Hall, NJ, 2001.
64. G. Held, "Understanding Broadband over Power Line", Auerbach Publications, New York, 2001.
65. H. C. Ferreira, L. Lampe, J. Newbury and T. G. Swart, "Power Line Communications: Theory and applications for narrowband and broadband communications over power lines", John Wiley & Sons, 2006.
66. X. Carcelle, "Power Line Communications in Practice", Artech House, London, 2006.
67. M. S Yousuf and M. El-Shafei, "Power line communications: an overview - part 1", *Proc. of Innovations '07*, pp. 218-222. Nov. 2007.
68. M. S Yousuf, S. Z. Rizvi and M. El-Shafei, "Power line communications: an overview - part 2", *Proc. 3rd Int'l Conf. Info. and Commun. Technologies: From Theory to Applications*, pp. 1-6. Apr. 2008.
69. K. S. Al Mawali, "Techniques for Broadband Power Line Communications: Impulse Noise Mitigation and Adaptive Modulation," *Doctoral Thesis*, RMIT University, July 2011
70. M. Zimmermann and K. Dostert, "Analysis and modelling of impulsive noise in broad-band powerline communications", *IEEE Trans. Electromagn. Compat.*, Vol. 44, No. 1, pp. 249-258, Feb. 2002.

- 71 M. Götz, M. Rapp and K. Dostert, "Power line channel characteristics and their effect on communication systems design", *IEEE Commun.Magazine*, Vol. 42, No. 4, pp. 78-86, Apr. 2004.
- 72 H. Meng, Y. L. Guan and S. Chen, "Modeling and analysis of noise effects on broadband power-line communications", *IEEE Trans. Power Delivery.*, Vol. 20, No. 2, pp. 630-637, Apr. 2005.
- 73 E. Biglieri and P. Torino, "Coding and modulation for a horrible channel", *Commun. Magazine*, Vol. 41, No. 5, pp. 92-98, May 2003.
- 74 T. Banwell and S. Galli, "A novel approach to the modeling of the indoor power line channel part 1: circuit analysis and companion model", *IEEE Trans. Power Delivery*, Vol. 20, No. 2, pp. 655-663, Apr. 2005.
- 75 M. Zimmermann, K. Dostert, "A multipath model for the power line channel", *IEEE Trans. Commun.*, Vol. 50, No. 4, pp. 553-559, Apr. 2002.
- 76 H. Philipps, "Modelling of powerline communication channels", *Proc. of the Int'l Symp. Power Line Commun. and its Applic. (ISPLC 1999)*,UK, pp. 14-21, Mar. 1999.
- 77 S. Meng, S. Chen, Y.L. Guan; C.L. Law, P.L. So, E. Gunawan and T.T. Lie, "A transmission line model for high-frequency power line communication channel", *Proc. of Int'l Conf. Power Sys. Tech. (PowerCon)*,Vol. 2, pp. 1290-1295, Oct. 2002.
- 78 O. G. Hooijen, "On the relation between network topology and power line signal attenuation", *Proc. of the Int'l Symp. Power Line Commun. and its Applic. (ISPLC 1998)*, Japan, pp. 45-56, Mar. 1998.
- 79 M. Zimmermann, K. Dostert, "A multi-path signal propagation model for the power line channel in the high frequency range", *Proc. of the Int'l Symp. Power Line Commun. And its Applic. (ISPLC 1999)*, pp. 45-51, Mar. 1999.
- 80 C. R. Paul, "Analysis of Multiconductor Transmission Lines", John Wiley & Sons, 1994.
- 81 P. Amirshahi, S. M. Navidpour and M. Kavehrad, "Performance analysis of uncoded and coded OFDM broadband transmission over low voltage power-line channels with impulsive noise", *IEEE Trans. Power Delivery*, Vol. 21, No. 4, pp. 1927-1934, Oct. 2006.
- 82 M. H. Chan and R. W. Donaldson, "Amplitude, width and interarrival distributions for noise impulses on intrabuilding power line communication networks", *IEEE Trans. Electromagn. Compat.*, Vol. 31, No. 3, pp.320-323, Aug. 1989.

- 83 L. T. Tang, P. L. So, E. Gunawan, S. Chen, T. T. Lie and Y. L. Guan, "Characterization of power distribution lines for high-speed data transmission", *Proc. of Int'l. Conf. Power Sys. Tech. (PowerCon 2000)*, Vol. 1, pp. 445-450, Aug. 2002.
- 84 D. Middleton, "Statistical-physical models of electromagnetic interference", *IEEE Trans. Electromagn. Compat.*, Vol. EMC-19, No. 3, pp.106-127, Aug. 1977.
- 85 A. Spaulding and D. Middleton, "Optimum Reception in an Impulsive Interference Environment—Part I: Coherent Detection", *IEEE Trans. Commun.*, Vol. 25, No. 9, pp. 910-923, Sep. 1977.
- 86 D. Middleton, "Procedures for Determining the Parameters of the First-Order. Canonical Models of Class A and Class B Electromagnetic Interference", *IEEE Trans. Electromagn. Compat.*, Vol. EMC-21, No. 3, pp.190-208, Aug. 1979.
- 87 N. Andreadou and F.N Pavlidou, "PLC Channel: Impulsive Noise Modelling and Its Performance Evaluation Under Different Array Coding Schemes", *IEEE Trans. Commun.*, Vol. 24, No. 2, pp. 585-595, Apr.2009.
- 88 H. Matsuo, D. Umehara, M. Kawai and Y. Morihiro, "An iterative detection for OFDM over impulsive noise channel", *Proc. of the Int'l Symp. Power Line Commun. and Its Applic. (ISPLC 2002)*, pp. 213-217, Mar. 2002.
- 89 R. Pighi, M. Franceschini, G. Ferrari and R. Raheli, "Fundamental performance limits for PLC systems impaired by impulsive noise", *Proc. of the IEEE Int'l Symp. Power Line Commun. and its Applic. (ISPLC2006)*, pp. 277-282, Mar. 2006.
- 90 R. Pighi, M. Franceschini, G. Ferrari and R. Raheli, "Fundamental performance limits of communications systems impaired by impulsive noise", *IEEE Trans. Commun.*, Vol. 57, No. 1, pp. 171-182, Jan. 2009.
- 91 M. Ghosh, "Analysis of the effect of impulsive noise on multicarrier and single carrier QAM systems", *IEEE Trans. Commun.*, Vol. 44, No. 2, pp. 145-147, Feb 1996.
- 92 Y. H. Ma, P. L. So, and E. Gunawan, "Performance analysis of OFDM systems for broadband power line communications under impulsive noise and multipath", *IEEE Trans. Power Delivery*, Vol. 20, No. 2, pp. 674-681, Apr. 2005.
- 93 O. G. Hooijen, "On the channel capacity of the residential power circuit used as a digital communications medium", *IEEE Commun. Letters*, Vol. 2, No. 10, pp. 267-268, Oct. 1998.

- 94 S. Zhidkov, "Analysis and comparison of several simple impulsive noise mitigation schemes for OFDM receivers", *IEEE Trans. Commun.*, Vol. 56, No. 1, pp. 5-9, Jan. 2008.
- 95 S. Zhidkov, "Performance analysis and optimization of OFDM receivers with blanking nonlinearity in impulsive noise environment", *IEEE Trans. Vehicular Technology*, Vol. 55, No. 1, pp. 234-238, Jan. 2006.
- 96 S. V. Vaseghi, "Advanced digital signal processing and noise reduction", 3<sup>rd</sup> ed, John & Wiley Sons, England, 2006.
- 97 L. Di Bert, P. Caldera, D. Schwingshack, and A. M. Tonello, "On Noise Modeling for Power Line Communications", *Proceedings of the IEEE ISPLC 2011*, p. 283-288.
- 98 H. dai and H. V. Poor, "Advanced Signal Processing for Power line Communications", *IEEE Communications Magazine*, vol. 41, no. 5, pp. 100-107, 2004.
- 99 A. Maiga, J. Y. Baudais, and J. F. Herald, "Very High Bit Rate Power Line Communications for Home Networks", *Proceedings of the IEEE ISPLC 2009*, Dresden, Germany, p. 313-318, 2009.
- 100 N. Sawada, T. Yamazato, and M. katayama, "Bit and Power Allocation for Power-Line Communications Under Nonwhite and Cyclostationery Noise Environment", *Proceeding of the IEEE ISPLC 2009*, Dresden, Germany, p. 307-312, 2009.
- 101 M. Tlich, A. Zeddami, F. Moulin, and F. Gauthier, "Indoor Powerline Communications Channel Characterisation up to 100 MHz-Part I: One-Parameter Deterministic Model", *IEEE Trans. Power Delivery*, 23(3): p. 1392-1401, 2008.
- 102 M. Tlich, A. Zeddami, F. Moulin, and F. Gauthier, "Indoor Powerline Communications Channel Characterisation up to 100 MHz-Part II: Time-Frequency Analysis", *IEEE Trans. on Power Delivery*, 23(3): p. 1402-1409, 2008.
- 103 M. Tlich, H. Chaouche, A. Zeddami, and P. Pagani, "Novel Approach for PLC Impulse Noise Modeling", *Proceeding of the IEEE ISPLC 2009*, Dresden, Germany, p. 20-25, 2009.
- 104 D. Umehara, S. Denno, and M. Morikura, "The influence of Compact AC Adapter on PLC Equipment", in *IEICE*, 2008, p. 55-60, 2008.
- 105 M. Zimmermann, "An Analysis of the Broadband Noise Scenario in Power-Line Networks", *proceeding of the IEEE ISPLC 2000*, Limerick, Ireland, p. 131-138, 2000.

- 106 V. Guillet, G. Lamarque, P. Ravier, and C. Leger, "Improving the Power Line Communication Signal-to-Noise Ratio During a Resistive Load Commutation", *Journal of Communication Magazine*, 4(2): p. 126-132, 2009.
- 107 J. A. Cortes, L. Diez, F. J. Canete, and J. J. Sanchez-Matinez, "Analysis of the Indoor Broadband Power-Line Noise Scenario," *IEEE transactions on Electromagnetic Compatibility*, VOL. 52, NO. 4, November 2010.
- 108 J. Lin and B. L. Evans, "Cyclostationary Noise Mitigation in Narrowband Powerline Communications," *Proc. APSIPA Annual Summit and Conference*, Dec 2012
- 109 Regis J. Bates, Donald W. Gregory, Bud Bates, "Voice and Data Communications Handbook", ISBN-0-07-213188-8, Osborne/McGraw-Hill, 2001.
- 110 T. Esmalian, F. R. Kschischang, and P. Glenn Gulak, "In-building Power Lines as High Speed Communication Channels: Channel Characterization and a test Channel Ensemble", *Int. J. Comm. Sys.* Vol. 16, pp. 381-400, June 2003.
- 111 V. degardin, M. Lienard, A. Zeddami, F. Gauthier, and P. Degauque, "Classification and Characterization of Impulse noise on Indoor Power Lines and for Data Communications", *IEEE Transactions on Consumer Electronics*, vol. 48, November 2002.
- 112 J. A. Cortes, L. Diez, F. J. Canete and J. Lopez, "Analysis of the periodic impulsive noise asynchronous with the mains in indoor PLC channels", in *Proc. IEEE Int. Symp. Power Line Commun. Appl. (ISPLC)*, Mar./Apr., 2009, pp. 26-30.
- 113 E. Liu, Y. Gao, O. Bilal, and T. Korhonen, "Broadband Characterization of indoor Powerline Channel", *proceeding of the IEEE ISPLC 2004*, Zaragoza, Spain, p. 5, 2004.
- 114 T. Esmailian, F. R. Kschischang, and P. G. Gulak, "Characteristics of In-Building Power Lines at High Frequencies and their Channel Capacity", *proceeding of the IEEE ISPLC 2000*, Limerick, Ireland, p. 52-59, 2000.
- 115 V. Guillet and G. Lamarque, "Unified Background Noise Model for Power Line Communications", *proceedings of the IEEE ISPLC 2010*, Rio de Janeiro, Brazil, p. 131-136, 2010.
- 116 R. Garcia, L. diez, J. A. cortes, and F. J. Canete, "Mitigation of cyclic short-time noise in indoor power line channels", in *Proc. IEEE Int. Symp. Power Line Commun. Appl. (ISPLC)*, Mar. 2007, pp. 396-400.

- 117 J. G. Proakis, "Digital Communications", 2<sup>nd</sup> ed, New York, McGraw Hill, 1989.
- 118 W. C. Jakes, "Microwave Mobile Communications", New York, Willey, 1974.
- 119 W. C. Y. Lee, "Mobile Communications Design Fundamentals", 2<sup>nd</sup> ed, New York, Willey, 1993.
- 120 M. S. Varela and M. G. Sanchez, "RMS Delay and Coherence Bandwidth Measurements in Indoor radio Channels in the UHF Band", *IEEE Transactions on veh., Tech.*, vol. 50, No. 2, March 2001.
- 121 H. Philipps, "Development of a Statistical Model for Power Line Communications Channels", *Proceedings of ISPLC 2000*, Limerick, Ireland, April 2000.
- 122 T. V. Pasad, S. Srikanth, C. N. Krishnan, and P. V. Ramakrishna, "Wideband characterization of Low Voltage outdoor Powerline Communication Channels in India", *International Symposium on Power-Line Communications (ISPLC'2001)*, Sweden, April 2001.
- 123 M. Tlich, G. Avril, A. Zeddani, "Coherence Bandwidth and its Relationship with the RMS delay spread for PLC Channels using Measurements up to 100 MHz", *1<sup>st</sup> International Home Networking Conference (IHN 2007)*, Paris-France, 10-12 December 2007.
- 124 Bo Tan, John S. Thompson, "Power line Communications Channel Modeling Methodology Based on Statistical Features", *Proceedings of the IEEE*, March 2012.
- 125 T. K. Sarkav, Zhong Ji, Kyungjung Kim, A. Medouri, and M. Salazar-Palma, "A Survey of Various Propagation Models for Mobile Communication", *IEEE Antenna and Propagation Magazine*, vol. 45, No. 3, June 2003.
- 126 H. R. Anderson and J. P. McGeehan, "Direct Calculation of Coherence Bandwidth in Urban Microcells Using a Ray-Tracing Propagation Model", *IEEE Int. Symp. On Wireless Networks*, vol. 1, pp. 20-24, September 1994.
- 127 H. Lutz, J. Lampe and Johannes B. Huber, "Bandwidth Efficient Power Line Communications Based on OFDM", *AEU Int. J. Electr. Commun.*, 1999.
- 128 D. J. Purle, A. R. Nix, M. A. Beach, and J. P. McGeenhan, "A Preliminary Performance Evaluation of a linear frequency Hopped Modem", *proceedings of the 1992*, veh. Tech. Society conf., Denver, pp. 120-124, May 1992.
- 129 C. R. Loubery, "Einrichtung zur elektrischen zeichengebung an die teilnehmereines starkstromnetzes," *Kaiserliches Patenamnt*, March 1901.

- 130 A. Sanz, J. I. Garcia, I. Urriza, and A. Valdovinos, "A complete node for the power line medium of european home systems specifications," in *Proceedings of the International Symposium on Power Line Communications and its Applications (ISPLC)*, 2001, pp.53-58.
- 131 X10 Technology Transmission Theory. [Online]. Available: [www.x10.com/technology1.htm](http://www.x10.com/technology1.htm), *Last visited* 10-08-2014.
- 132 CENELEC, "Signalling on low-voltage electrical installations in the frequency range 3 kHz to 148.5 kHz," *EN 50065*, 1991.
- 133 J. A. C. Arrabal, "Modulation and Multiple Access Techniques for Indoor Broadband Power-Line Communications," *Doctoral thesis*, Universidad de Malaga, 17 June 2007.
- 134 The Wi-Fi Alliance. [Online]. Available: <http://www.wifi.org>, *Last visited*: 15-08-2014.
- 135 F. J. Canete, J. A. Cortes, L. Diez, and J. T. Entrambasaguas, "Modeling and evaluation of the indoor power line channel," *IEEE Communications Magazine*, vol. 41, no. 4, pp. 41-47, Apr 2003.
- 136 F. J. Canete-Corripio, L. Diez-del Rio, J. T. Entrambasaguas-Mnoz, "Indoor Power-Line Communications: Channel Modelling and Measurements," *Proceedings of ISPLC 2000*, pp. 117-122.
- 137 L.T. Tang, P.L. So, E. Gunawan, Y.L. Guan, S. Chen, T.T. Lie, "Characterization and modeling of in-building power lines for high-speed data transmission," *IEEE Transactions on Power Delivery*, vol.18, no.1, pp. 69- 77, Jan 2003
- 138 D. Anastasiadou, T. Antonakopoulos, "Multipath characterization of indoor power-line networks," *Transactions on Power Delivery*, vol.20, no.1, pp. 90- 99, Jan. 2005
- 139 S. Galli, T. Banwell, "A novel approach to the modeling of the indoor power line channel-Part II: power line transmission medium," *IEEE Communications Magazine*, vol.41, no.4, pp. 41- 47, April 2003
- 140 H. Meng, Y.L. Guan, C.L. Law, P.L. So, E. Gunawan and T.T. Lie, "Modeling of Transfer Characteristics for the Broadband Power Line Communications Channel" in *IEEE Transactions on Power Delivery*, Vol. 19, no. 3, pp. 1057–1064, 2004.
- 141 [http://www.testequipmentdepot.com/rohdeschwarz/pdf/zv113\\_data.pdf](http://www.testequipmentdepot.com/rohdeschwarz/pdf/zv113_data.pdf) (Access date: 10/09/14)

- 142 Giuseppe Marrocco, Driton Statovci, Steffen Trautmann, “A PLC Broadband Channel Simulator for Indoor Communications,” *IEEE International symposium on Power Line and its Applications (ISPLC)*, pp. 321-326, March 2013.
- 143 H. Philipps, “Modeling of powerline communication channels,” in *Proc. 3rd Int. Symp. Powerline Communications and its Applications*, Lancaster, U.K., 1999, pp. 14–21.
- 144 “Seventh Framework Programme: Theme 3. ICT-213311 OMEGA, PLC Channel Characterization and Modelling.” [Online]. Available: [http://www.ict-omega.eu/fileadmin/documents/deliverables/Omega D3.2 v1.1.pdf](http://www.ict-omega.eu/fileadmin/documents/deliverables/Omega_D3.2_v1.1.pdf)
- 145 H. Phillips, “Performance Measurements of Powerline Channels at High Frequencies,” *PLC'98* ISBN: 90-74249-18-3